

**International
Progress Report**

IPR-03-08

Äspö Hard Rock Laboratory

Canister Retrieval test

**Sensors data Report
(Period 001026-021101)
Report no: 5**

Reza Goudarzi
Lennart Börgesson
Clay Technology AB

Kennert Röshoff
Nancy Bono
BBK

November 2002

Svensk Kärnbränslehantering AB

Swedish Nuclear Fuel
and Waste Management Co
Box 5864
SE-102 40 Stockholm Sweden
Tel +46 8 459 84 00
Fax +46 8 661 57 19



**Äspö Hard Rock
Laboratory**

Report no.	No.
IPR-03-08	F69K
Author	Date
Goudarzi, Börgesson Röshoff, Bono	02-11-01
Checked by	Date
Approved	Date
Christer Svemar	03-01-30

Äspö Hard Rock Laboratory

Canister Retrieval test

Sensors data Report (Period 001026-021101) Report no: 5

Reza Goudarzi
Lennart Börgesson
Clay Technology AB

Kennert Röshoff
Nancy Bono
BBK

November 2002

Keywords: Buffer, bentonite, rock, temperature, stress, strain, test, measurements, swelling, full scale, in situ

This report concerns a study which was conducted for SKB. The conclusions and viewpoints presented in the report are those of the author(s) and do not necessarily coincide with those of the client.

Abstract

This report presents data from the measurements in the Canister Retrieval Test from 001026 to 021101.

The following measurements are made in the bentonite: Temperature is measured in 32 points, total pressure in 27 points, pore water pressure in 14 points and relative humidity in 55 points. Temperature is also measured by all relative humidity gauges. The positions of the measuring points in the bentonite are related to a coordinate system in the deposition hole.

The following measurements are made in the rock: Temperature is measured in 40 points, stresses are measured in 8 points and strain is measured in 9 points. Stresses and strains are also measured in the rock around the empty deposition hole located 6 m south of the test hole.

The following measurements are made in the canister: Temperature is measured every meter along two fiber optic cables and strain is measured in 76 points on the surface of the copper envelop. Temperature is measured in the steel insert in 18 points.

The following measurements are made on the plug: Force is measured in 3 of the 9 anchors and vertical displacement is measured in three points.

The water inflow to the filter mats on the rock surface is also measured.

The general conclusion is that the measuring systems and transducers seem to work well but the following problems have been noted: The strain measurements in the canister are not reported due to question marks regarding the relevance of the results. Most Vaisala relative humidity transducers have failed due to water saturation. Four Kulite total pressure transducers out of six seem to yield erroneous results.

The wetting has continued during the last 6-months period and the relative humidity sensors indicate that the bentonite between the rock and the canister is close to water saturation although the wetting seems to be somewhat uneven and the total pressure has not reached the expected values yet. Some clogging of the filters may explain the inhomogeneous appearance.

In order to increase the rate of saturation the water pressure in the mats was increase in steps to 800 kPa during the autumn 2002 and in order to reduce the risk of heater failure the power of the canister was reduced from 2600 to 2100 W at September 10.

Sammanfattning

I denna rapport presenteras data från mätningar i Återtag under perioden 001026-021101.

Följande mätningar görs i bentoniten: Temperaturen mäts i 32 punkter, totaltryck i 27 punkter, porvattentryck i 14 punkter och relativa fuktigheten i 55 punkter. Temperaturen mäts även i alla relativa fuktighetsmätare. Varje mätpunkt relateras till ett koordinatsystem i deponeringshålet.

Följande mätningar görs i berget: Temperaturen mäts i 40 punkter, bergspänningar mäts i 8 punkter och töjningar i 9 punkter. Bergspänningar och töjningar mäts också i berget runt det tomma deponeringshålet 6 m söder om försökshålet.

Följande mätningar görs på ytan i kapselns kopparhölje: Temperaturen mäts varje meter längs två fiberoptiska kablar och töjning mäts i 76 punkter. Temperaturen mäts i stålinsatsen i kanistern i 18 punkter.

Följande mätningar görs på pluggen: Kraften mäts i 3 av de 9 stagen och vertikala förskjutningen mäts i tre punkter.

Vatteninflödet till filtermattorna mäts också.

En generell slutsats är att mätsystemen och givarna tycks fungera bra, men följande problem har noterats: Töjningsmätningarna i kapseln har inte redovisats p. g. a frågetecken beträffande mätresultatets relevans. Några av Visalas relativa fuktighetsmätare, de flesta belägna i ring 10, har slutat fungera p. g. a. vattenmättnad. Fyra Kulite totaltrycksgivare av totalt sex tycks ge felaktiga resultat.

Bevätningen har fortsatt under den senaste 6-månadersperioden och fuktighetsmätarna indikerar att bentoniten mellan berget och kapseln är nära vattenmättnad, fastän bevätningen tycks vara något ojämn och totaltrycket ännu inte har nått de förväntade värdena. En viss igensättning av filterna kan förklara det inhomogena uppförandet.

För att öka bevätningshastigheten har vattentrycket i mattorna ökats stegvis till 800 kPa under hösten 2002 och för att reducera risken för värmarkortslutning har kapselns effekt minskats från 2600 W till 2100 W (10 september).

Contents

1 Introduction	9
2 Comments	11
2.1 General	11
2.2 Total pressure, Geocon (App. A pages 35-38)	12
2.3 Total Pressure, Kulite (App. A page 39)	12
2.4 Suction, Wescor Psychrometers (App. A pages 40-49)	12
2.5 Relative humidity, Vaisala (App. A pages 50-54)	12
2.6 Pore water pressure, Geocon (App. A pages 55-56)	13
2.7 Pore water pressure, Kulite (App. A page 57)	13
2.8 Water flow into the filters (App. A page 58)	13
2.9 Forces on the plug (App. A page 59)	13
2.10 Displacement of the plug (App. A page 60)	14
2.11 Canister power (App. A page 61)	14
2.12 Temperature in the buffer (App. A pages 62-66)	14
2.13 Temperature in the rock (App. A pages 67-70)	14
2.14 Temperature on the canister surface, Optical fiber cables (App. A pages 71-72)	14
2.15 Temperature inside the canister (App. A pages 73-75)	15
2.16 Strain in the canister	15
2.17 Rock stresses and strains	15
3 Geometry	17
4 Location of instruments	19
4.1 Brief description of the instruments	19
4.2 Strategy for describing the position of each device	20
4.3 Position of each instrument in the bentonite	21
4.4 Instruments in the rock	26
4.5 Instruments in the canister	27
4.6 Instruments at the plug	30
References	31
Appendix A	33
Appendix B	77

1 Introduction

The installation of the Canister Retrieval Test was made during autumn 2000. In general the data in this report are presented in diagrams covering the time period 2000-10-26 to 2002-11-01. The time axis in the diagrams represents days from 2000-10-26. The diagrams are attached in Appendix A. The stress and strain measurements in the rock are reported separately by BBK. That report is attached as Appendix B.

A test overview with the positions of the measuring points and a brief description of the instruments is also presented in this report (chapters 3 and 4).

General comments concerning the collected data are given in chapter 2.

2 Comments

2.1 General

In this chapter short comments on general trends in the measurements are given. Sensors that are not delivering reliable data or no data at all are noted and comments on the data in general are given.

The slot between rock and bentonite block was filled with bentonite pellets and water at 001026. This date is also marked as start date. 1 m water head in the water supply tank was connected to the filters on 001102.

The heating of the canister started with an initially applied constant power of 700 W at 001027 that is one day after test start. The power was raised to 1700 W on 001113. The power was further raised to 2600 W on 010213.

At the end of last year two of the 36 electrical heaters failed due to short circuit to earth and no power was generated during one day between November 5 and 6 2001 (day 375). The heaters were also shut off during one week between March 4 and 11 2002 (days 495 to 502) for control measurements.

The following events, which are important for understanding the results, have occurred this reporting half-year period:

- Day 678 (5/9 –02): The water pressure in the mats on the rock wall was increased to 200 kPa.
- Day 683 (10/9 –02): The power in the heater has been reduced from 2600 W to 2100 W in order to lower the temperature in the canister and thus increase the resistance to earth in the heater elements.
- Day 690 (17/9 –02): The water pressure in the mats on the rock wall was increased to 400 kPa.
- Day 697 (24/9 –02): The water pressure in the mats on the rock wall was increased to 520 kPa. During that day the water pressure in the top of the mats was temporarily reduced to atmospheric for a few hours (flow testing of mats).
- Day 710 (7/10 –02): The water pressure in the mats on the rock wall was increased to 600 kPa.
- Day 713 (10/10 –02): The water pressure in the mats on the rock wall was increased to 800 kPa. During that day the water pressure in the top of the mats was temporarily reduced to atmospheric for a few hours (flow testing of mats).

The fourth report covered the period up to 020501. This report is the fifth one and covers the results up to 021101.

2.2 Total pressure, Geocon (App. A pages 35-38)

The two periods of power shut off with decreased temperature are clearly reflected by the pressure measurements with decreasing pressure and a rather fast recovery.

The measured pressure range is from 0 to 6.1 MPa. The highest pressure is indicated in the periphery of the bottom block (C1) and the center ring (R5), where all transducers yield a pressure between 2.5 and 6 MPa except for P116.

If each section is considered separately all Geocon total pressure sensors show logical increase in pressure with increased radial distance from the canister surface except for section C in ring 5, where P116 close to the rock yields 1.2 MPa and P115 close to the canister yields 3.6 MPa.

P114 failed at the end of the reporting period.

Sensor P104 was not installed. U106 was originally intended to be a pore pressure sensor but was replaced by a total pressure sensor. 1 of 21 sensors is out of order.

2.3 Total Pressure, Kulite (App. A page 39)

Six Kulite total pressure transducers are installed in the bentonite blocks. Unfortunately they don't seem to work properly. The reason for the malfunction is probably brakeage of the transducer connections at high pressures.

4 out of 6 sensors seem to be malfunctioning.

2.4 Suction, Wescor Psychrometers (App. A pages 40-49)

Wescor psychrometers are only working at suction below 5000 kPa, which correspond to high relative humidity (above about 96%). 19 out of 26 transducer yield values that can be evaluated and have thus a high relative humidity. The interpretation of the values should be done with care since the evaluation is done with an automatic technique and the plateau required for proper evaluation not always formed. This explains why most transducers start their appearance from very low value. These low values are not correct but only an indication of that the relative humidity or suction is getting close to the measuring range. All diagrams are included (also diagrams with no evaluated values).

In Ring 5 eight out of nine transducers are indicating a high relative humidity, which confirm the total pressure measurements. In ring 10 all eight transducers indicate a high relative humidity.

3 out of 26 sensors are out of order.

2.5 Relative humidity, Vaisala (App. A pages 50-54)

App. A pages 37-41 show relative humidity and temperature measured with Vaisala transducers. The relative humidity results and the temperature results in ring 10 have been split into two diagrams (pages 52 and 53) since the data were interfering with each other.

All transducers in Cyl.1, Ring5 and Ring10 (except W134 and W135 which are placed above the canister) have stopped to work.

The reason for the successive malfunction of these is not clear but the transducers do not work very well at high relative humidity. It is interesting to note that the drying indicated by transducers W134 and W135, which are placed just above the canister, has stopped and turned into a slow wetting. All transducers between the rock and the canister in rings 5 and 10 indicate a high degree of saturation, which confirm the results of the Wescor psychrometers.

19 out of 25 sensors are out of order, mainly due to water saturation.

2.6 Pore water pressure, Geocon (App. A pages 55-56)

U105, U107, U108 and U110 yield a water pressure of between 170 and 220 kPa. They are placed in Ring 5. The pressure measured by these transducers is most likely a pore gas pressure. The remaining sensors of this type yield pressure close to zero. No increase in pore water pressure from the applied water pressure in the mats is yet noted.

U106 is replaced by a total pressure sensor. All 11 sensors are working

2.7 Pore water pressure, Kulite (App. A page 57)

There are only one sensor of this type in Ring 10 and one in Cylinder 4. Both are working and indicate pressure close to zero.

2.8 Water flow into the filters (App. A page 58)

Measurement of water inflow into the filters started on 001102. The total inflow to the filters has since that date been 315 liter.

The inflow rate has strongly increased after start pressurizing the water in the mats on 020905 (day 678). The inflow is at present about 0.80 l/day.

2.9 Forces on the plug (App. A page 59)

The forces on the plug have been measured since 001106. The total force is about 6000 kN on 021101.

During the first about 50 days the plug was only fixed with 3 rods. When the total force exceeded 1500 kN the rest of the 9 rods were fixed in a prescribed manner. This procedure took place 12-14 December 2000 that is 46-48 days after test start. From that time only every third anchor is measured and the results should thus be multiplied with 3. The diagram shows both the actual measurements and after multiplication with 3.

2.10 Displacement of the plug (App. A page 60)

A strange behavior with jumps up and down of the measured values is observed in the last months. This behavior cannot be real and the data is excluded. The system will be checked.

2.11 Canister power (App. A page 61)

A constant power of 2600 W is applied and measured. The failure at day 375 and the turn off at days 495 to 502 are noted as intermissions in the curve.

In this latest half-year period (day 683) the power has been decreased from 2600 W to 2100 W.

2.12 Temperature in the buffer (App. A pages 62-66)

After reduction of power at 020909 (day 683) from 2600 W to 2100 W the highest temperature near the canister in Ring 5 has decreased from 86 °C to 77 °C.

The highest temperature gradient is about 0.75 degrees/cm (ring 5).

1 out of 32 sensors is out of order.

2.13 Temperature in the rock (App. A pages 67-70)

The maximum temperature measured in the rock (58 degrees) is measured in the central section on the surface of the deposition hole. Almost complete axial symmetry of the temperature measured in the rock is observed.

One thermocouple (TR139) has stopped working during last period. All other sensors are working.

2.14 Temperature on the canister surface, Optical fiber cables (App. A pages 71-72)

The first diagram shows the maximum temperature plotted as a function of time. The maximum temperature measured on the canister surface has decreased from between 95 and 100 to between 83 and 86 °C due to the decrease in power. The second diagram shows the distribution of the temperature along the cables at 021101. The length of the cable on the canister surface is only about 20 m and close to the entrances the lower surrounding temperatures affect the measured temperature.

2.15 Temperature inside the canister (App. A pages 73-75)

After reduction of the power with 500 W, the max temperature inside the canister has been reduced from 107 °C to 95 °C.

Five of these sensors have stopped working. All these sensors are placed near canister surface.

2.16 Strain in the canister

Continuous measurements have been made but so far no results have been produced due to evaluation problems.

2.17 Rock stresses and strains

Rock stresses and strains are reported in Appendix B.

3 Geometry

The test installation consists of a full-scale deposition hole, a copper canister equipped with electrical heaters and bentonite blocks (cylindrical and ring shaped). A plug of concrete and steel is anchored to the rock on top of the bentonite.

The saturation of the bentonite is attained artificially by vertical filter stripes. 16 stripes with a width of 0.1 meters and a length of 5.5 meters are applied on the surrounding rock.

Measurements are made in four vertical sections A, B, C and D according to Figure 3-1. Direction A-B is parallel to the tunnels axial with A headed almost against north.

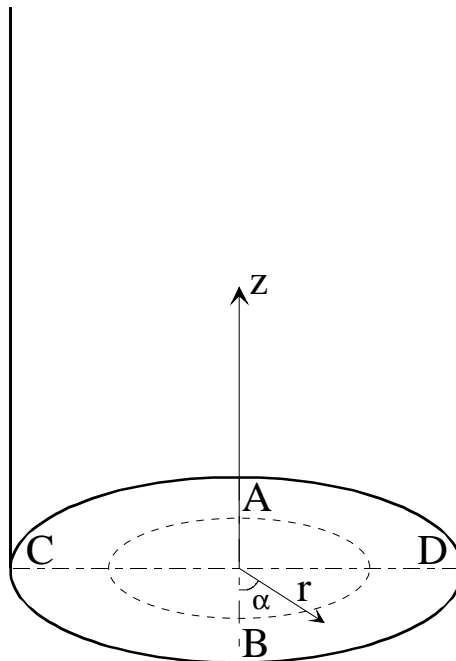


Figure 3-1. Figure describing the instrument planes (A-D) and the coordinate system used when describing the instrument positions.

4 Location of instruments

4.1 Brief description of the instruments

The different instruments that are used in the experiment are briefly described in this chapter.

Measurements of temperature

Buffer

Thermocouples from BICC have been installed for measuring temperature in the buffer. Measurements are done in 32 points in the test hole. In addition, temperature gauges are built in into the capacitive relative humidity sensors (29 sensors) as well as in the pressure gauges of vibrating wire type (13 gauges). Temperature is also measured in the psychrometers.

Canister

Temperature is measured inside the canister (on the insert) in 19 points with PT-100 gauges. In addition temperature is measured on the surface of the canister with optical fiber cables. An optical measuring system called FTR (Fiber Temperature Laser Radar) from BICC is used.

Rock

Temperature in the rock and on the rock surface of the hole is measured in 40 points with thermocouples from BICC.

Measurement of total pressure in the buffer

Total pressure is the sum of the swelling pressure and the pore water pressure. It is measured with the following instrument types:

- Geocon total pressure cells with vibrating wire transducers. 15 cells of this type have been installed.
- Kulite total pressure cells with piezo resistive transducers. 6 cells of this type have been installed.

Measurement of pore water pressure in the buffer

Pore water pressure is measured with the following instrument types:

- Geocon pore pressure cells with vibrating wire transducer. 13 cells of this type have been installed.
- Kulite pore pressure cells with piezo resistive transducer. 2 cells of this type have been installed.

Measurement of the water saturation process

The water saturation process is recorded by measuring the relative humidity in the pore system, which can be converted into water ratio or total suction (negative water pressure). The following techniques and devices are used:

- Vaisala relative humidity sensor of capacitive type. 29 cells of this type have been installed. The measuring range is 0-100 % RH.
- Wescor psychrometers model PST-55. The devices measure the relative humidity in the pore system. The measuring range is 95.5-99.6 % RH corresponding to the pore water pressure -0.5 to -6MPa. 26 cells of this type have been installed.

Measurements of strain in the Canister

These measurements are not reported.

Measurements of stresses and strain in the rock

These measurements are not reported.

Measurements of forces on the plug

The force on the plug caused by the swelling pressure of the bentonite is measured in 3 of the 9 anchors. The force transducers are of the type GLÖTZL.

Measurements of plug displacement

Due to straining of the anchors the swelling pressure of the bentonite will cause not only a force on the plug but also displacement of the plug. The displacement is measured in three points with transducers of the type LVDT with the range 0 – 50 mm.

Measurement of water flow into the permeable mats

Water is supplied to the bentonite with filter strips attached to the rock surface. The water flow into these mats is measured by measuring the water volume in the supply tank with a differential pressure transmitter that measures the difference in pressure between the nitrogen in the top of the tank and the water in the bottom of the tank.

4.2 Strategy for describing the position of each device

Every instrument is named with a short unique name consisting of 1-2 letters describing the type of measurement and 3 figures numbering the device. Every instrument position in the buffer and rock is described with three coordinates according to Figure 3-1.

The r-coordinate is the horizontal distance from the center of the hole and the z-coordinate is the height from the bottom of the hole (the block height is set to 500 mm). The α -coordinate is the angle from the vertical direction B (almost south).

The short description of the positions in the diagrams differs between the buffer and the rock.

Buffer: Three positions with the following meaning: (bentonite block or cylinder number counted from the bottom \ direction A, B, C, or D \ radius in mm from center line)

Rock: Three positions with the following meaning: (distance in meters from the bottom \ α according to Fig 3-1 \ distance in meters from the hole surface)

The bentonite blocks are called cylinders and rings. The cylinders are numbered C1-C4 and the rings R1-R10 respectively (Figure 4-1).

4.3 Position of each instrument in the bentonite

Measurements are done in four vertical sections A, B, C and D according to Figure 3-1. Direction A and B are placed in the tunnels axial direction.

An overview of the positions of the instruments is shown in Fig 4-1. Exact positions are described in Tables 4-1 to 4-4.

The instruments are located in two main levels in the blocks, 50 mm and 160 mm, from the upper surface. The thermocouples have mostly placed in the 50mm level and the other gauges in the 160 mm level.

- pore water pressure + temp.
- total pressure + temp.
- × temp.
- △ relative humidity (+ temp.)

1m

A

B+C

D

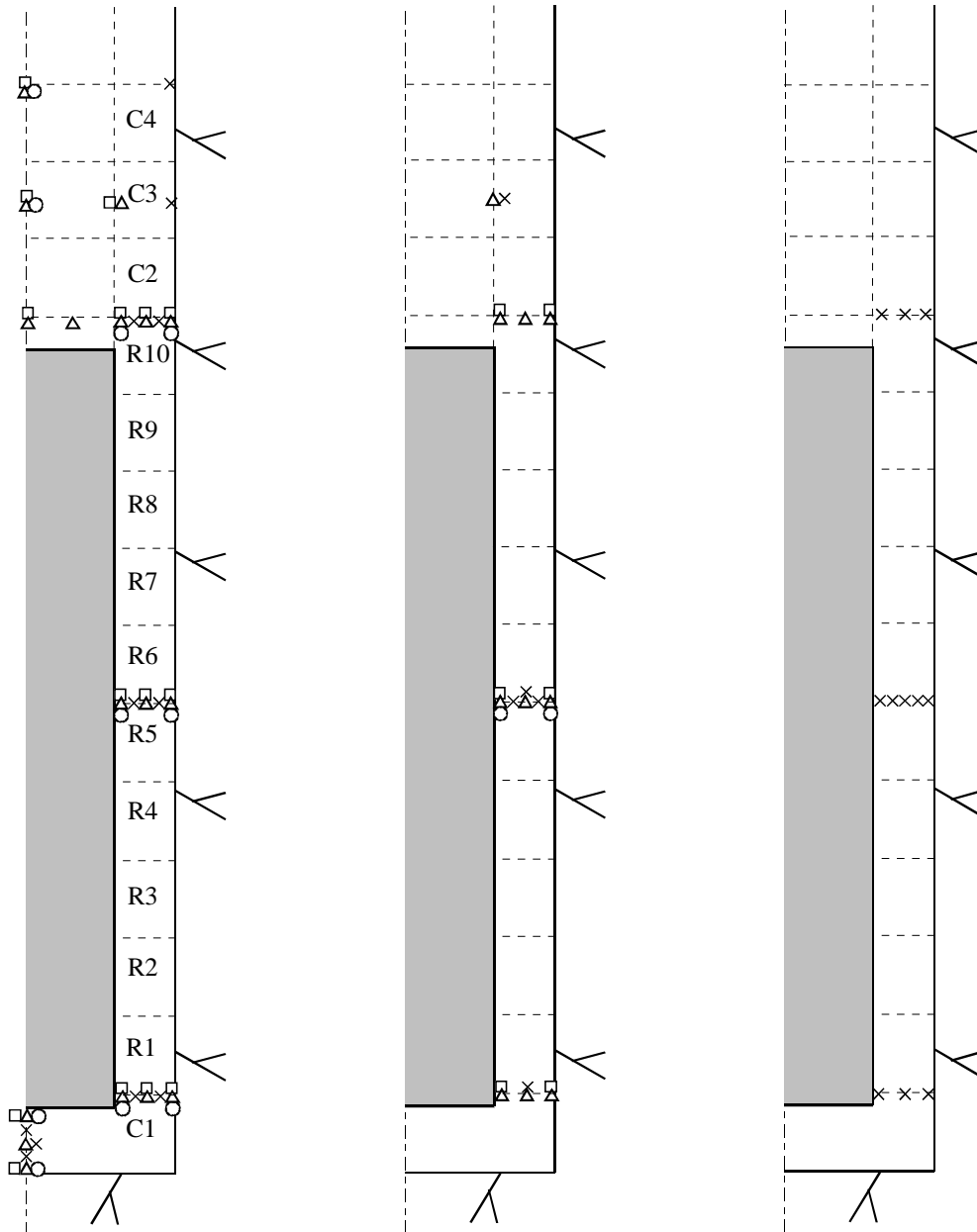


Figure 4-1 Schematic view over the instruments in four vertical sections and the block designation.

Table 4-1 Numbering and position of instruments for measuring temperature (T)

Type and number	Block	Instrument position in block				Cable pos.		Remark
		Direction	α	r	Z	α	Fabricate	
T101	Cyl. 1	Center	90	50	50	242	BICC	
T102	Cyl. 1	Center	90	50	250	238	BICC	
T103	Cyl. 1	Center	90	50	450	230	BICC	
T104	Cyl. 1	A	180	635	450	206	BICC	
T105	Cyl. 1	A	180	735	450	202	BICC	
T106	Cyl. 1	B	365	685	450	38	BICC	
T107	Cyl. 1	C	275	685	450	274	BICC	
T108	Cyl. 1	D	90	585	450	96	BICC	
T109	Cyl. 1	D	90	685	450	94	BICC	
T110	Cyl. 1	D	90	785	450	92	BICC	
T111	Ring 5	A	180	635	2950	224	BICC	
T112	Ring 5	A	180	735	2950	218	BICC	
T113	Ring 5	B	360	610	2950	318	BICC	
T114	Ring 5	B	360	685	2950	322	BICC	
T115	Ring 5	B	360	735	2950	324	BICC	
T116	Ring 5	C	270	610	2950	258	BICC	
T117	Ring 5	C	270	685	2950	260	BICC	
T118	Ring 5	C	270	735	2950	262	BICC	
T119	Ring 5	D	90	585	2950	44	BICC	
T120	Ring 5	D	90	635	2950	46	BICC	
T121	Ring 5	D	90	685	2950	48	BICC	
T122	Ring 5	D	90	735	2950	50	BICC	
T123	Ring 5	D	90	785	2950	52	BICC	
T124	Ring 10	A	180	635	5450	200	BICC	
T125	Ring 10	A	180	735	5450	194	BICC	
T126	Ring 10	D	90	585	5450	54	BICC	
T127	Ring 10	D	90	685	5450	56	BICC	
T128	Ring 10	D	90	785	5450	58	BICC	
T129	Cyl. 3	A	180	785	6250	166	BICC	
T130	Cyl. 3	B	365	585	6250	358	BICC	
T131	Cyl. 3	C	275	585	6250	280	BICC	
T132	Cyl. 4	A	180	785	6950	66	BICC	

Table 4-2 Numbering and position of instruments for measuring total pressure (P)

Type and number	Block	Instrument position in block				Cable pos.		Fabricate	Remark
		Direction	α	r	Z	α			
P101	Cyl. 1	Center	180	50	50	244	Geocon		
P102	Cyl. 1	Center	180	50	250	232	Geocon		
P103	Cyl. 1	A	185	585	250	208	Geocon		
P104	Cyl. 1	A	185	685	250	204	Geocon		
P105	Cyl. 1	A	185	785	250	186	Geocon		
P106	Cyl. 1	B	365	585	250	40	Geocon		
P107	Cyl. 1	B	365	785	250	2	Geocon		
P108	Cyl. 1	C	275	585	250	278	Geocon		
P109	Cyl. 1	C	275	785	250	270	Geocon		
P110	Ring 5	A	185	585	2750	228	Geocon		
P111	Ring 5	A	185	685	2750	222	Geocon		
P112	Ring 5	A	185	785	2750	188	Geocon		
P113	Ring 5	B	365	535	2750	36	Geocon		
P114	Ring 5	B	365	825	2750	16	Geocon		
P115	Ring 5	C	275	585	2750	296	Geocon		
P116	Ring 5	C	275	785	2750	290	Geocon		
P117	Ring 10	Center	180	50	5250	24	Kulite		
P118	Ring 10	A	180	585	5250	216	Geocon		
P119	Ring 10	A	180	685	5250	198	Geocon		
P120	Ring 10	A	180	785	5250	192	Geocon		
P121	Ring 10	B	365	585	5250	20	Kulite		
P122	Ring 10	B	365	785	5250	18	Kulite		
P123	Ring 10	C	275	585	5250	286	Kulite		
P124	Ring 10	C	275	785	5250	284	Kulite		
P125	Cyl. 3	Center	180	50	6250	158	Geocon		
P126	Cyl. 3	A	180	585	6250	162	Geocon		
P127	Cyl. 4	Center	180	50	6750	64	Kulite		

Table 4-3 Numbering and position of instruments for measuring pore water pressure (U)

Type and number	Block	Instrument position in block				Cable pos.		Fabricate	Remark
		Direction	α	r	Z	α			
U101	Cyl. 1	Center	270	50	50	246	Geocon		
U102	Cyl. 1	Center	270	50	250	236	Geocon	Horizontal	
U103	Cyl. 1	A	175	585	250	126	Geocon		
U104	Cyl. 1	A	175	785	250	178	Geocon		
U105	Ring 5	A	175	585	2750	138	Geocon		
U106	Ring 5	A	175	785	2750	180	Geocon		
U107	Ring 5	B	355	535	2750	314	Geocon		
U108	Ring 5	B	355	825	2750	348	Geocon		
U109	Ring 5	C	265	585	2750	256	Geocon	In the slot	
U110	Ring 5	C	265	825	2750	264	Geocon	In the slot	
U111	Ring 10	A	175	585	5250	146	Geocon		
U112	Ring 10	A	175	785	5250	152	Geocon		
U113	Cyl. 3	Center	270	50	6250	156	Geocon		
U114	Cyl. 4	Center	270	50	6950	62	Kulite		

Table 4-4 Numbering and position of instruments for measuring water content (W)

Type and number	Block	Instrument position in block				Cable pos.		Fabricate	Remark
		Direction	α	r	Z	α			
W101	Cyl. 1	Center	360	50	50	248	Vaisala		
W102	Cyl. 1	Center	360	400	160	240	Vaisala		
W103	Cyl. 1	Center	360	50	450	234	Vaisala	Horizontal	
W104	Cyl. 1	A	180	585	340	128	Vaisala		
W105	Cyl. 1	A	180	685	340	132	Vaisala		
W106	Cyl. 1	A	180	785	340	184	Vaisala		
W107	Cyl. 1	A	170	585	340	124	Wescor		
W108	Cyl. 1	A	170	685	340	130	Wescor		
W109	Cyl. 1	A	170	785	340	134	Wescor		
W110	Cyl. 1	B	360	585	340	304	Vaisala		
W111	Cyl. 1	B	360	785	340	360	Vaisala		
W112	Cyl. 1	B	360	685	340	308	Vaisala		
W113	Cyl. 1	B	355	585	340	302	Wescor		
W114	Cyl. 1	B	355	685	340	306	Wescor		
W115	Cyl. 1	B	355	785	340	310	Wescor		
W116	Cyl. 1	C	270	585	340	250	Wescor		
W117	Cyl. 1	C	270	685	340	252	Wescor		
W118	Cyl. 1	C	270	785	340	254	Vaisala		
W119	Ring 5	A	180	585	2840	226	Vaisala		
W120	Ring 5	A	180	685	2840	220	Vaisala		
W121	Ring 5	A	180	785	2840	182	Vaisala		
W122	Ring 5	A	170	585	2840	136	Wescor		
W123	Ring 5	A	170	685	2840	140	Wescor		
W124	Ring 5	A	170	785	2840	142	Wescor		
W125	Ring 5	B	360	535	2840	316	Vaisala	In the slot	
W126	Ring 5	B	360	685	2840	34	Vaisala		
W127	Ring 5	B	360	785	2840	350	Vaisala		
W128	Ring 5	B	350	535	2840	312	Wescor	In the slot	
W129	Ring 5	B	350	685	2840	320	Wescor		
W130	Ring 5	B	350	785	2840	346	Wescor		
W131	Ring 5	C	270	585	2840	294	Wescor	In the slot	
W132	Ring 5	C	275	685	2840	292	Wescor		
W133	Ring 5	C	270	785	2840	288	Wescor		
W134	Ring 10	Center	360	50	5340	22	Vaisala		
W135	Ring 10	A	180	262	5340	26	Vaisala		
W136	Ring 10	A	180	585	5340	214	Vaisala		
W137	Ring 10	A	180	685	5340	196	Vaisala		
W138	Ring 10	A	180	785	5340	190	Vaisala		
W139	Ring 10	A	170	585	5340	144	Wescor		
W140	Ring 10	A	170	685	5340	148	Wescor		
W141	Ring 10	A	170	785	5340	150	Wescor		
W142	Ring 10	B	360	585	5340	328	Vaisala		
W143	Ring 10	B	360	685	5340	332	Vaisala		
W144	Ring 10	B	360	785	5340	336	Vaisala		
W145	Ring 10	B	355	585	5340	326	Wescor		
W146	Ring 10	B	355	685	5340	330	Wescor		
W147	Ring 10	B	355	785	5340	334	Wescor		
W148	Ring 10	C	270	585	5340	266	Wescor		
W149	Ring 10	C	270	685	5340	268	Wescor		
W150	Ring 10	C	270	785	5340	272	Vaisala		
W151	Cyl. 3	Center	360	50	6250	154	Vaisala		
W152	Cyl. 3	A	180	585	6250	160	Vaisala		
W153	Cyl. 3	B	360	585	6250	356	Vaisala		
W154	Cyl. 3	C	270	585	6250	276	Wescor		
W155	Cyl. 4	Center	360	50	6840	60	Vaisala		

4.4 Instruments in the rock

Temperature measurements

40 thermocouples are placed in the rock and on the rock surface of the deposition hole. Holes have been bored in three directions on three levels and one additional hole has been bored in the bottom of the deposition hole i.e. totally 10 holes. They are led from the rock, over the gap between rock and bentonite and up along the bentonite block periphery. The position of the thermocouples in the rock is shown in Table 4-5.

Table 4-5 Numbering and positions of thermocouples in the rock

Type and number	Level	Direction	Distance from rock surface	Cable pos. α	Fabricate	Remark
TR101	0	Center	0.000	70°-90°	BICC	
TR102	0	Center	0.375	70°-90°	BICC	
TR103	0	Center	0.750	70°-90°	BICC	
TR104	0	Center	1.500	70°-90°	BICC	
TR105	0.61	10°	0.000	4°-14°	BICC	
TR106	0.61	10°	0.375	4°-14°	BICC	
TR107	0.61	10°	0.750	4°-14°	BICC	
TR108	0.61	10°	1.500	4°-14°	BICC	
TR109	0.61	80°	0.000	70°-90°	BICC	
TR110	0.61	80°	0.375	70°-90°	BICC	
TR111	0.61	80°	0.750	70°-90°	BICC	
TR112	0.61	80°	1.500	70°-90°	BICC	
TR113	0.61	170°	0.000	168°-176°	BICC	
TR114	0.61	170°	0.375	168°-176°	BICC	
TR115	0.61	170°	0.750	168°-176°	BICC	
TR116	0.61	170°	1.500	168°-176°	BICC	
TR117	3.01	10°	0.000	4°-14°	BICC	
TR118	3.01	10°	0.375	4°-14°	BICC	
TR119	3.01	10°	0.750	4°-14°	BICC	
TR120	3.01	10°	1.500	4°-14°	BICC	
TR121	3.01	80°	0.000	70°-90°	BICC	
TR122	3.01	80°	0.375	70°-90°	BICC	
TR123	3.01	80°	0.750	70°-90°	BICC	
TR124	3.01	80°	1.500	70°-90°	BICC	
TR125	3.01	170°	0.000	168°-176°	BICC	
TR126	3.01	170°	0.375	168°-176°	BICC	
TR127	3.01	170°	0.750	168°-176°	BICC	
TR128	3.01	170°	1.500	168°-176°	BICC	
TR129	5.41	10°	0.000	4°-14°	BICC	
TR130	5.41	10°	0.375	4°-14°	BICC	
TR131	5.41	10°	0.750	4°-14°	BICC	
TR132	5.41	10°	1.500	4°-14°	BICC	
TR133	5.41	80°	0.000	70°-90°	BICC	
TR134	5.41	80°	0.375	70°-90°	BICC	
TR135	5.41	80°	0.750	70°-90°	BICC	
TR136	5.41	80°	1.500	70°-90°	BICC	
TR137	5.41	170°	0.000	168°-176°	BICC	
TR138	5.41	170°	0.375	168°-176°	BICC	
TR139	5.41	170°	0.750	168°-176°	BICC	
TR140	5.41	170°	1.500	168°-176°	BICC	

Stress and strain measurements

See Appendix B .

4.5 Instruments in the canister

The canister is instrumented with optical fiber cables on the copper surface, thermocouples in the steel insert and strain gauges on the inner and outer surface of the copper envelop in canister.

Optical fiber cables

Figure 4-2 shows how the two optical fiber cables are placed on the canister surface. Both ends of a cable are used for measurements. This means that the two cables are used as four measuring channels as described in Table 4-6.

With this laying the cable will enter and exit the surface at almost the same position. Curvatures are shaped as a quarter circle with a radius of 20 cm. The cable is placed in a milled out channel on the surface. The channel has a width and a depth of just above 2 mm

Table 4-6. Combination of cables and channels

Channel 1	Outlet of cable 1
Channel 2	Inlet of cable 1
Channel 3	Outlet of cable 2
Channel 4	Inlet of cable 2

Figure 4-3 shows the location of the thermocouples on the steel insert inside the canister.

Thermocouple, PT100

Temperature in the steel insert measured at 18 point of measuring with. thermocouple of type PT100. Figure 4-4 shows how these thermocouple are placed

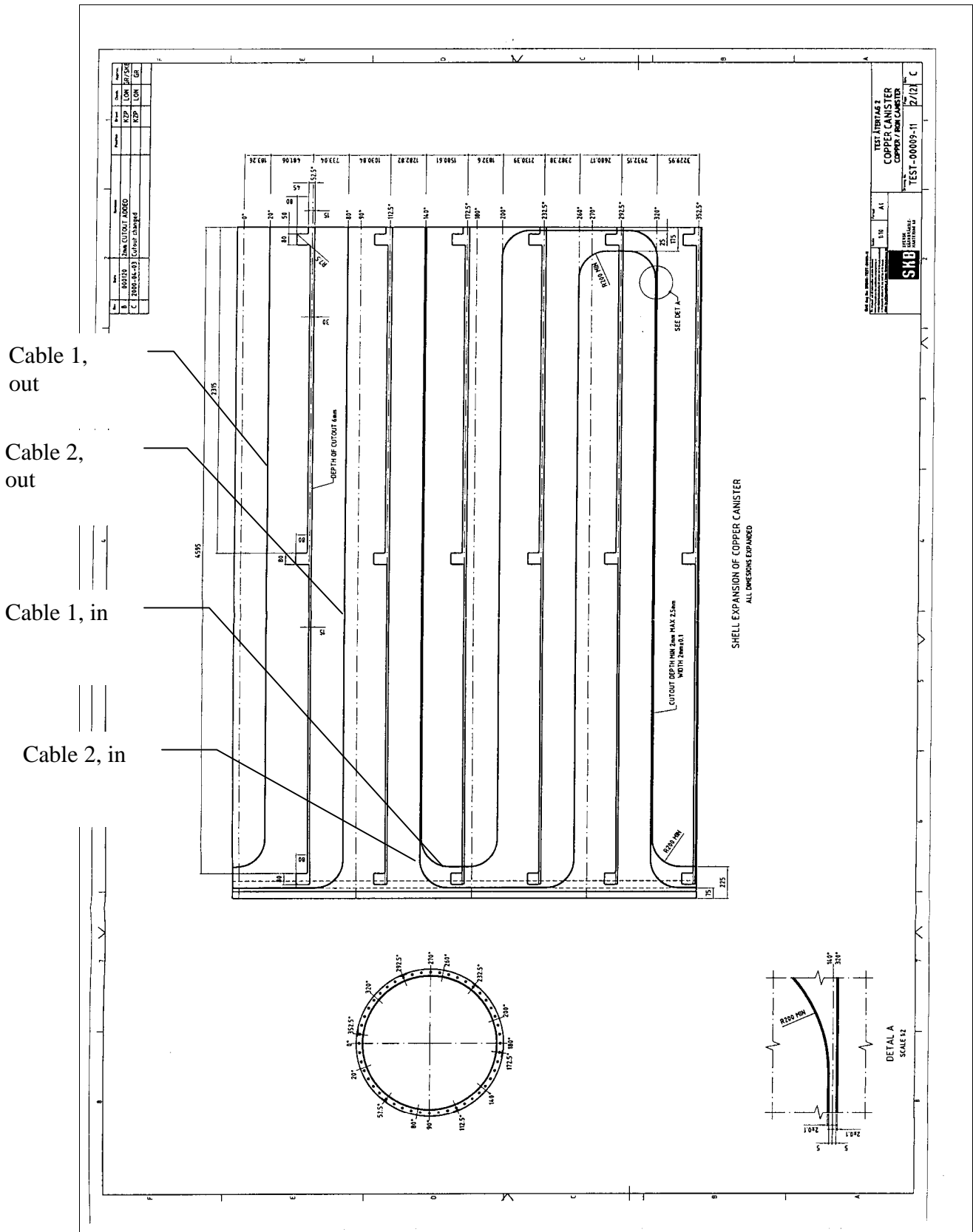
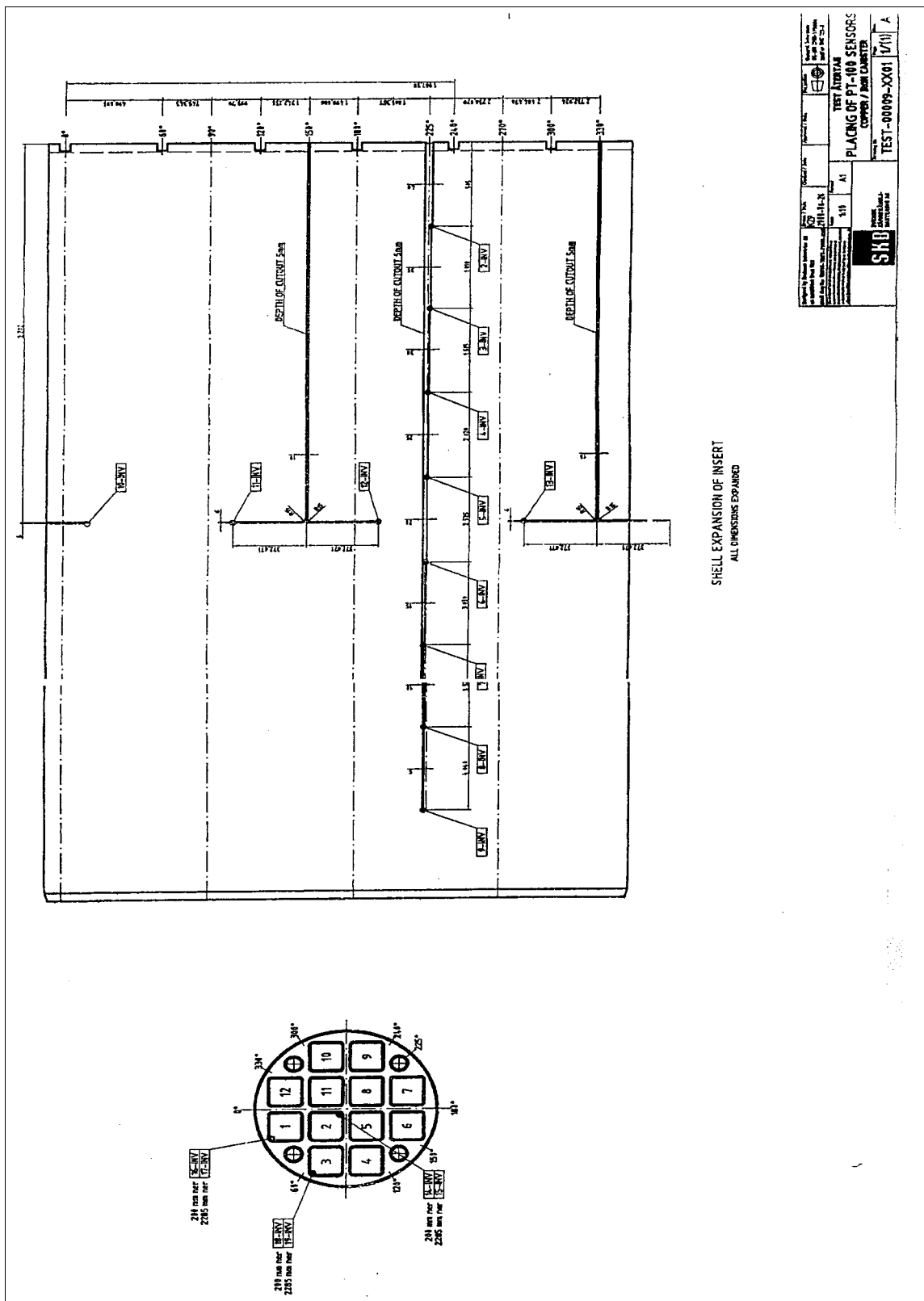


Figure 4-2. Laying of two optical fibre cables with protection tube of Inconel 625 (outer diameter 2 mm) for measurement of the canister surface temperature (surface unfolded).



Figur 4-3. Location of thermocouples inside the canister

4.6 Instruments at the plug

Three force transducers and three displacement transducers have been placed on the plug to measure the force of the anchors and the displacement of the plug. The location of these transducers can be described in relation to Fig 4-4, which shows a schematic view of the plug with the slots, rods and cables.

The rods are numbered 1-9 anti-clockwise and number 1 is assumed to be the northern rod in direction A. The force transducers are placed on rods 3, 6, and 9. The displacement transducers are placed between the rods 5 cm from the rock surface of the hole and according to Table 4-6. They are fixed on the rock surface and measure thus the displacement relative the rock.

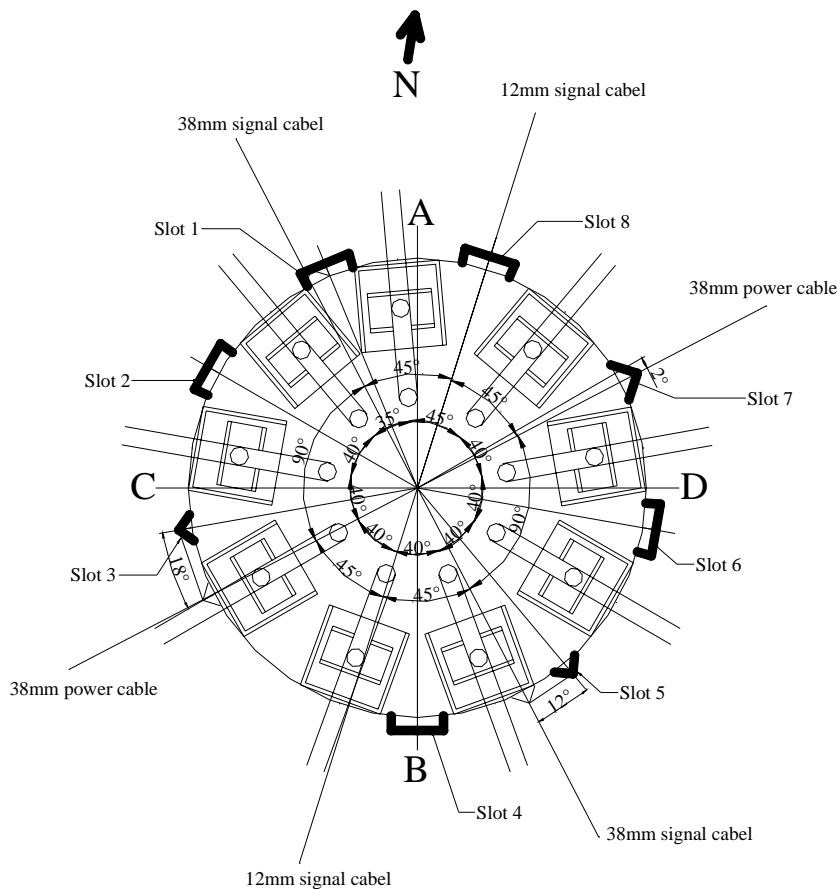


Figure 4-4. Schematic view of the deposition hole, showing the position of the slots, the rods and the cables from the canister.

Table 4-6. Location of displacement transducers

Transducer No.	Located between rods No.
1	4 and 5
2	7 and 8
3	1 and 2

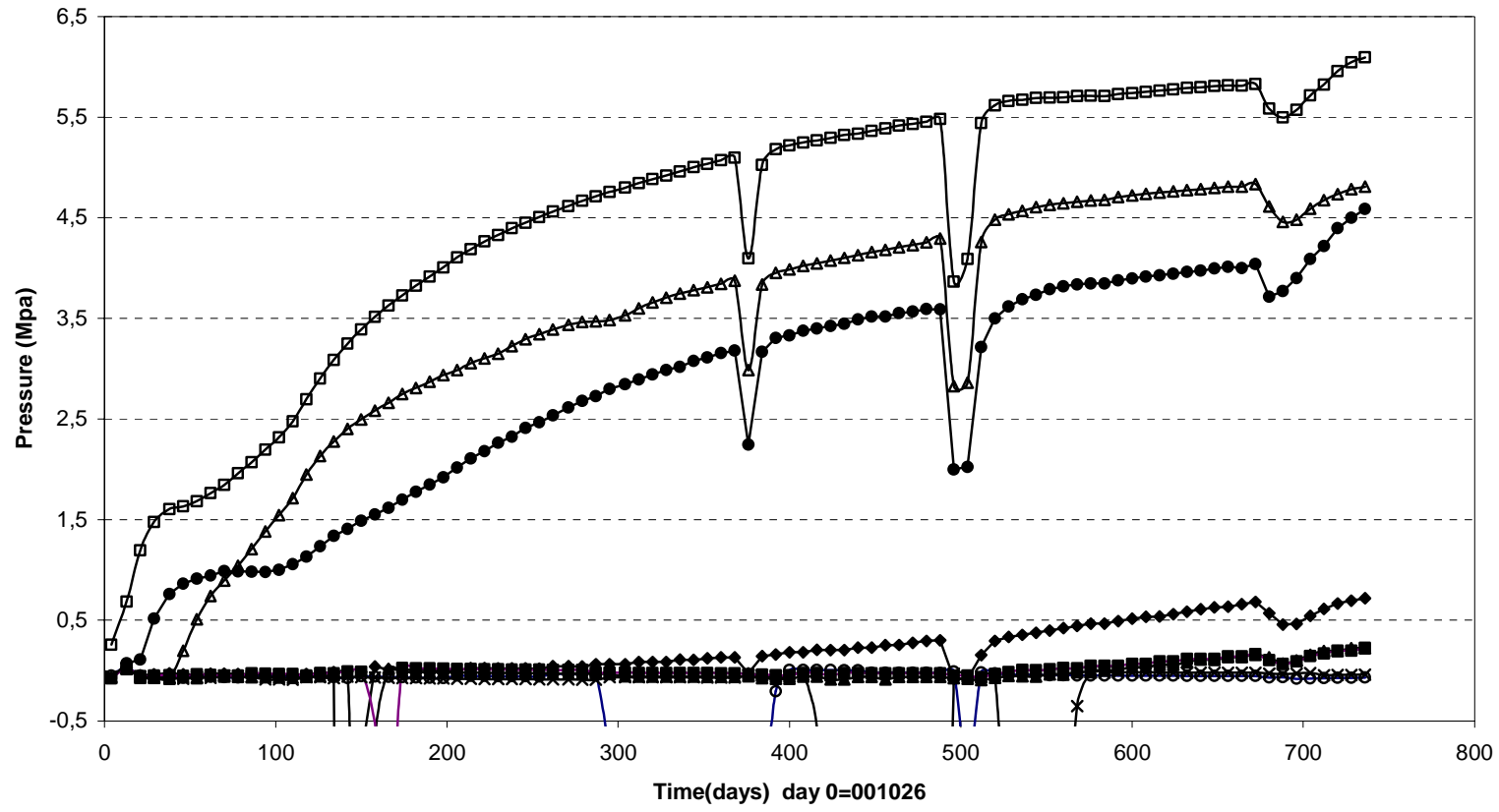
References

/1-1/ **Sanden T, Börgesson L.** Report on instrument positions and preparation of bentonite blocks for instruments and cables May 2000. SKB IPR-00-14

Appendix A

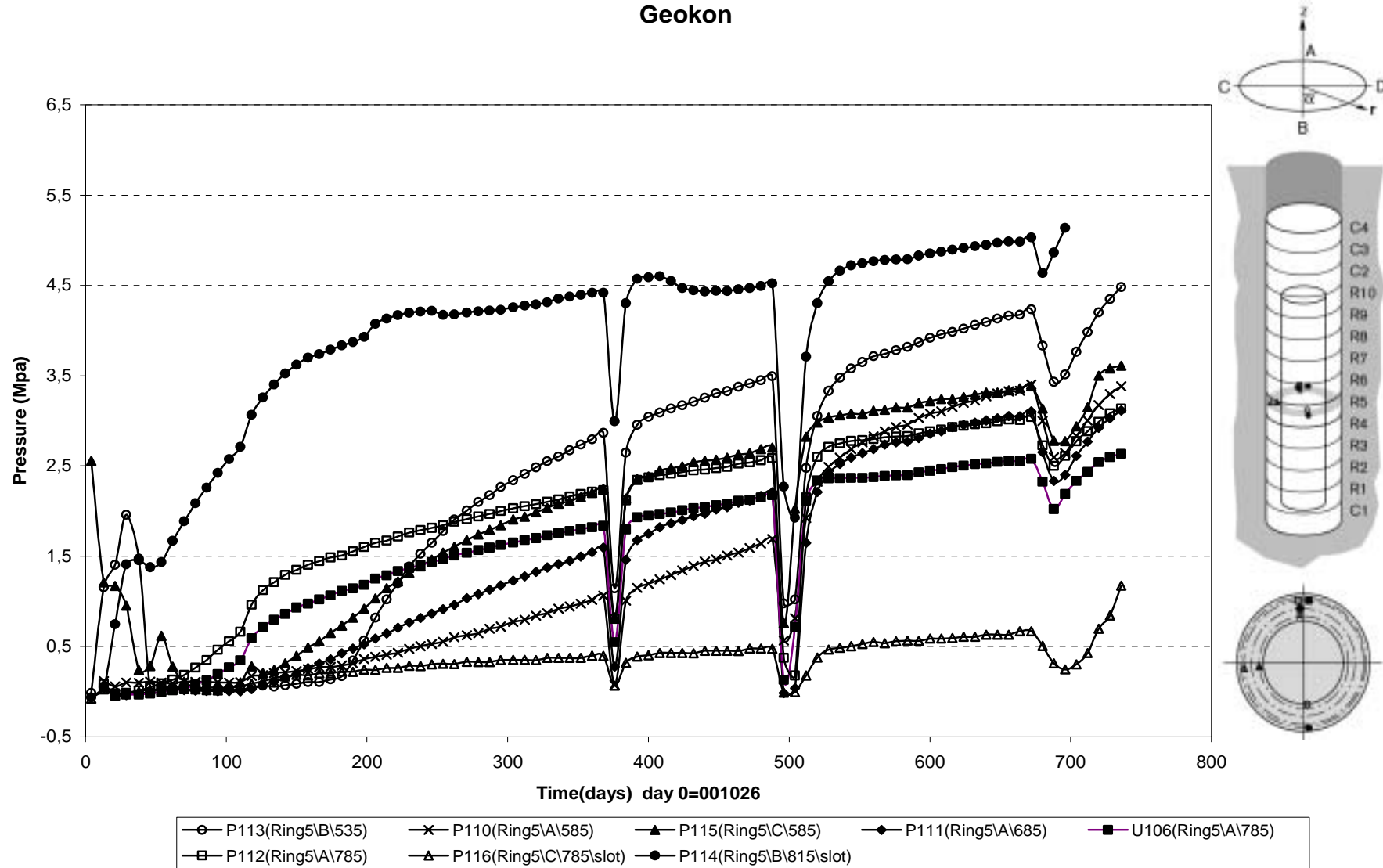
Measured data

Total pressure - Cylinder 1 (001026-021101) Geokon

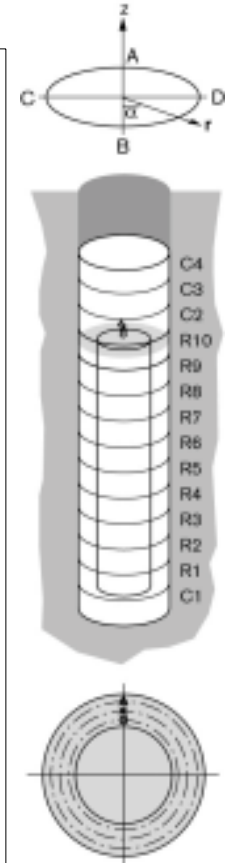
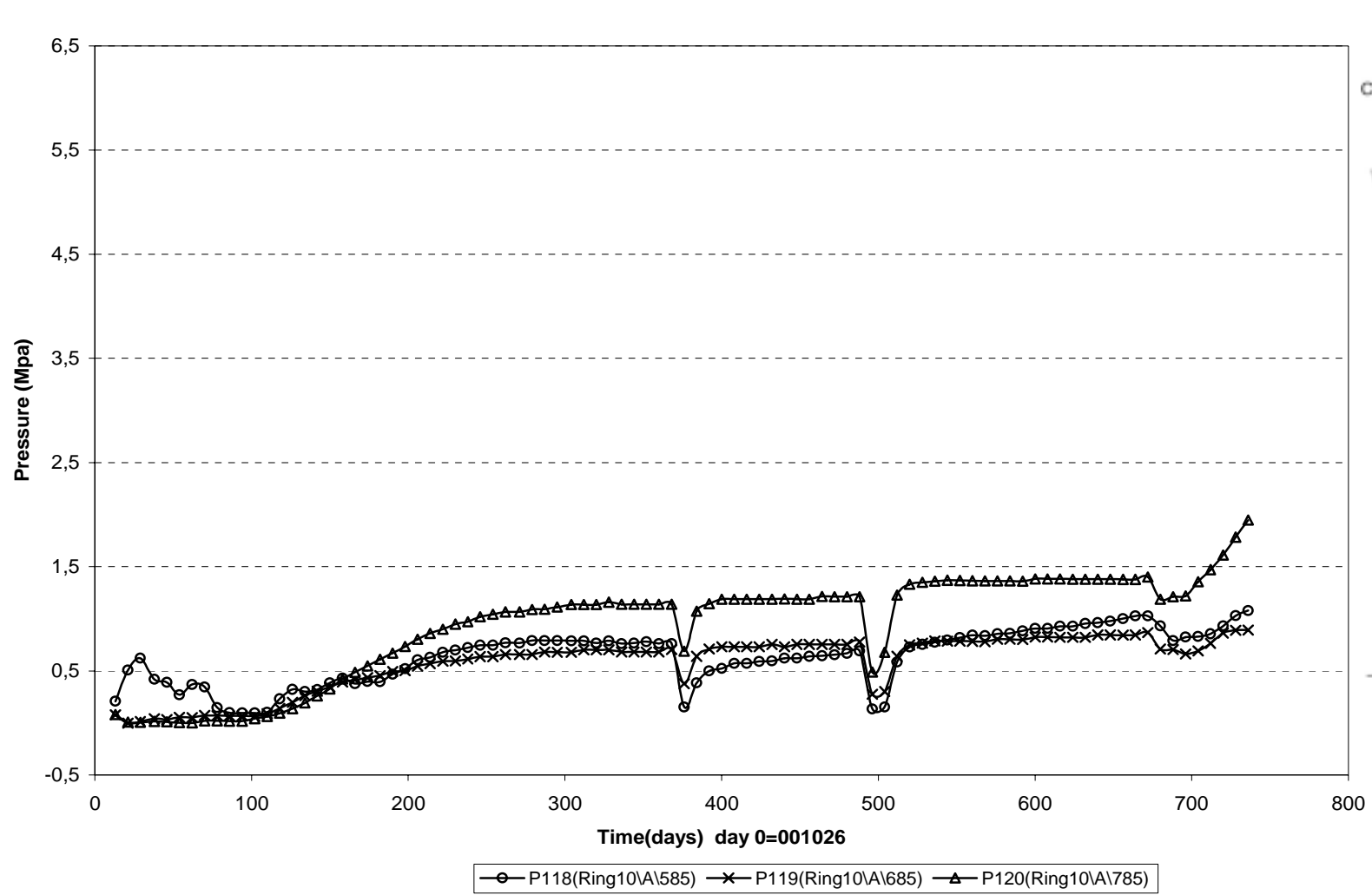


- | | | | | |
|-------------------------|-------------------------|---------------------|---------------------|---------------------|
| ○ P101(Cyl.1\center\50) | × P102(cyl.1\center\50) | ▲ P103(Cyl.1\A\585) | ◆ P106(Cyl.1\B\585) | ■ P108(Cyl.1\C\585) |
| □ P105(Cyl1\A\785) | △ P107(Cyl.1\B\785) | ● P109(Cyl1\C\785) | | |

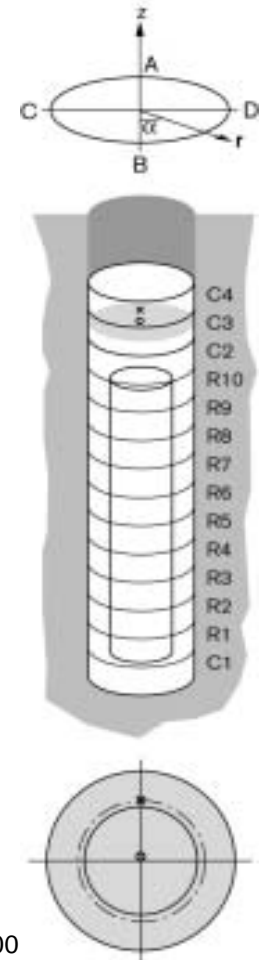
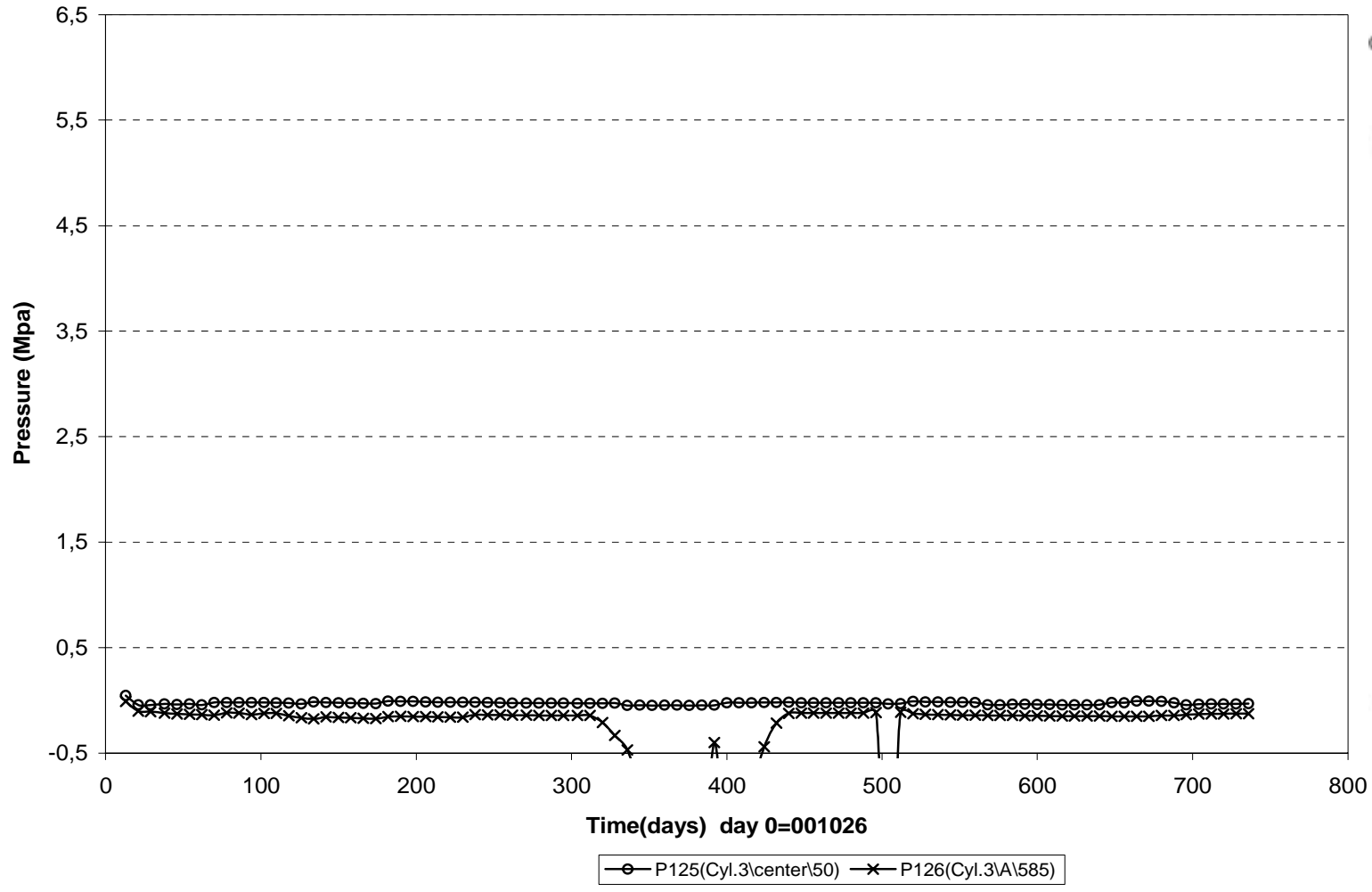
Total pressure - Ring 5 (001026-021101) Geokon



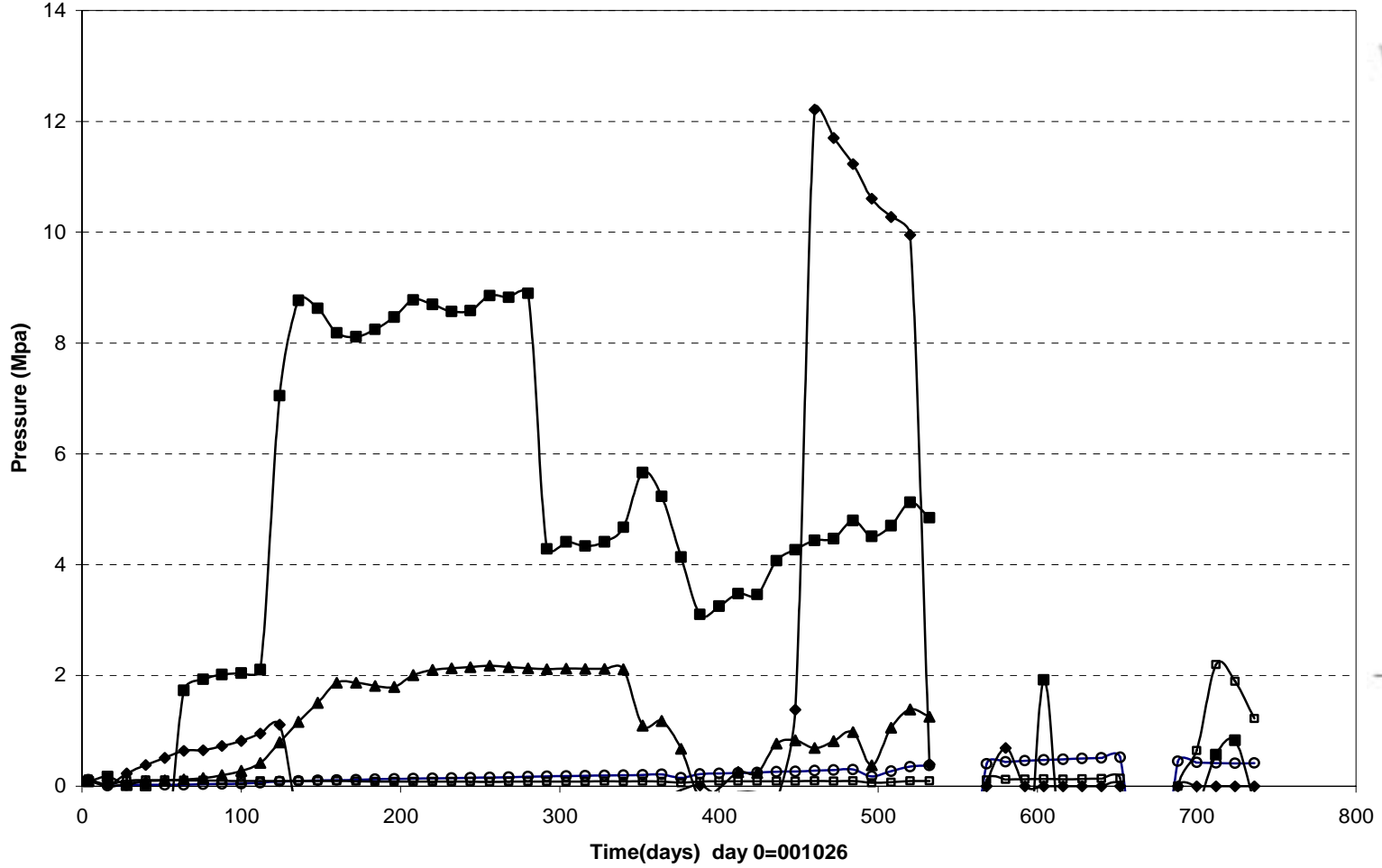
Total pressure - Ring 10 (001026-021101) Geokon



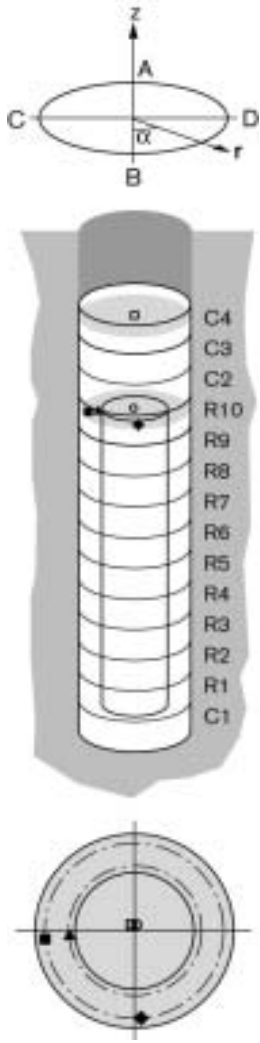
**Total pressure - Cylinder 3 (001026-021101)
Geokon**



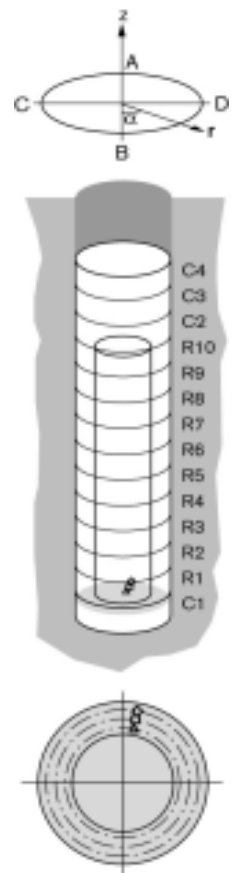
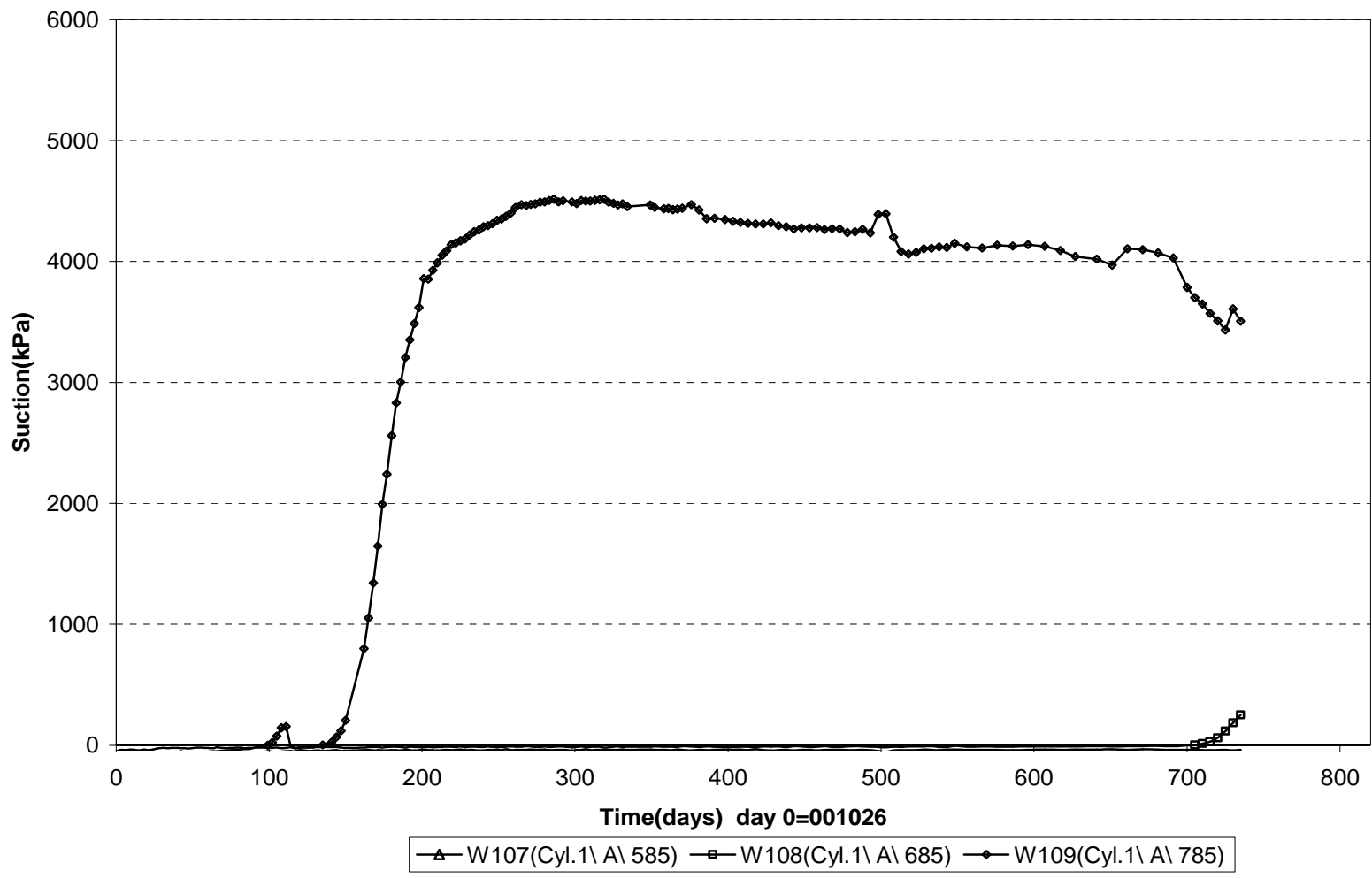
**Total pressure - Ring 10 (001026-021101)
Kulite**



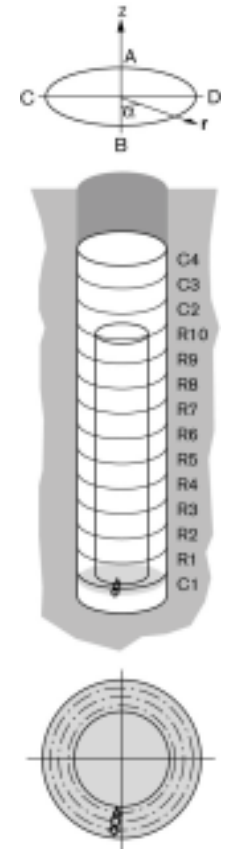
—○— P217(Ring10-center-50) —▲— P223(Ring10-C-585) —◆— P222(Ring10-B-785) —■— P224(Ring10-C-785) —■— P227(Cyl.4-center-50)



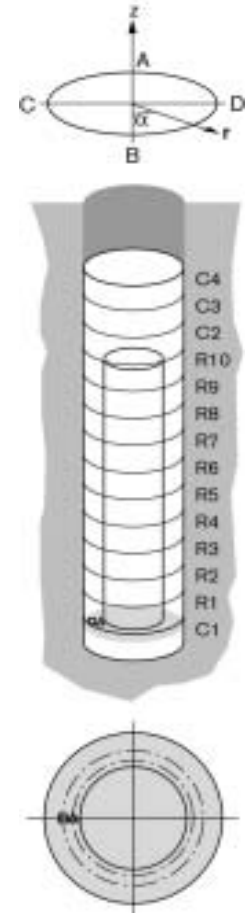
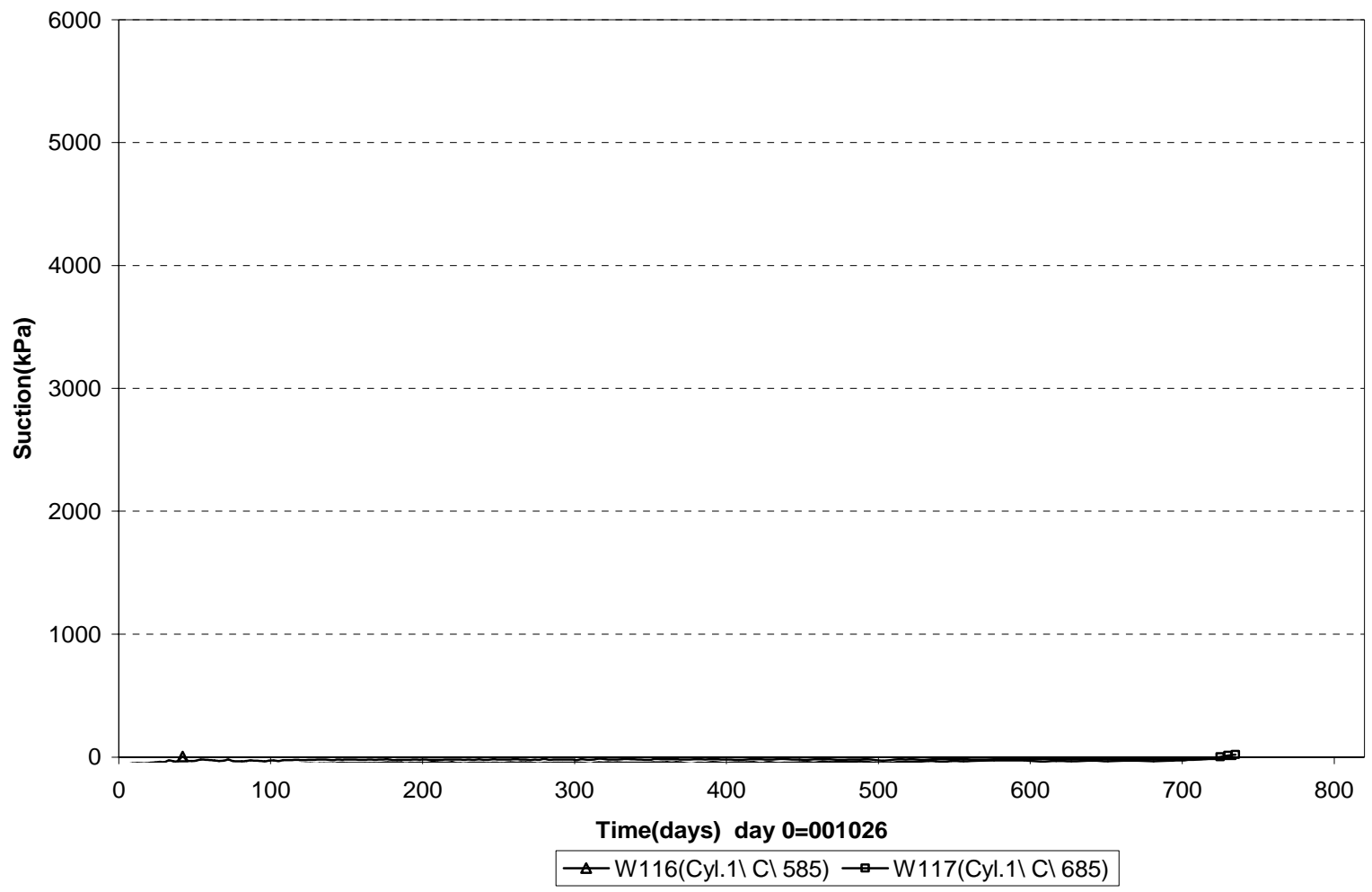
Suction in the buffer - Cyl.1 (001026-021101)
Wescor



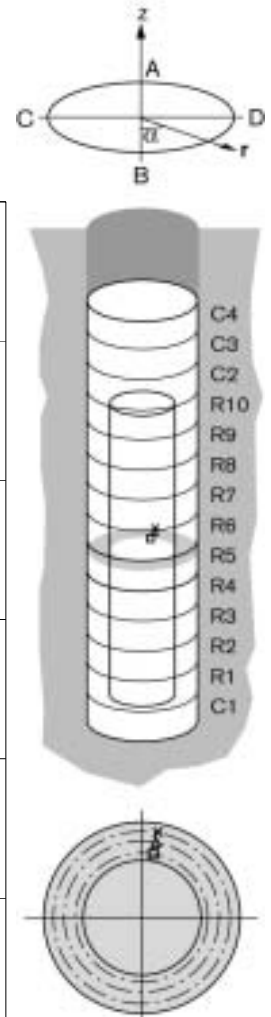
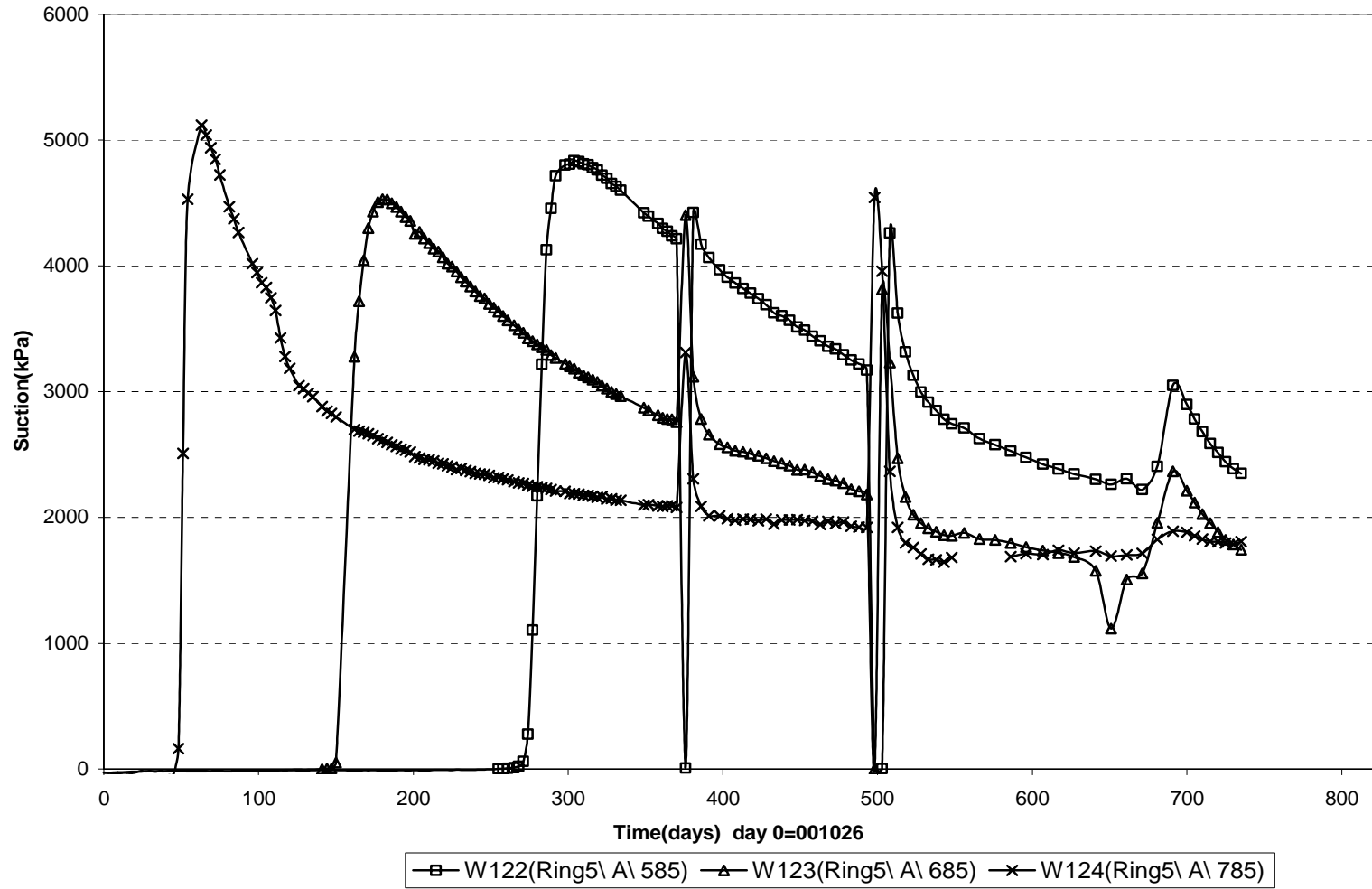
Suction in the buffer - Cyl.1 (001026-021101)
Wescor



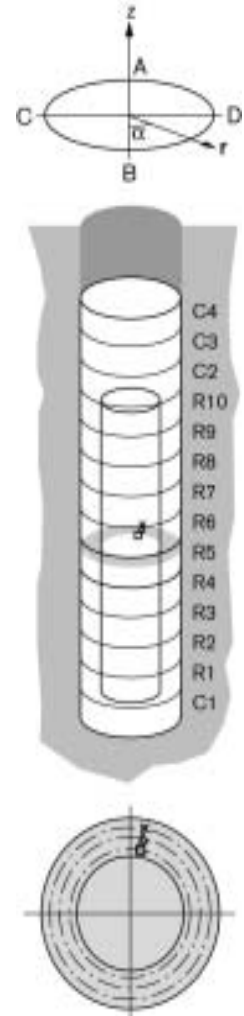
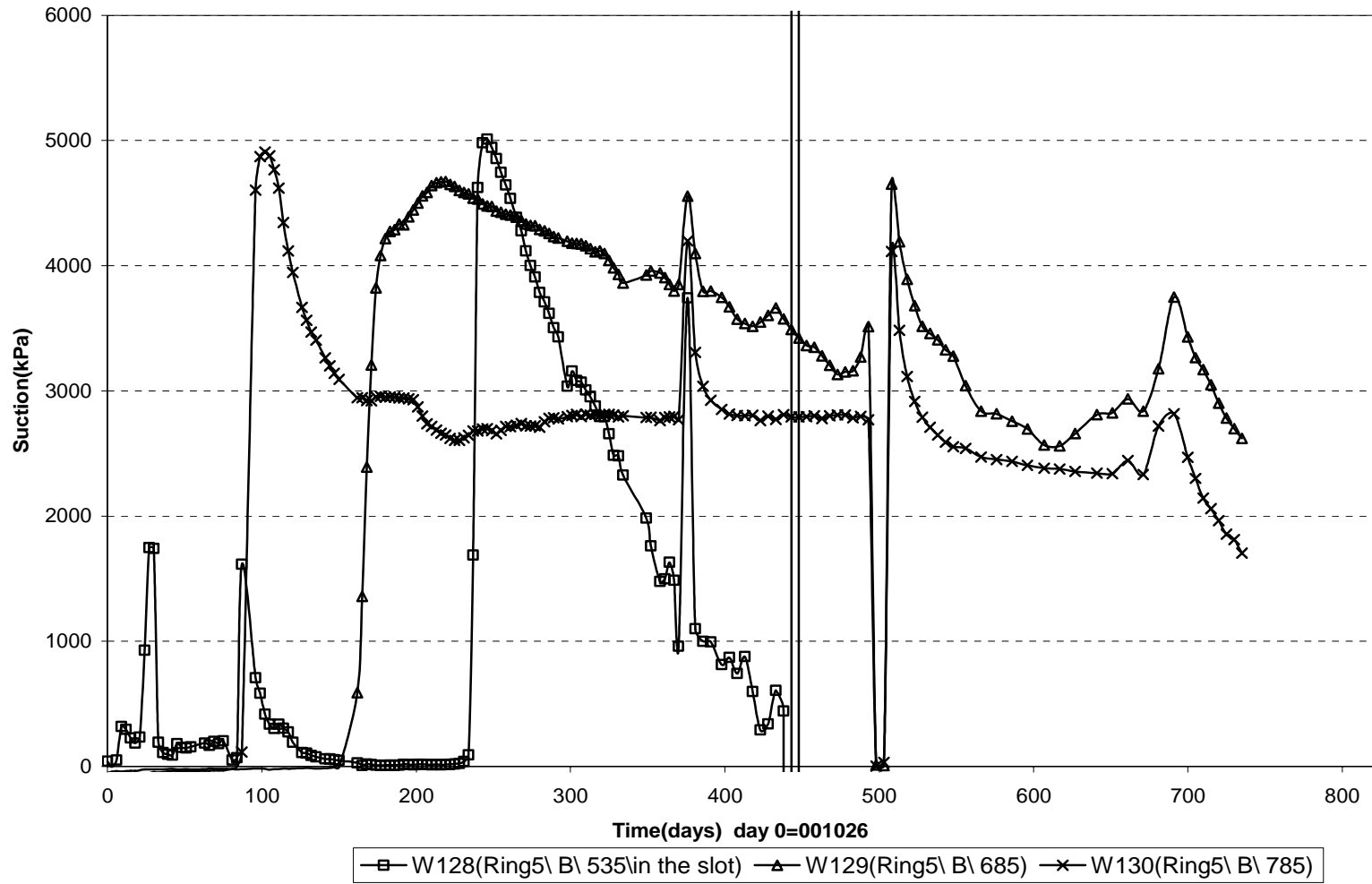
Suction in the buffer - Cyl.1 (001026-021101)
Wescor



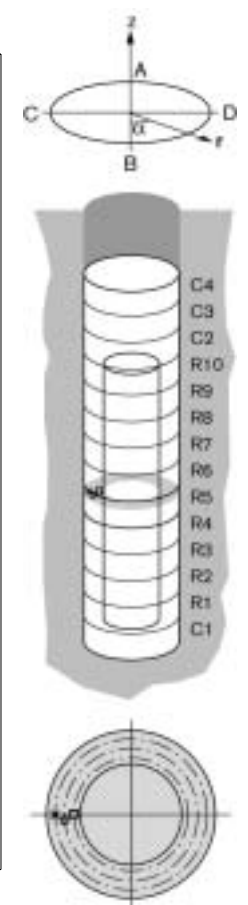
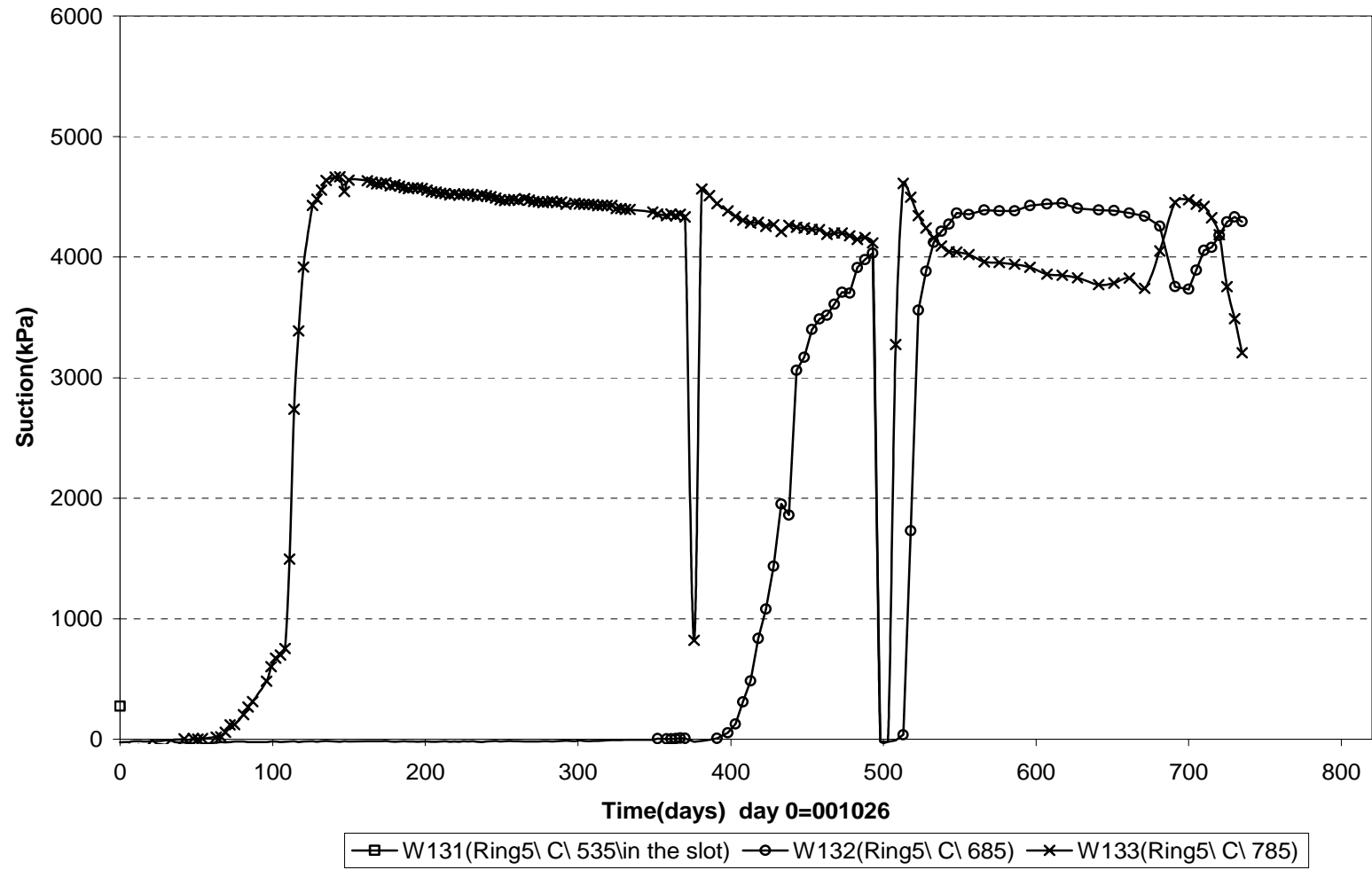
Suction in the buffer - Ring 5 (001026-021101)
Wescor



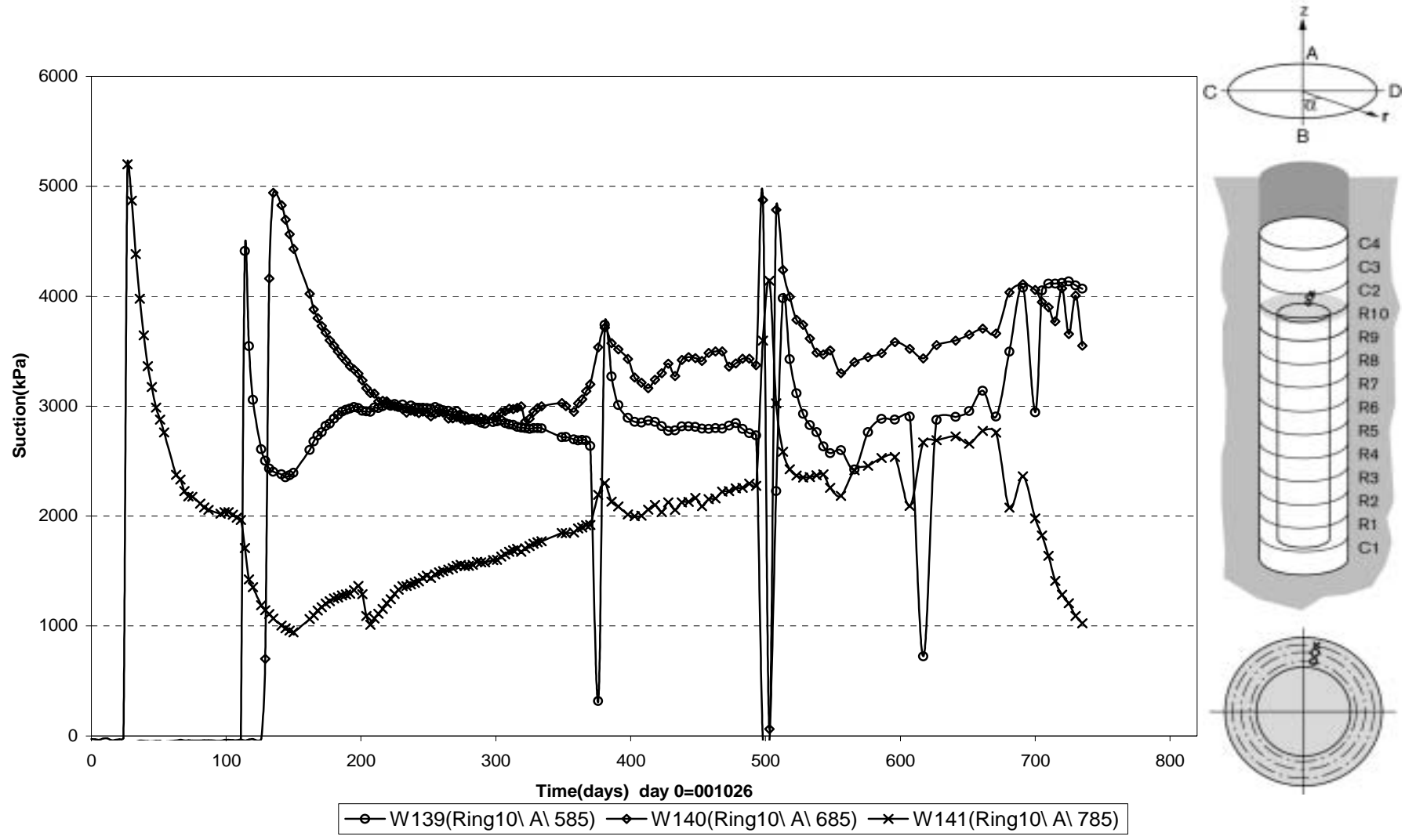
Suction in the buffer - Ring 5 (001026-021101)
Wescor



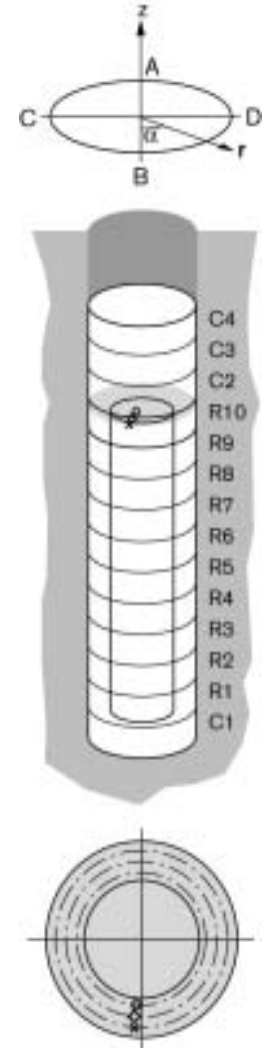
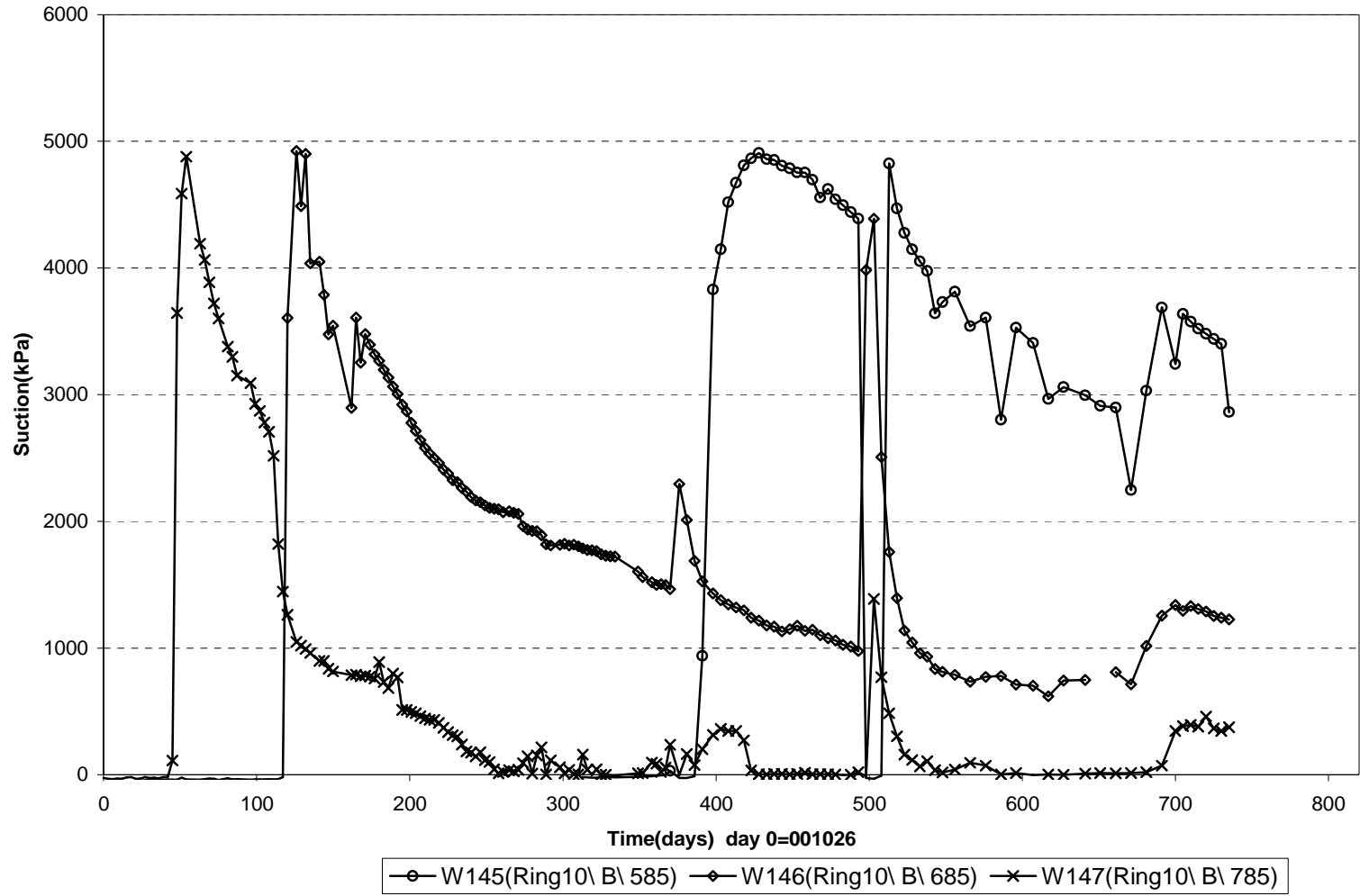
Suction in the buffer - Ring 5 (001026-021101)
Wescor



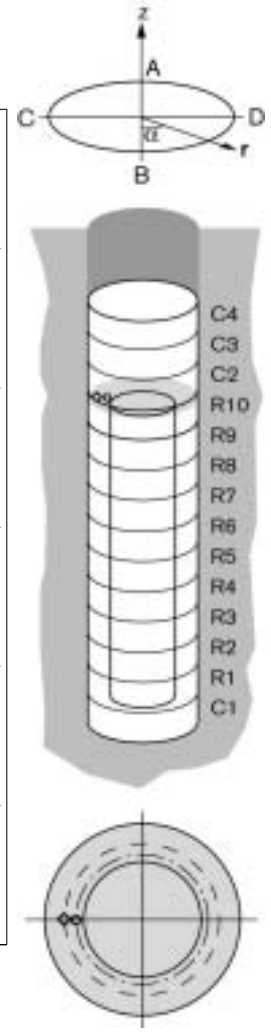
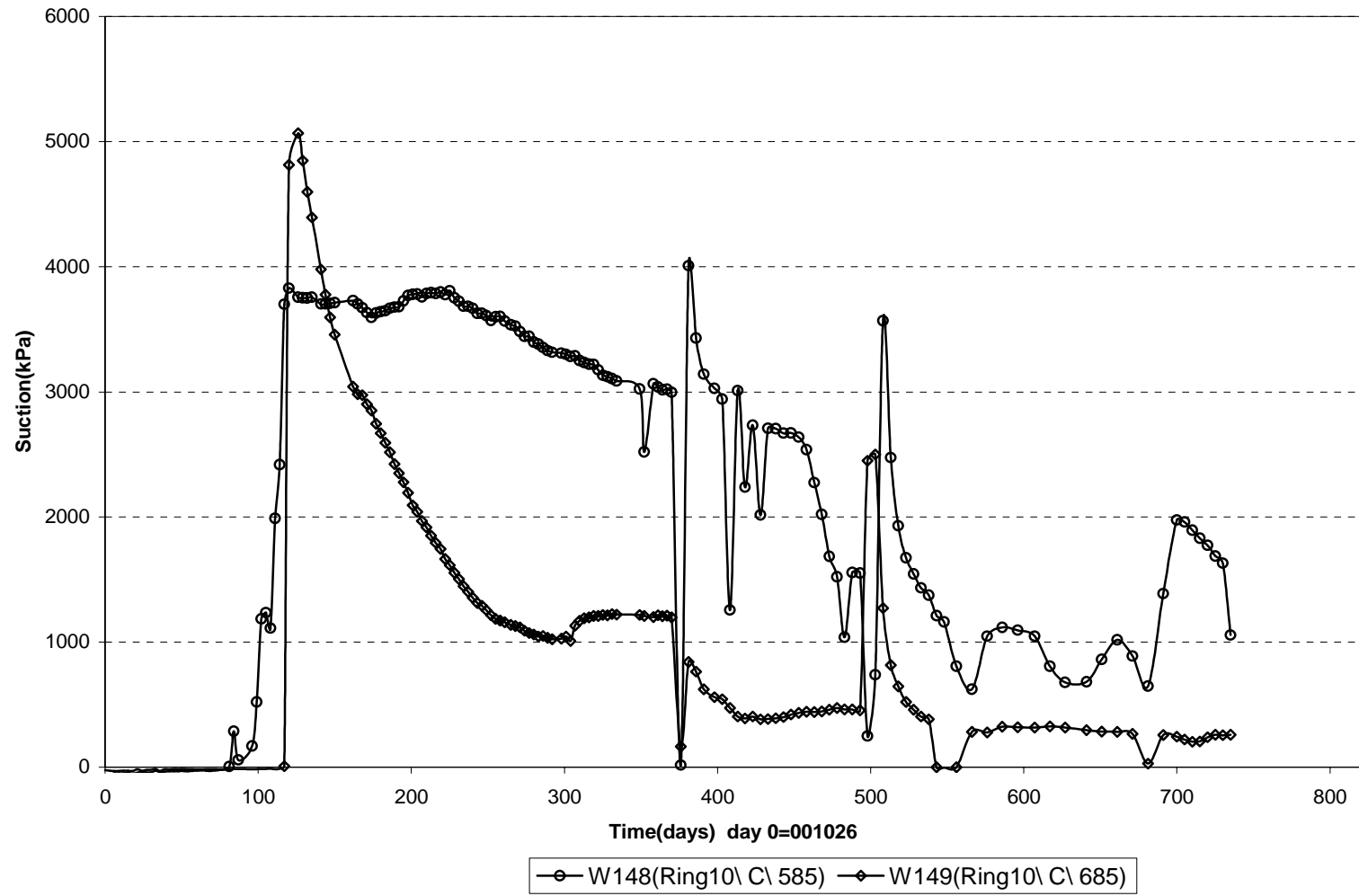
Suction in the buffer - Ring 10 (001026-021101)
Wescor



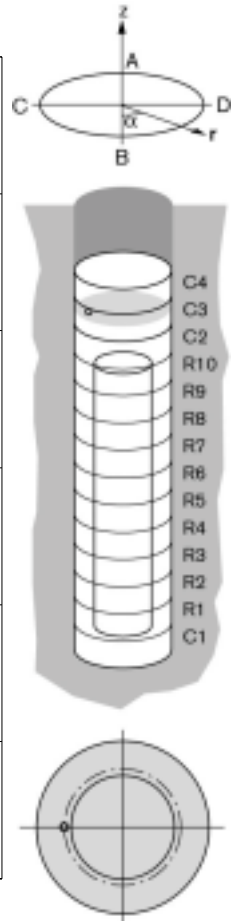
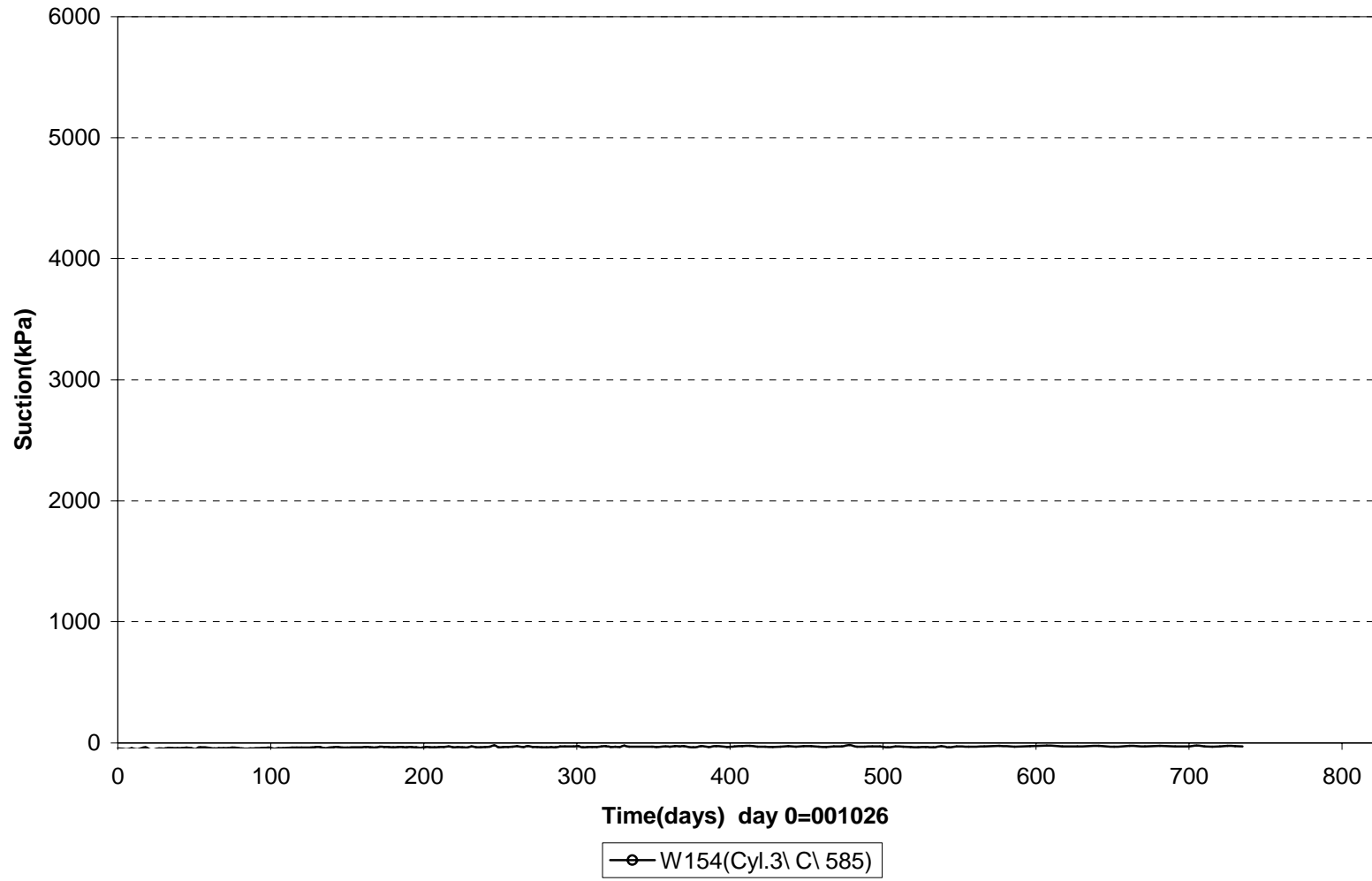
Suction in the buffer - Ring 10 (001026-021101)
Wescor



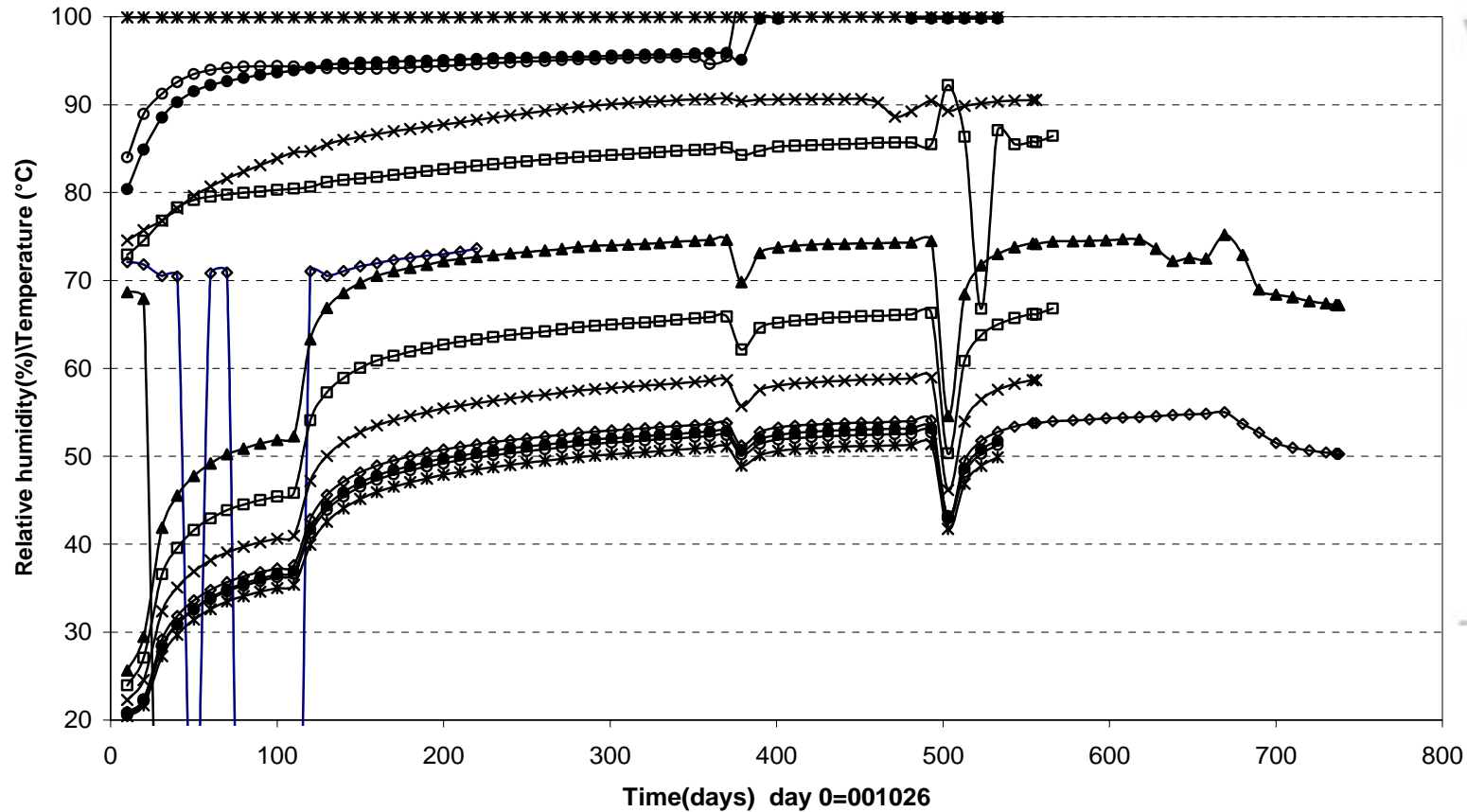
Suction in the buffer - Ring 10 (001026-021101)
Wescor



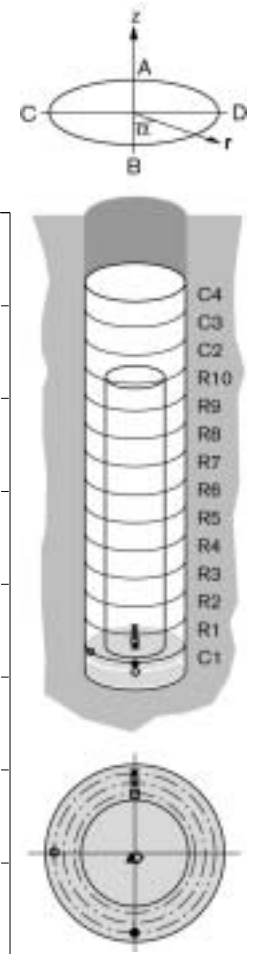
Suction in the buffer - Cyl.3 (001026-021101)
Wescor



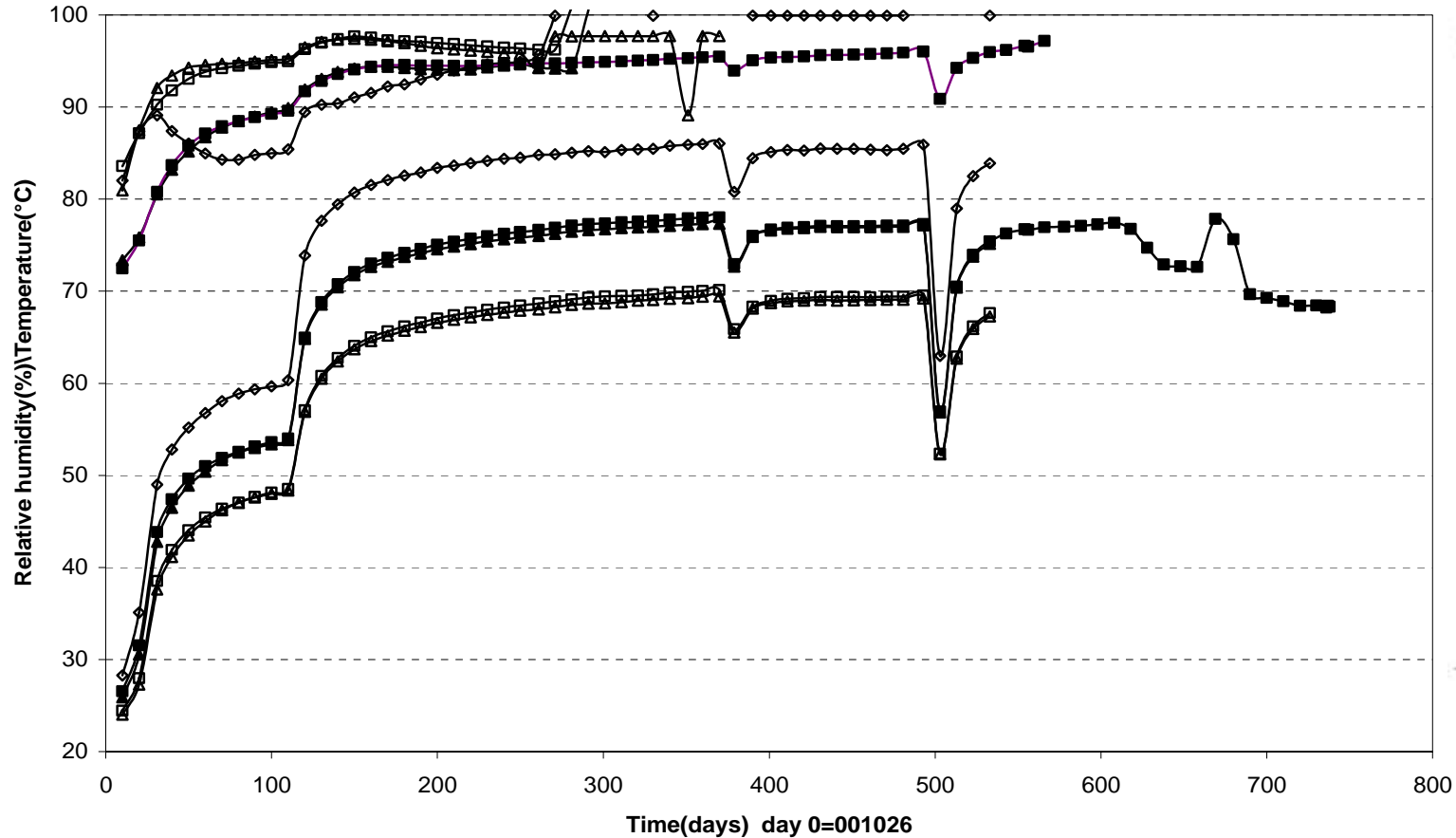
Relative humidity - Cylinder 1 (001026-021101) Vaisala



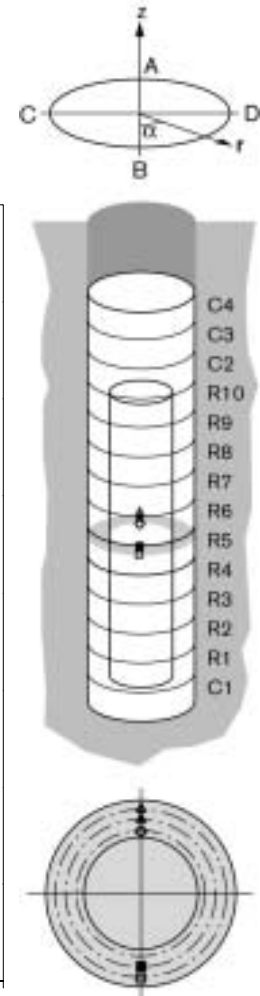
◆ W101(Cyl.1\Center\50)	◇ W101T	▲ W103(Cyl.1\Center\50)	▲ W103T
■ W104(Cyl.1\A\585)	■ W104T	× W105(Cyl.1\A\685)	× W105T
* W106(Cyl.1\A\785)	* W106T	● W111(Cyl.1\B\785)	● W111T
○ W118(Cyl.1\C\785)	○ W118T		



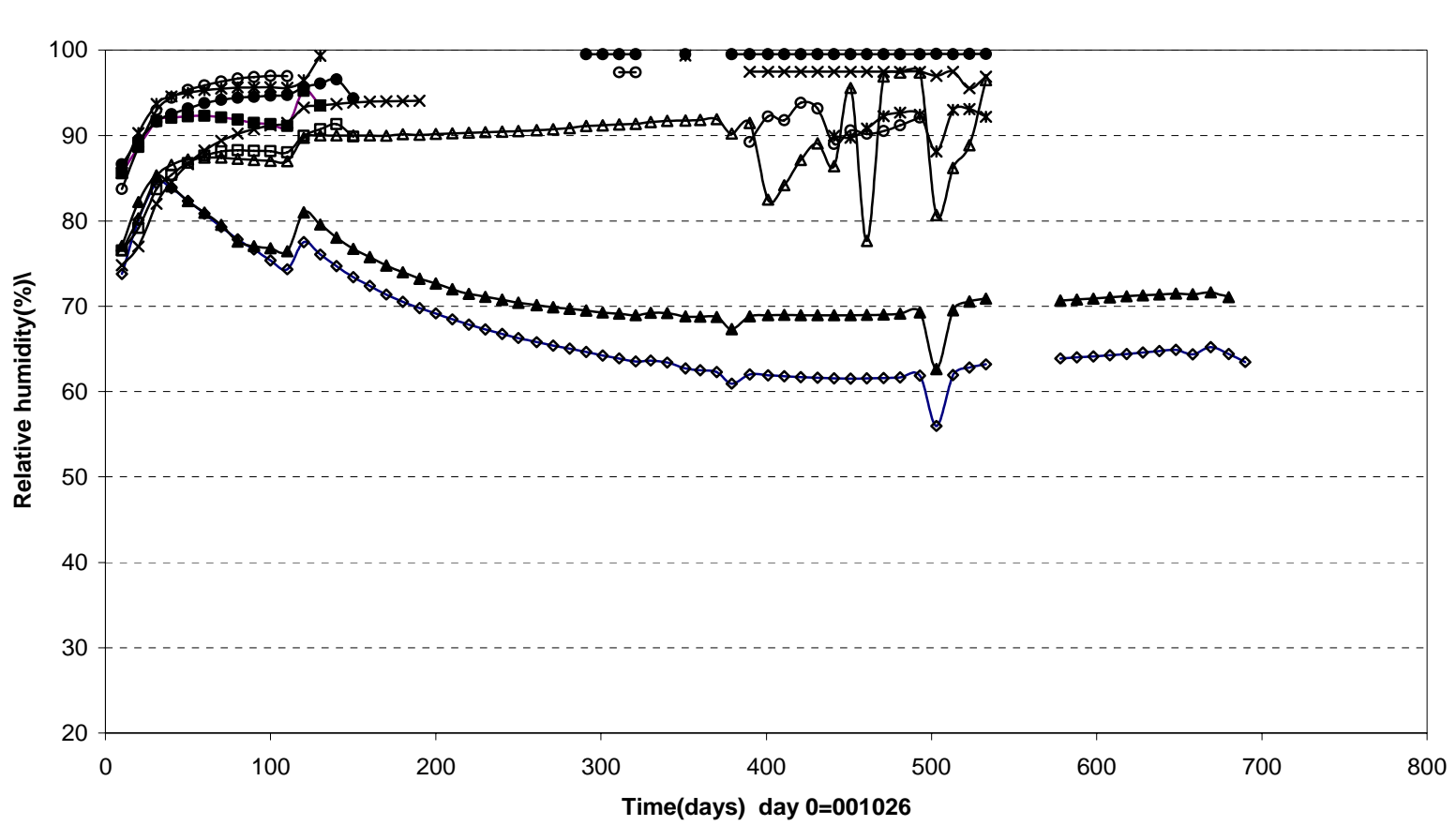
Relative humidity- Ring 5 (001026-021101)
Vaisala



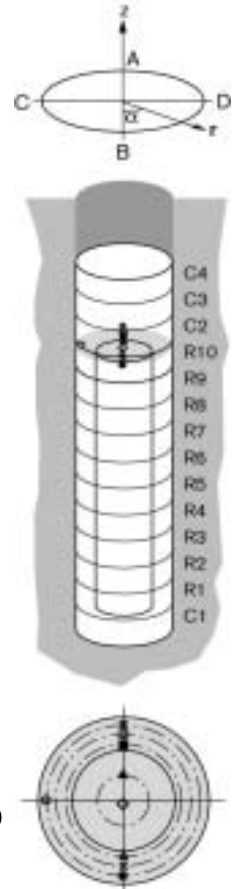
- | | | | |
|---------------------|---------|---------------------|---------|
| ◇ W119(Ring5\A\585) | ◇ W119T | ▲ W120Ring5\A\685) | ▲ W120T |
| ■ W126(Ring5\B\685) | ■ W126T | ▲ W121(Ring5\A\785) | ▲ W121T |
| □ W127(Ring5\B\785) | □ W127T | | |



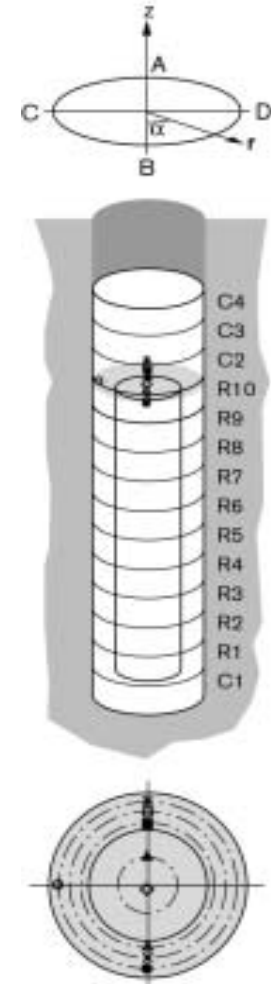
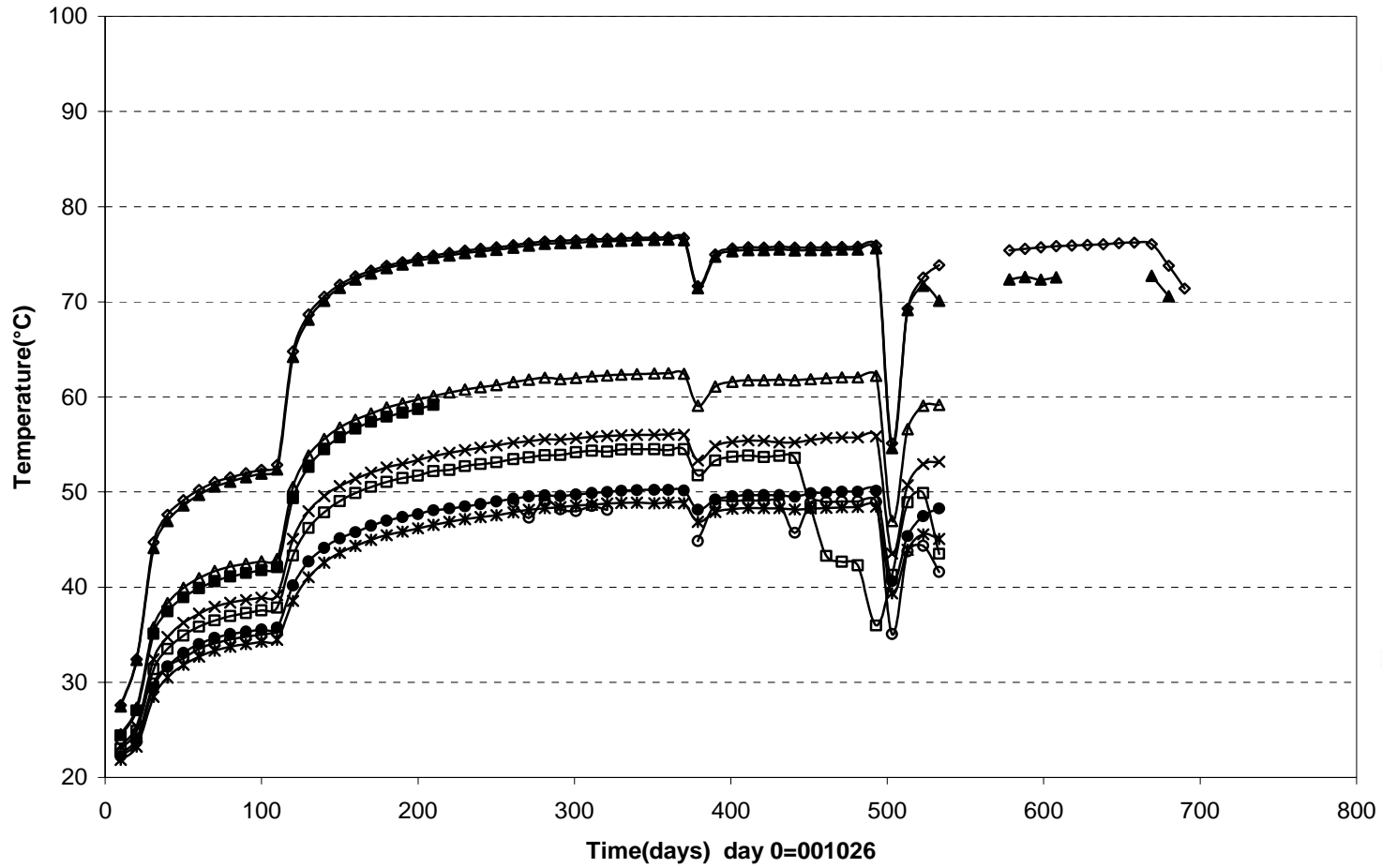
Relative humidity - Ring 10 (001026-021101) Vaisala



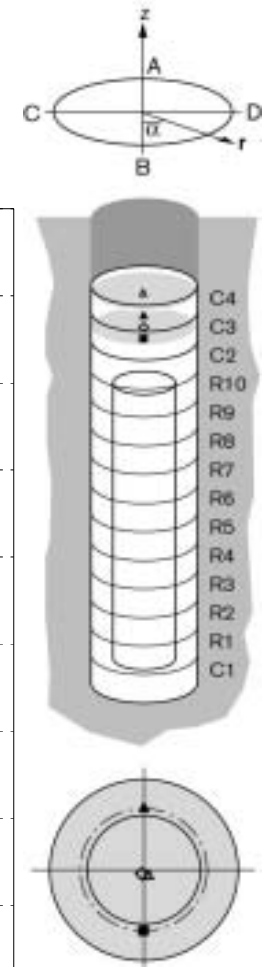
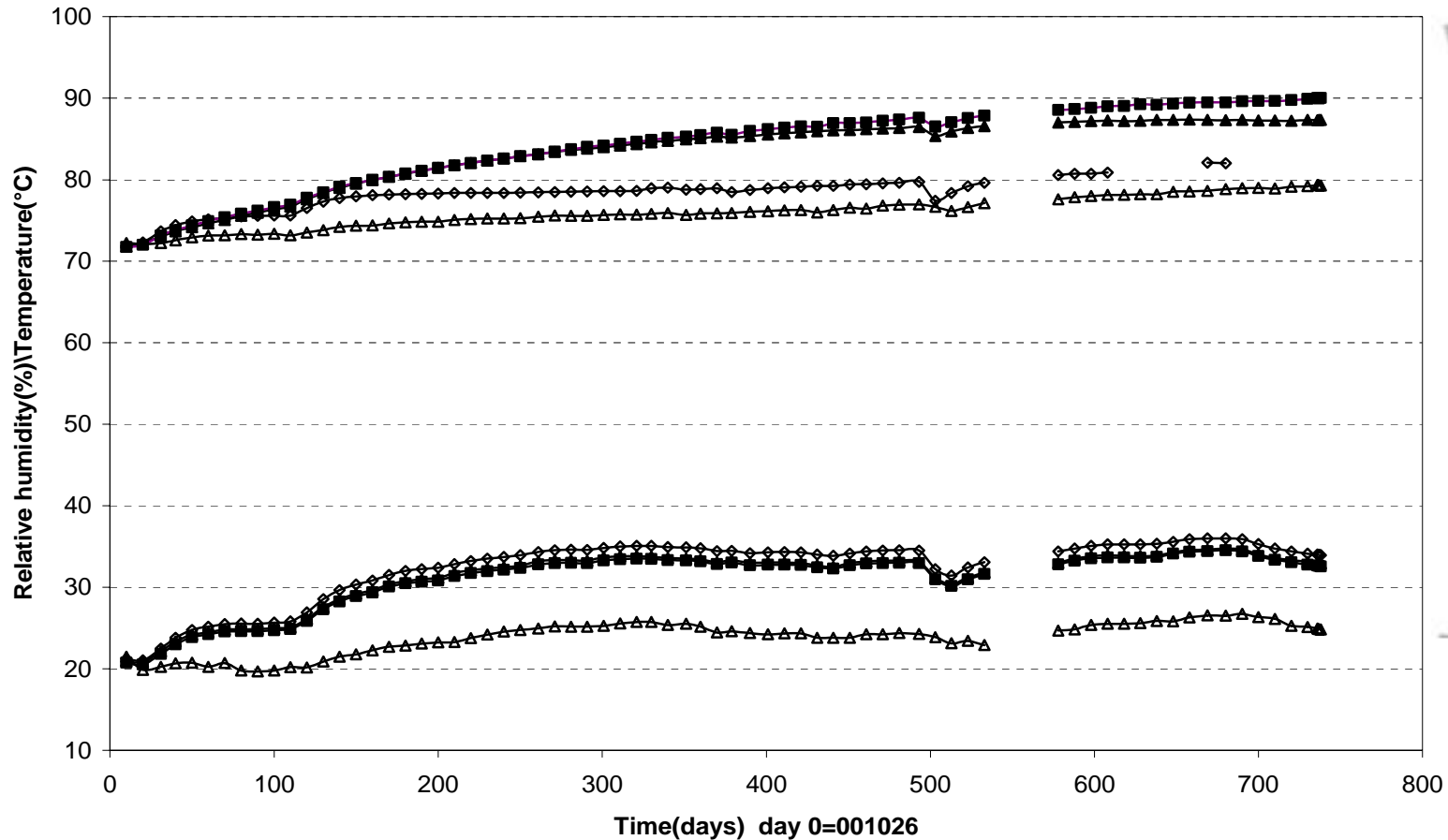
◆ W134(Ring.10\center\50)	▲ W135(Ring.10\A\262)	■ W136(Ring.10\A\585)
▲ W142(Ring.10\B\585)	◻ W137(Ring.10\A\685)	✕ W143(Ring.10\B\685)
✱ W138(Ring.10\A\785)	● W144(Ring.10\B\785)	○ W150(Ring.10\C\785)



Relative humidity - Ring 10 (001026-021101)
Vaisala

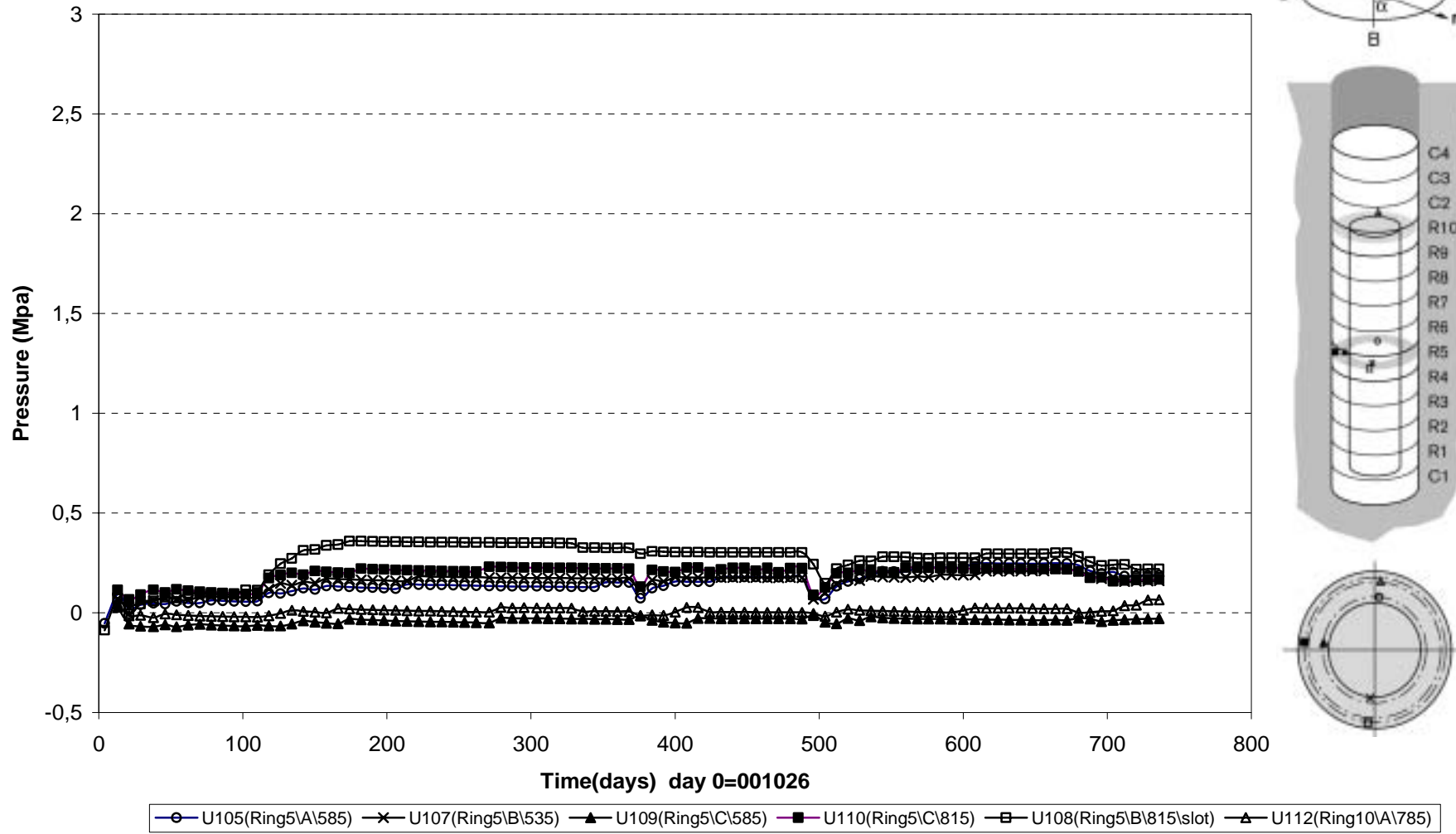


Relative humidity - Cylinder 3 and Cylinder 4 (001026-021101) Vaisala

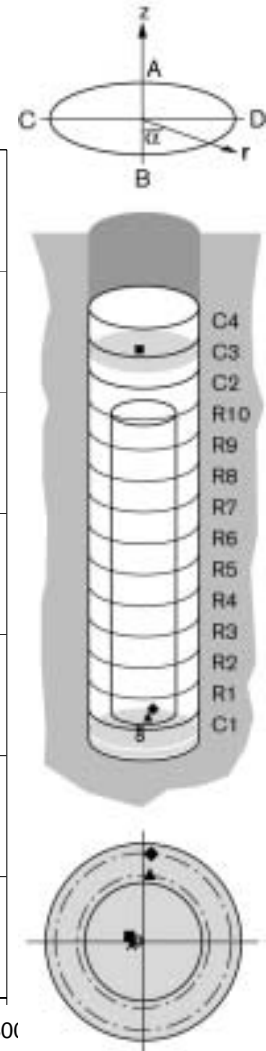
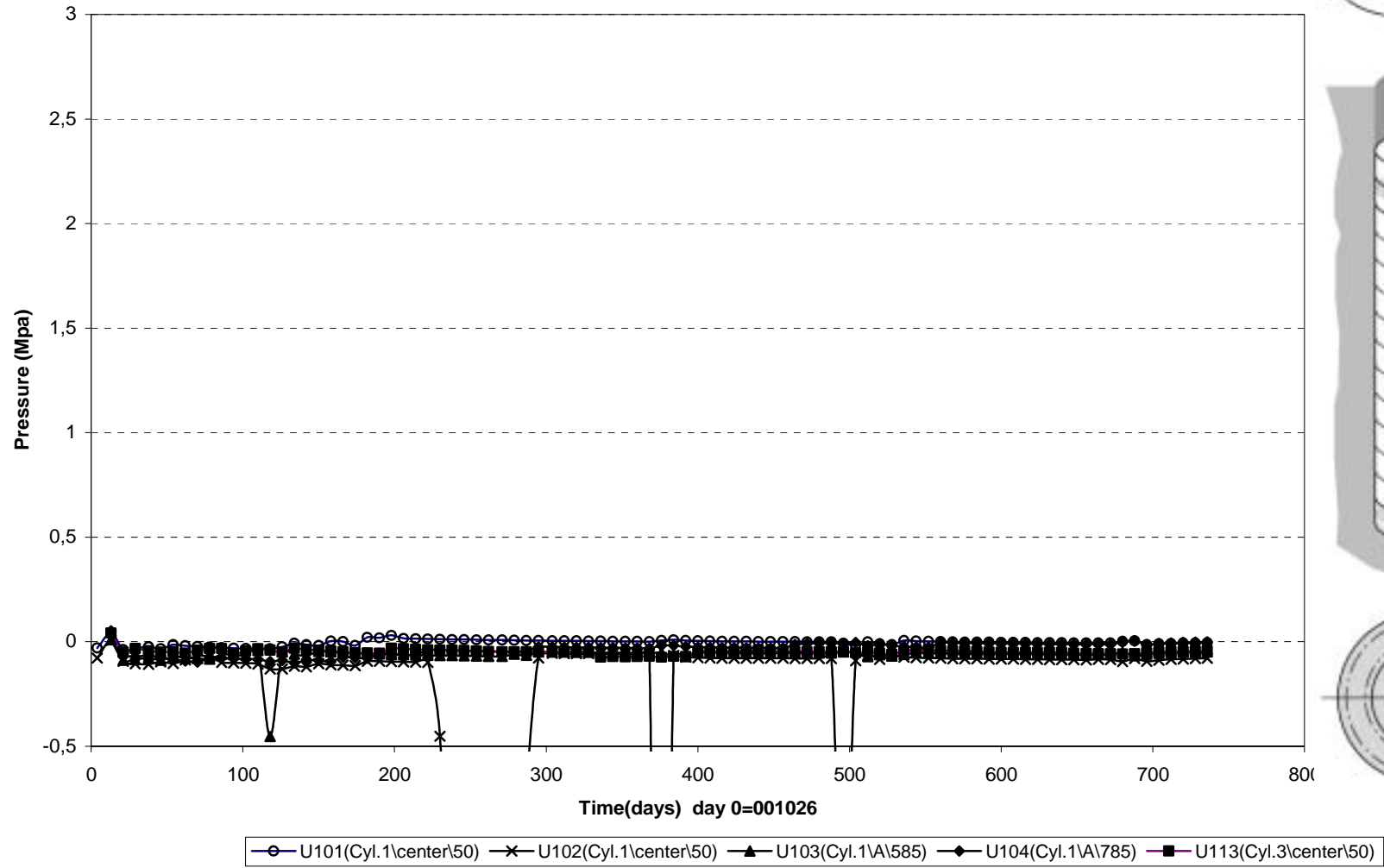


◆ W151(Cyl.3\Center\50)	◆ W151T	▲ W152(Cyl.3\A\585)	▲ W152T
■ W153(Cyl.3\C\585)	■ W153T	▲ W155(Cyl.4\center\50)	▲ W155T

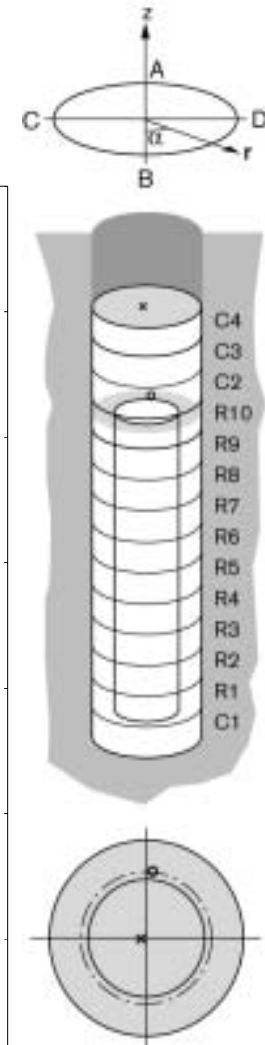
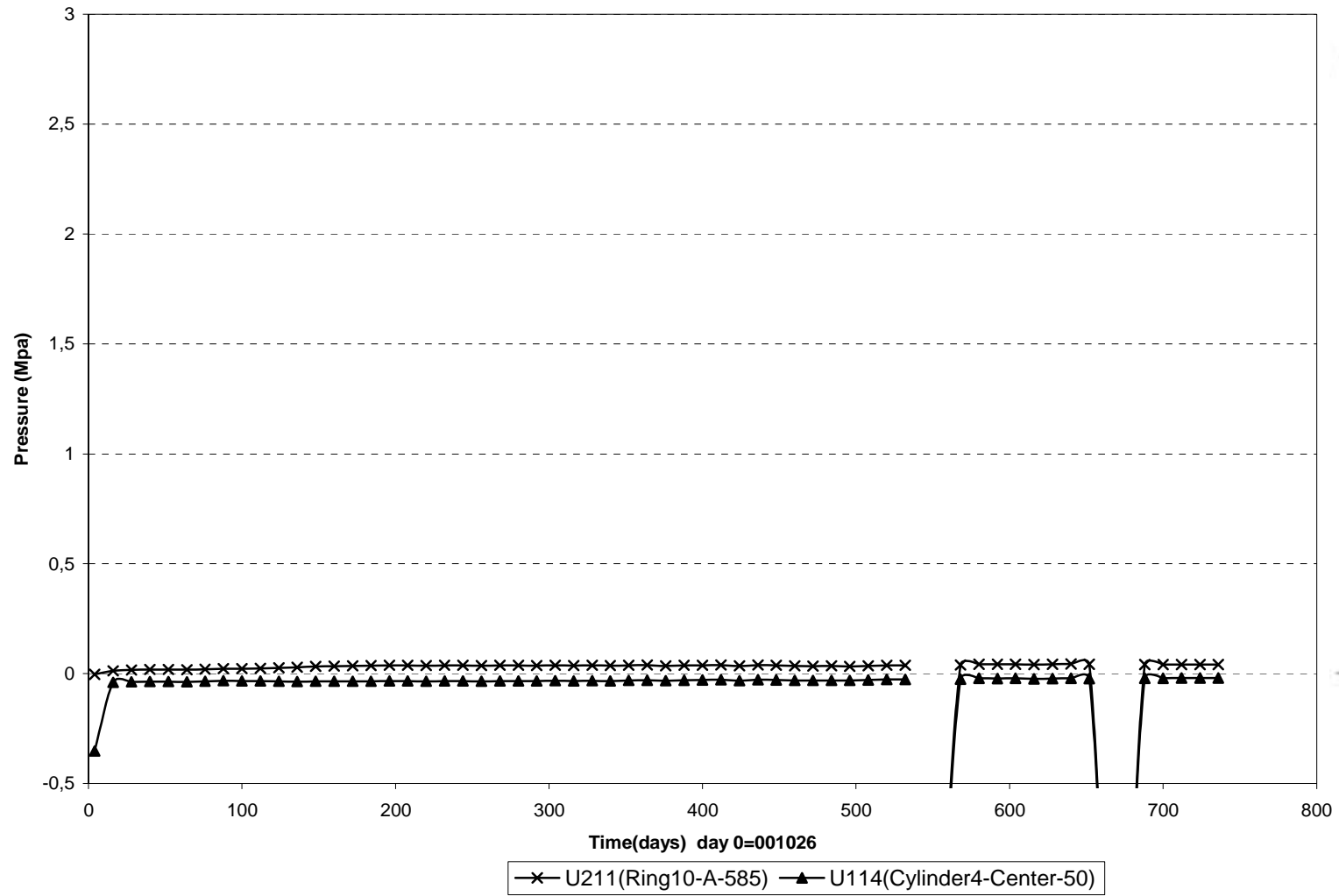
Pore water pressure - Ring 5 and Ring 10 (001026-021101)
Geokon



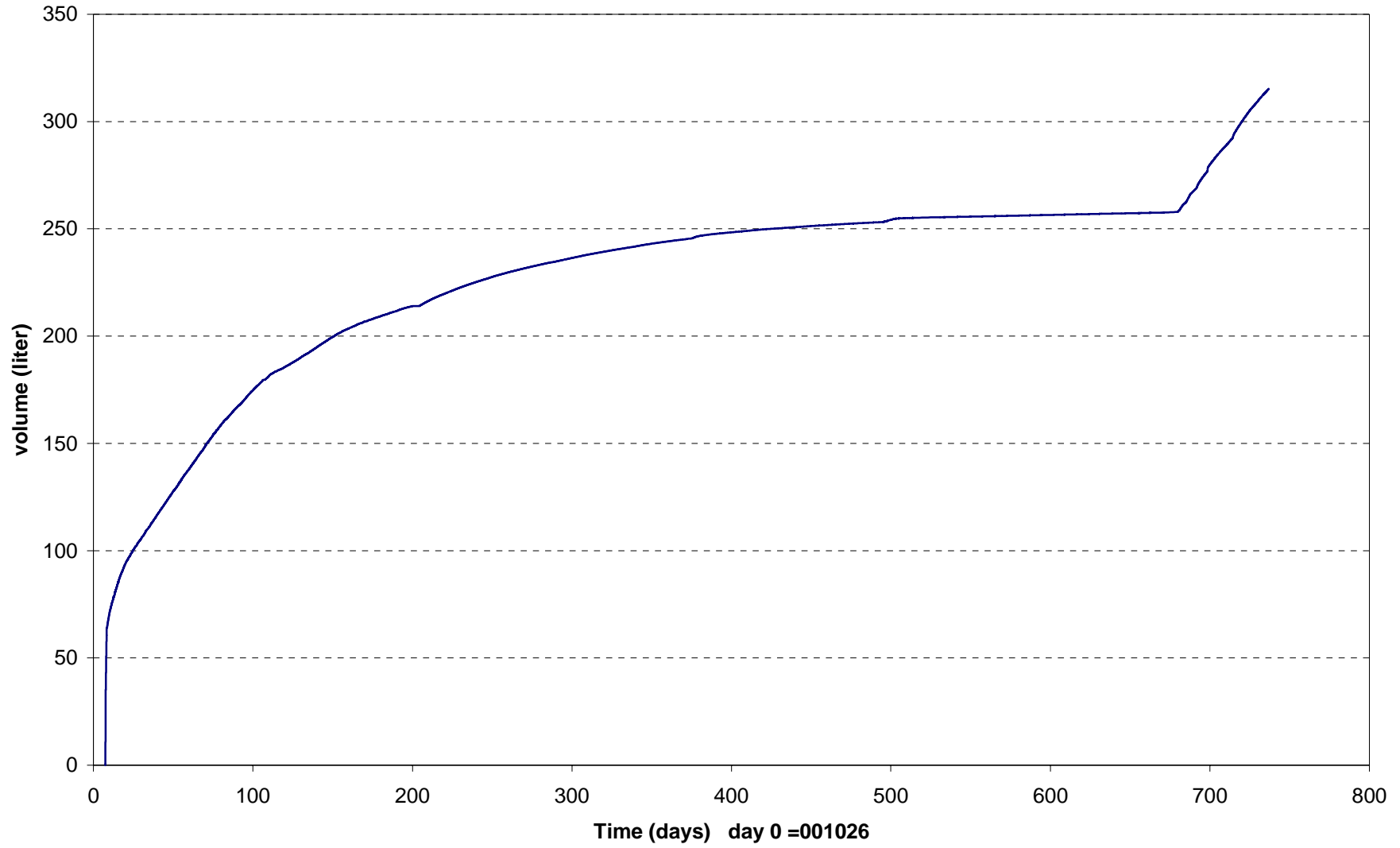
Pore water pressure - Cylinder 1 and Cylinder 3 (001026-021101) Geokon



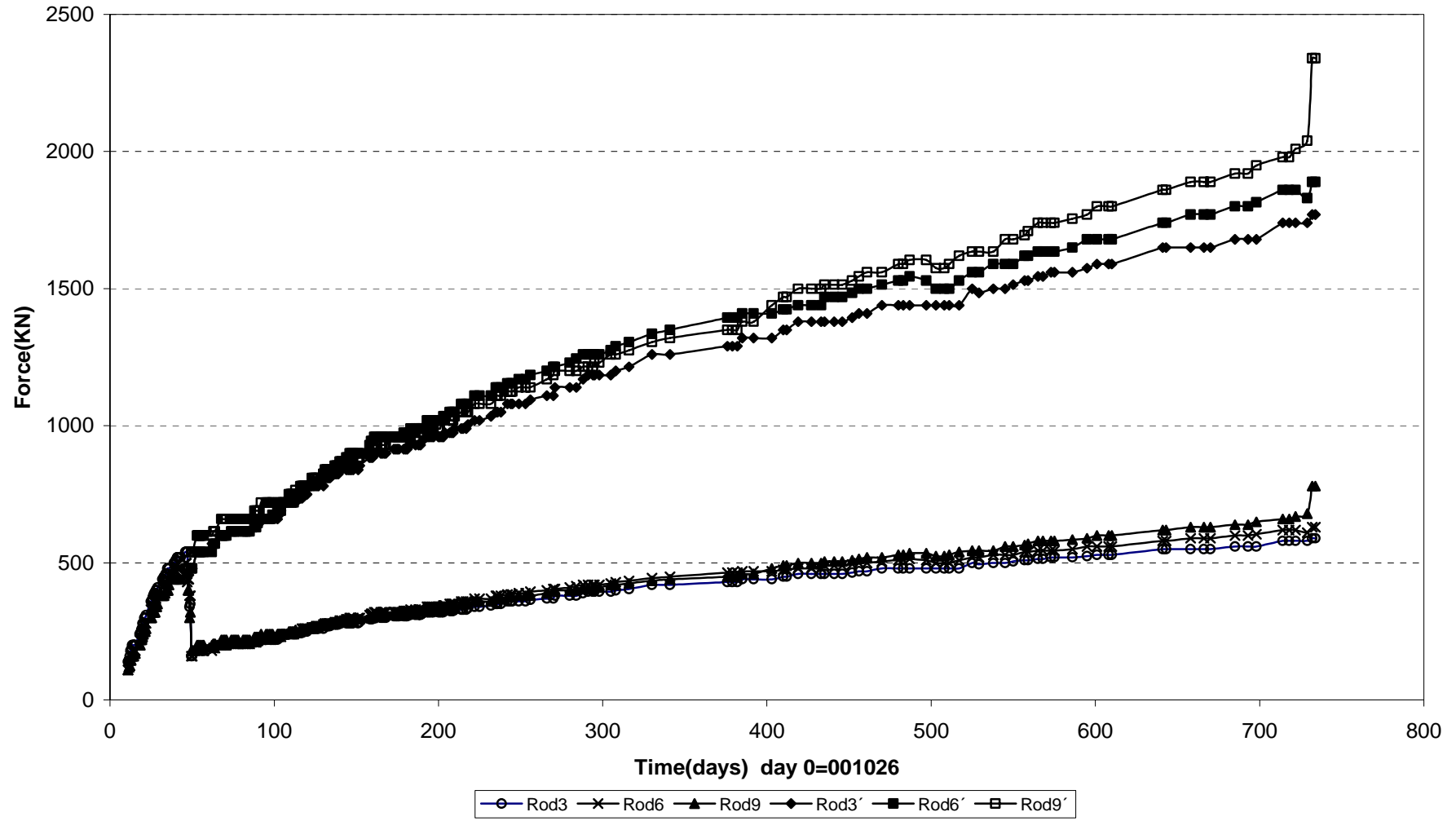
Pore water pressure - Ring 10 & Cylinder 4 (001026-021101)
Kulite



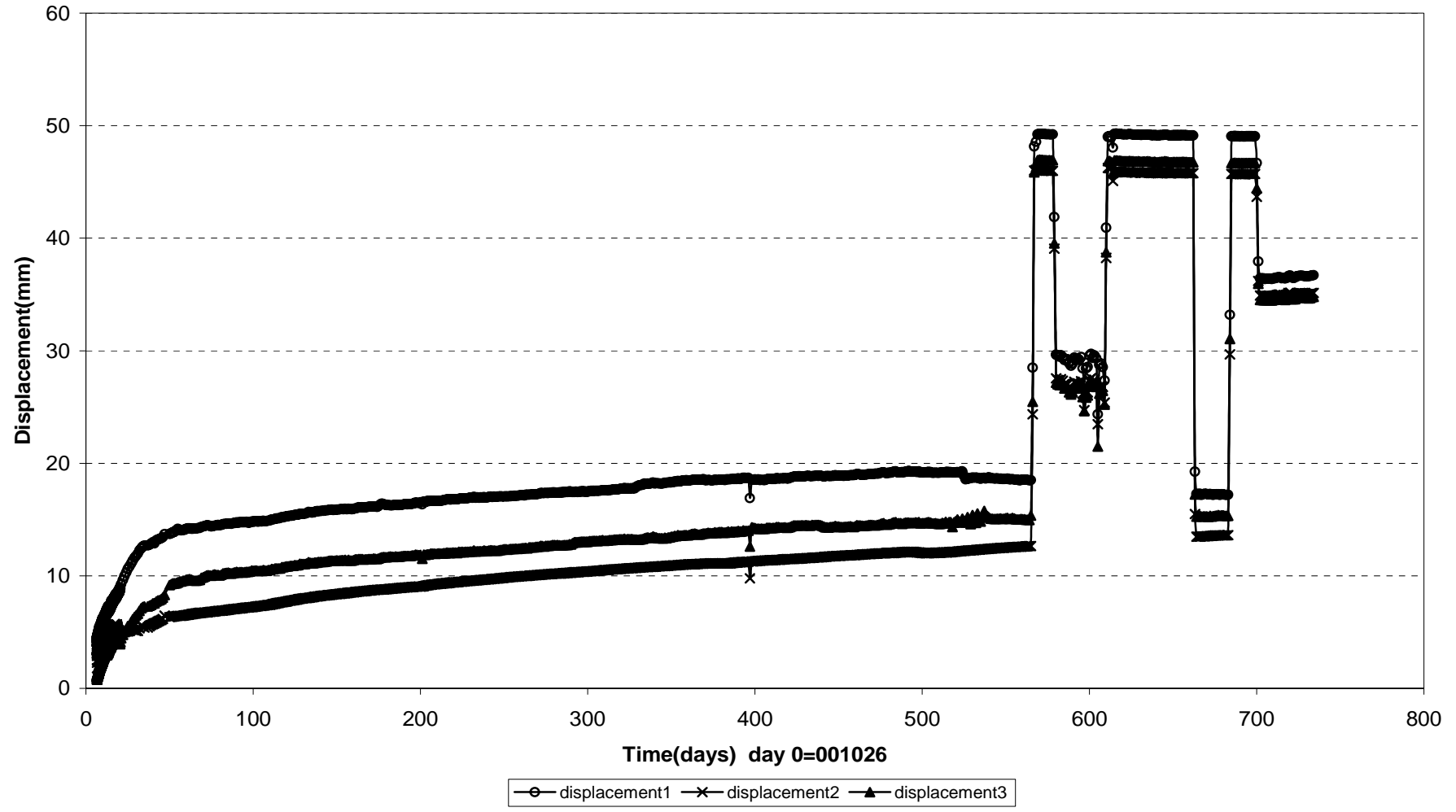
Inflow into filter (001026-021101)



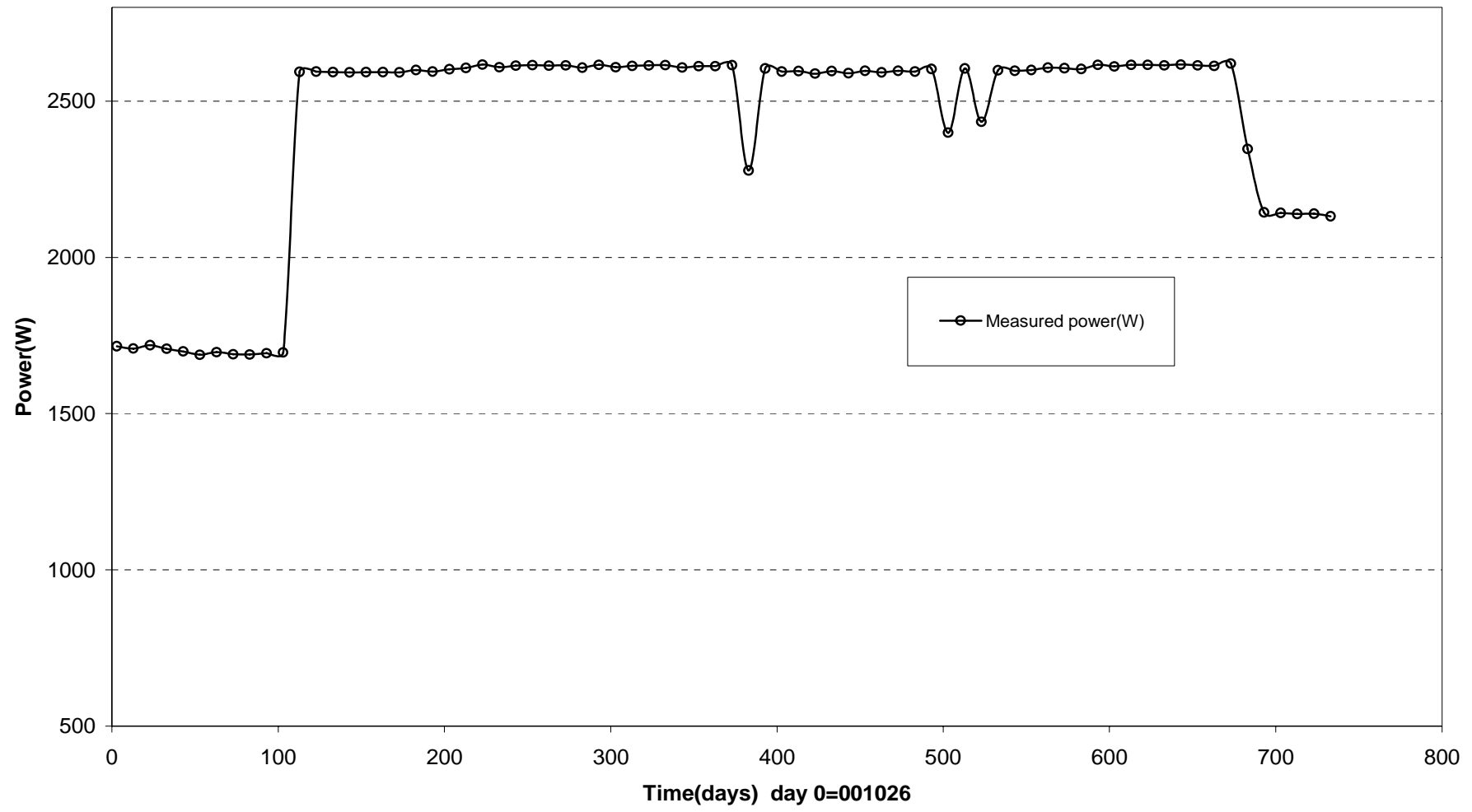
Forces on plug (001026-021101)



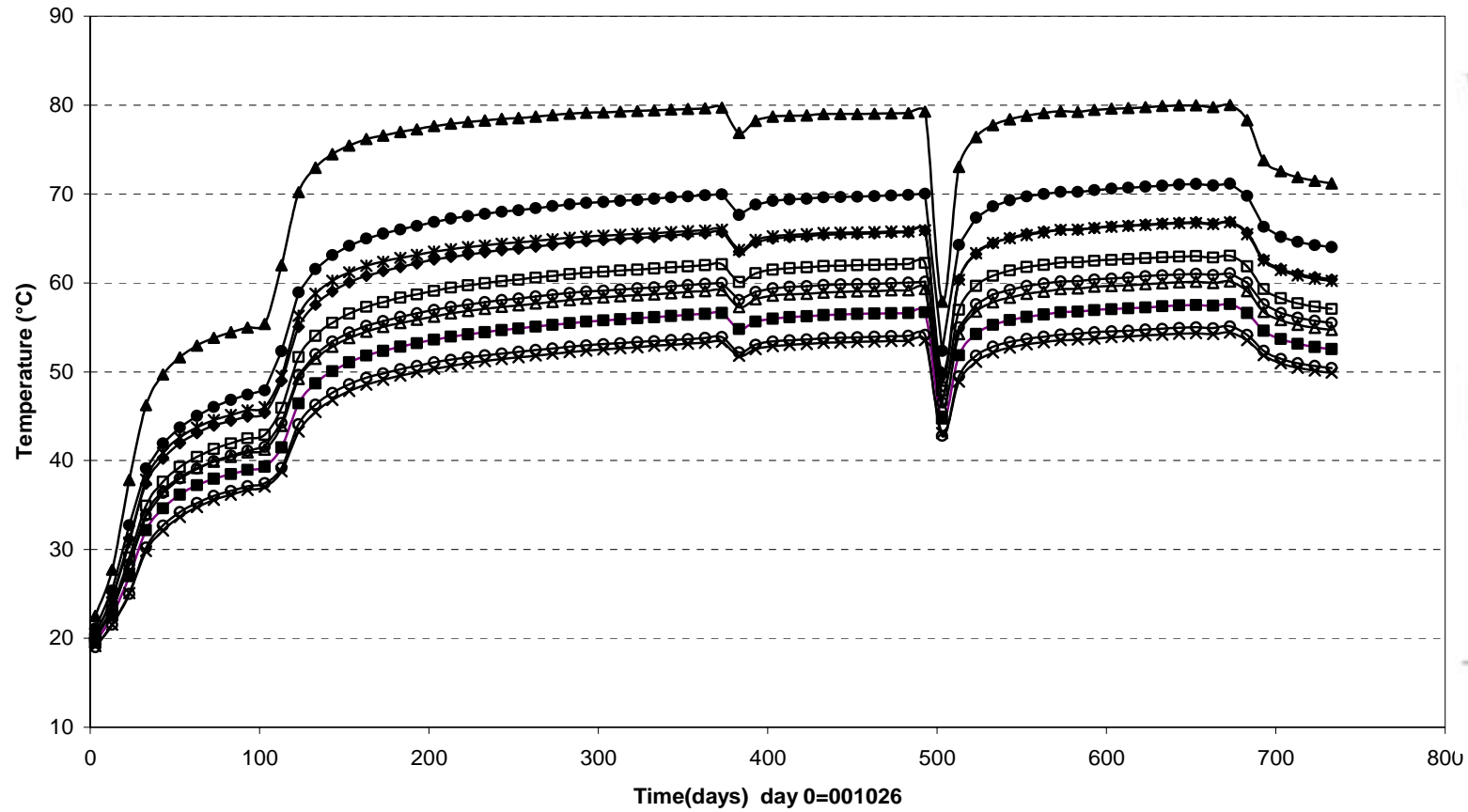
Displacement of plug (001026-021101)



Canister power (001026-021101)

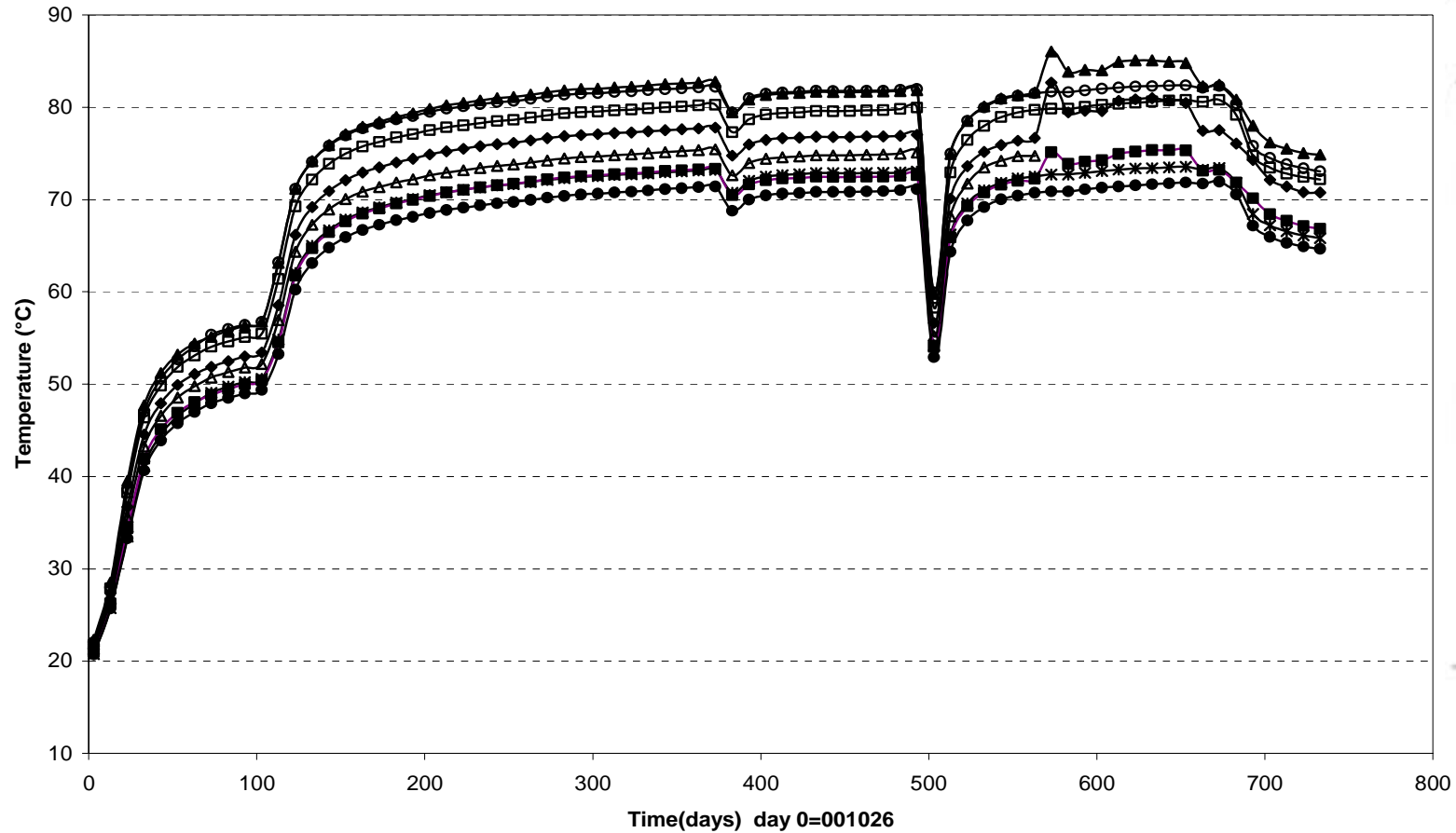


Temperature in the buffer - Cylinder 1 (001026-021101) Thermocouple

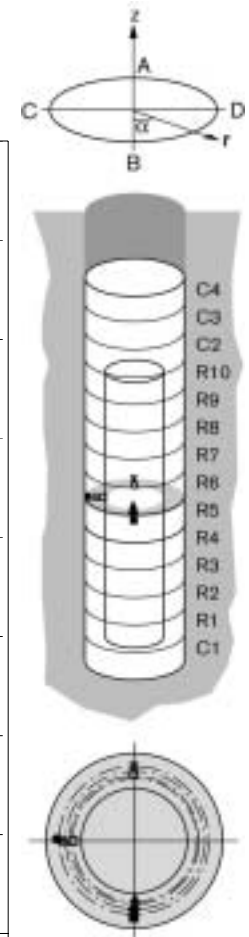


○ T101(Cyl.1\center\50)	* T102(Cyl.1\center\50)	▲ T103(Cyl.1\center\50)
◆ T104(Cyl.1\A\635)	■ T105(Cyl.1\A\735)	□ T106(Cyl.1\B\685)
△ T107(Cyl.1\C\685)	● T108(Cyl.1\D\585)	○ T109(Cyl.1\D\685)
× T110(Cyl.1\D\785)		

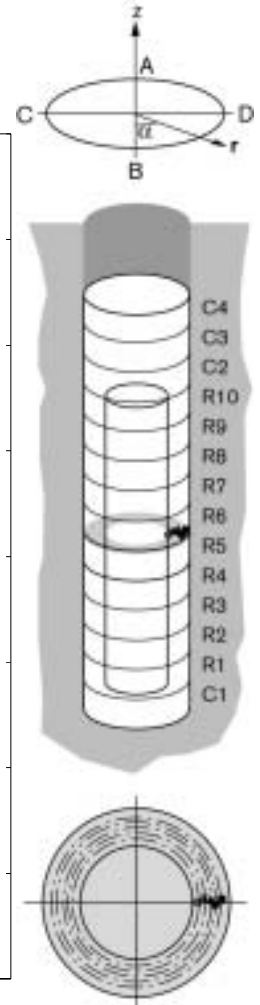
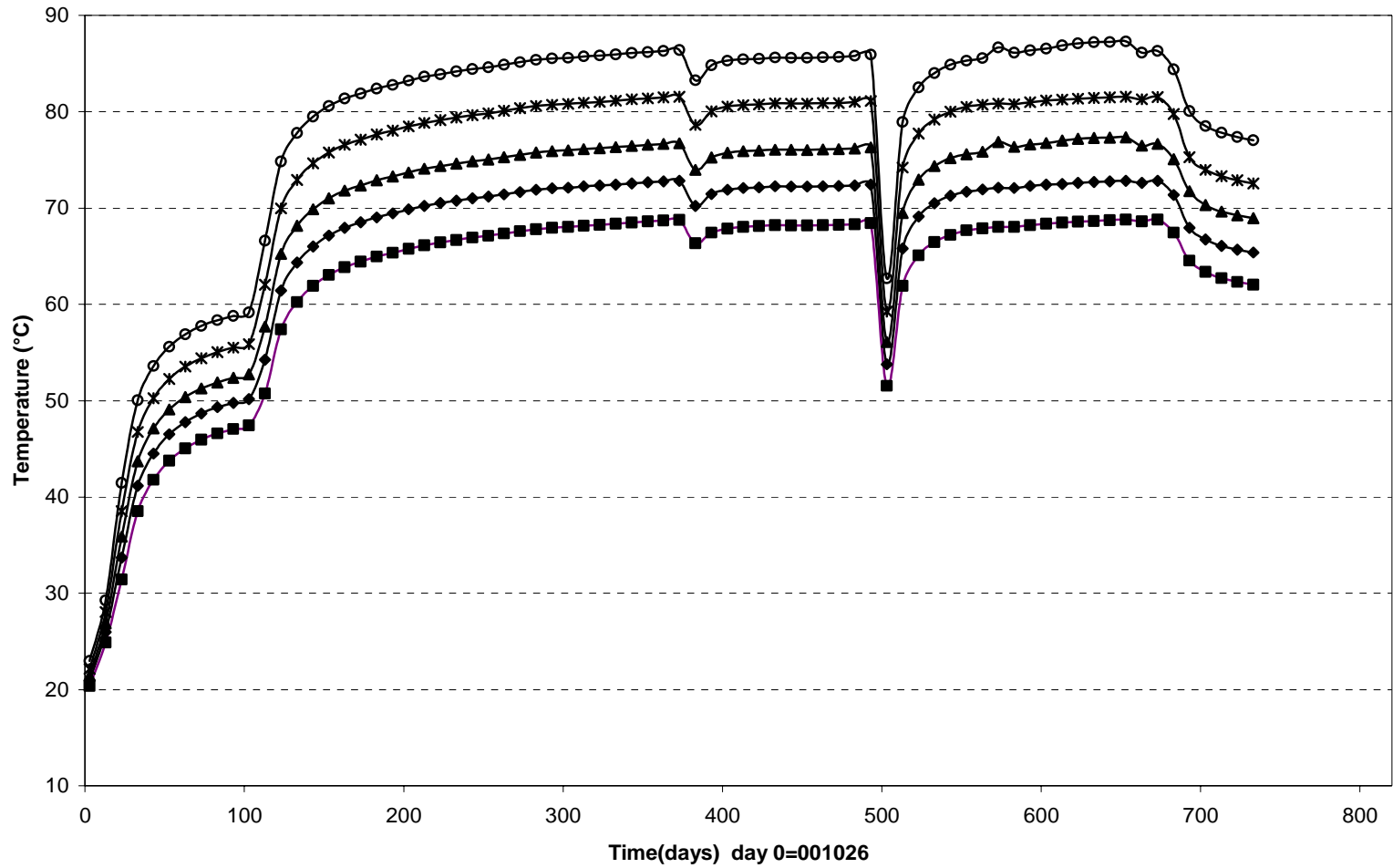
Temperature in the buffer - Ring 5 (001026-021101) Thermocouple



- | | | | | |
|---------------------|---------------------|---------------------|---------------------|---------------------|
| ○ T111(Ring5\A\635) | * T112(Ring5\A\735) | ▲ T113(Ring5\B\610) | ◆ T114(Ring5\B\685) | ■ T115(Ring5\B\735) |
| □ T116(Ring5\C\610) | △ T117(Ring5\C\685) | ● T118(Ring5\C\735) | | |

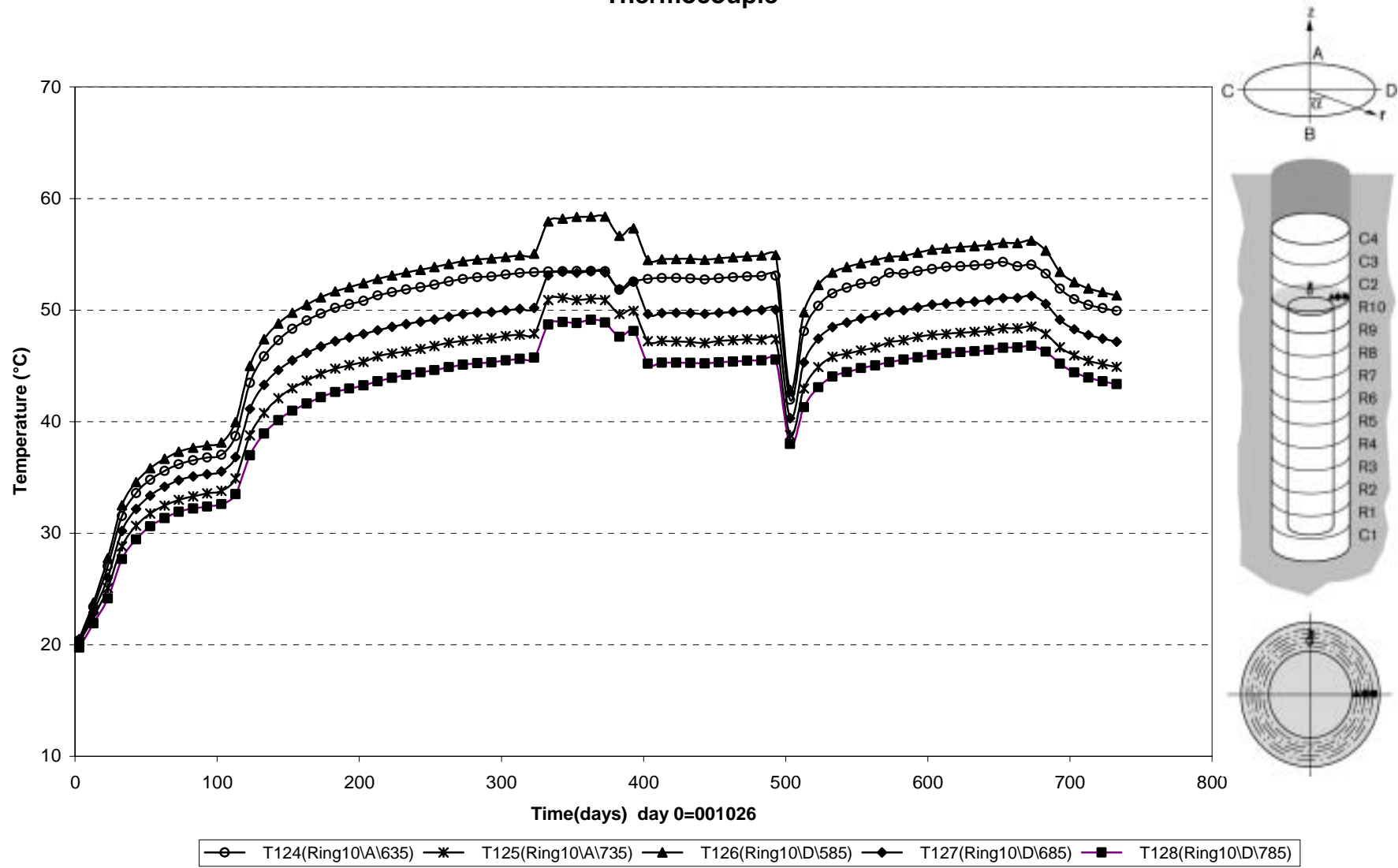


Temperature in the buffer - Ring 5 (001026-021101) Thermocouple

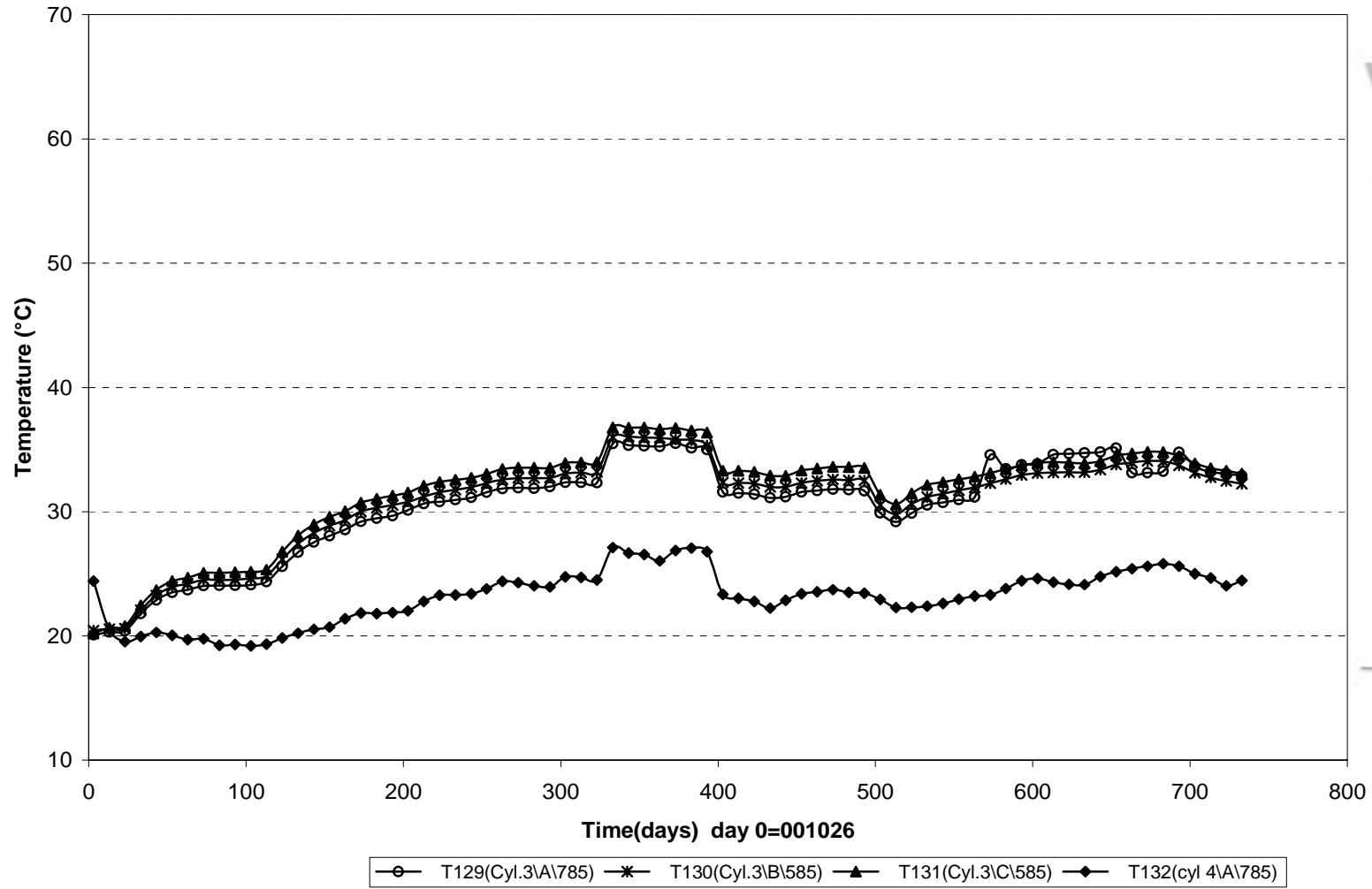


T119(Ring5\D\585)
 T120(Ring5\D\635)
 T121(Ring5\D\685)
 T122(Ring5\D\735)
 T123(Ring5\D\785)

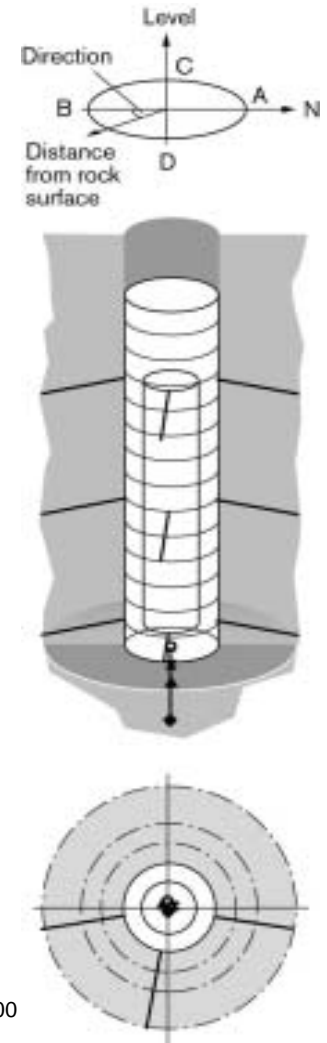
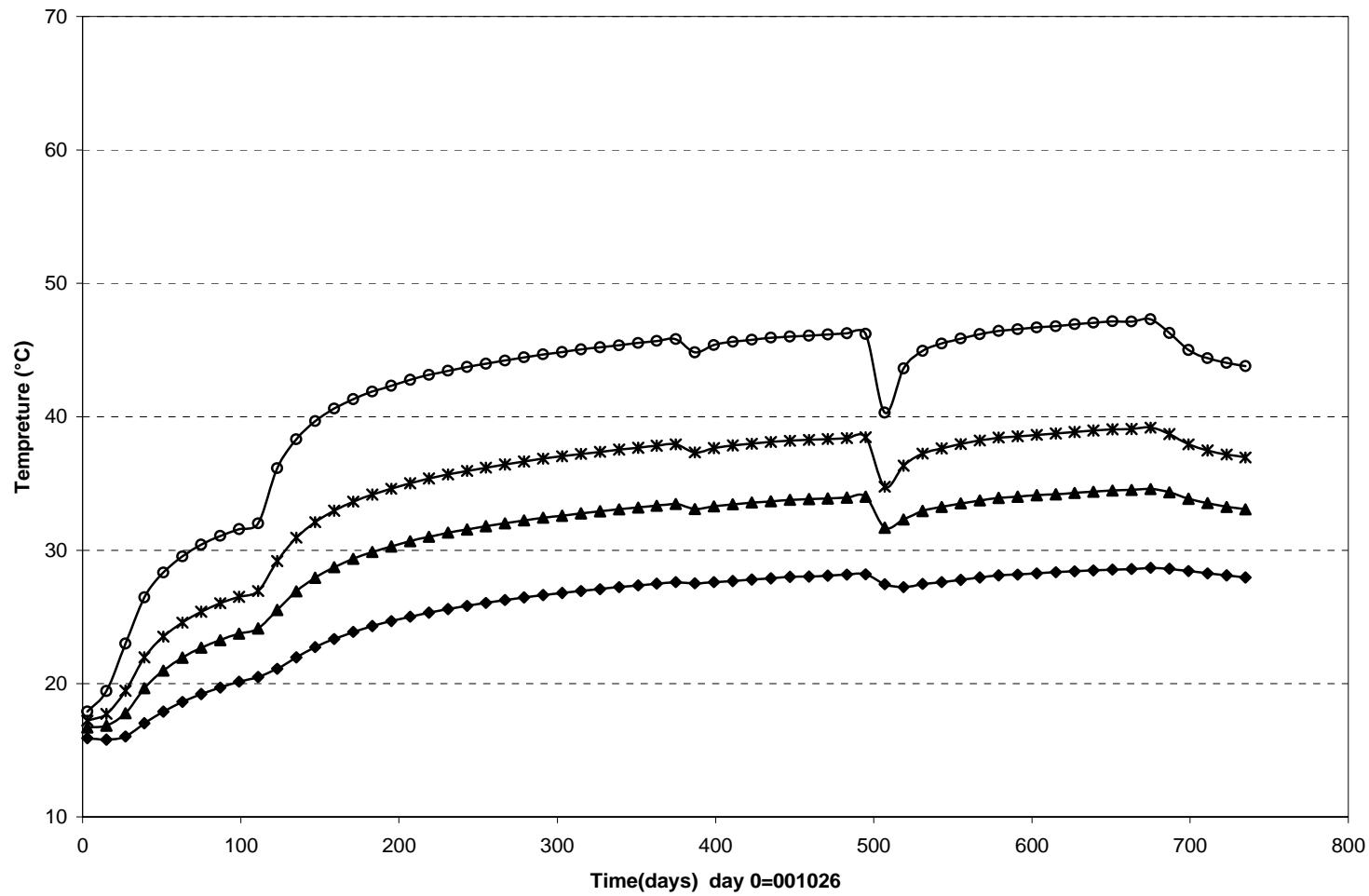
Temperature in the buffer - Ring 10 (001026-021101) Thermocouple



Temperature in the buffer - Cylinder 3 and Cylinder 4 (020501-021101) Thermocouple

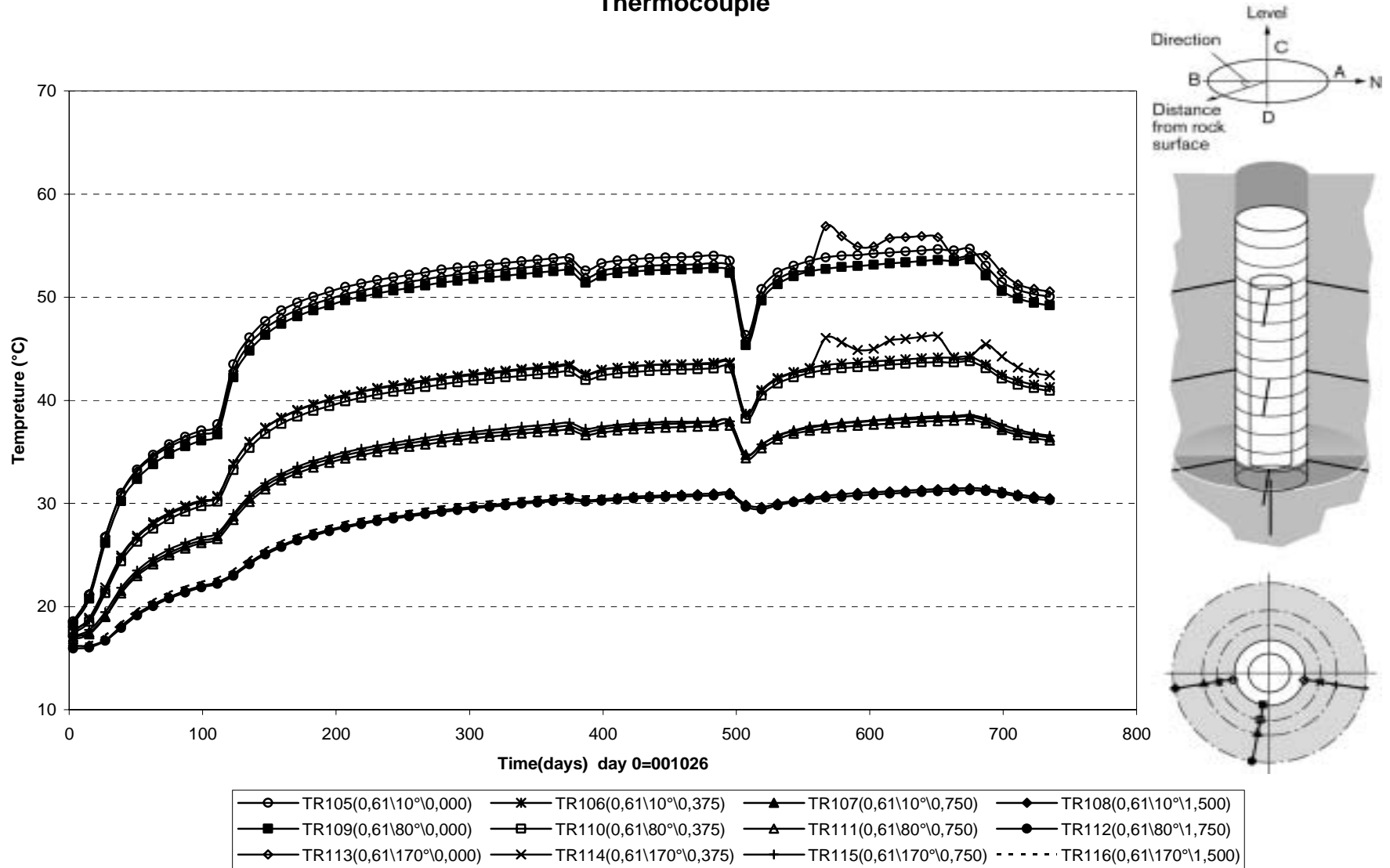


Temperature in the rock - below the dep. hole (001026-021101) Thermocouple

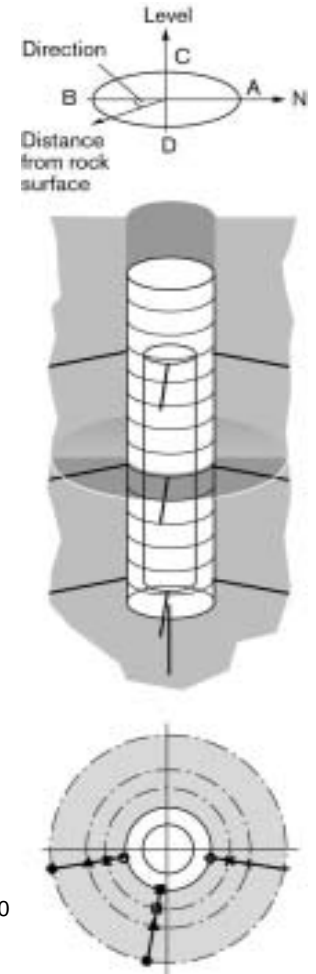
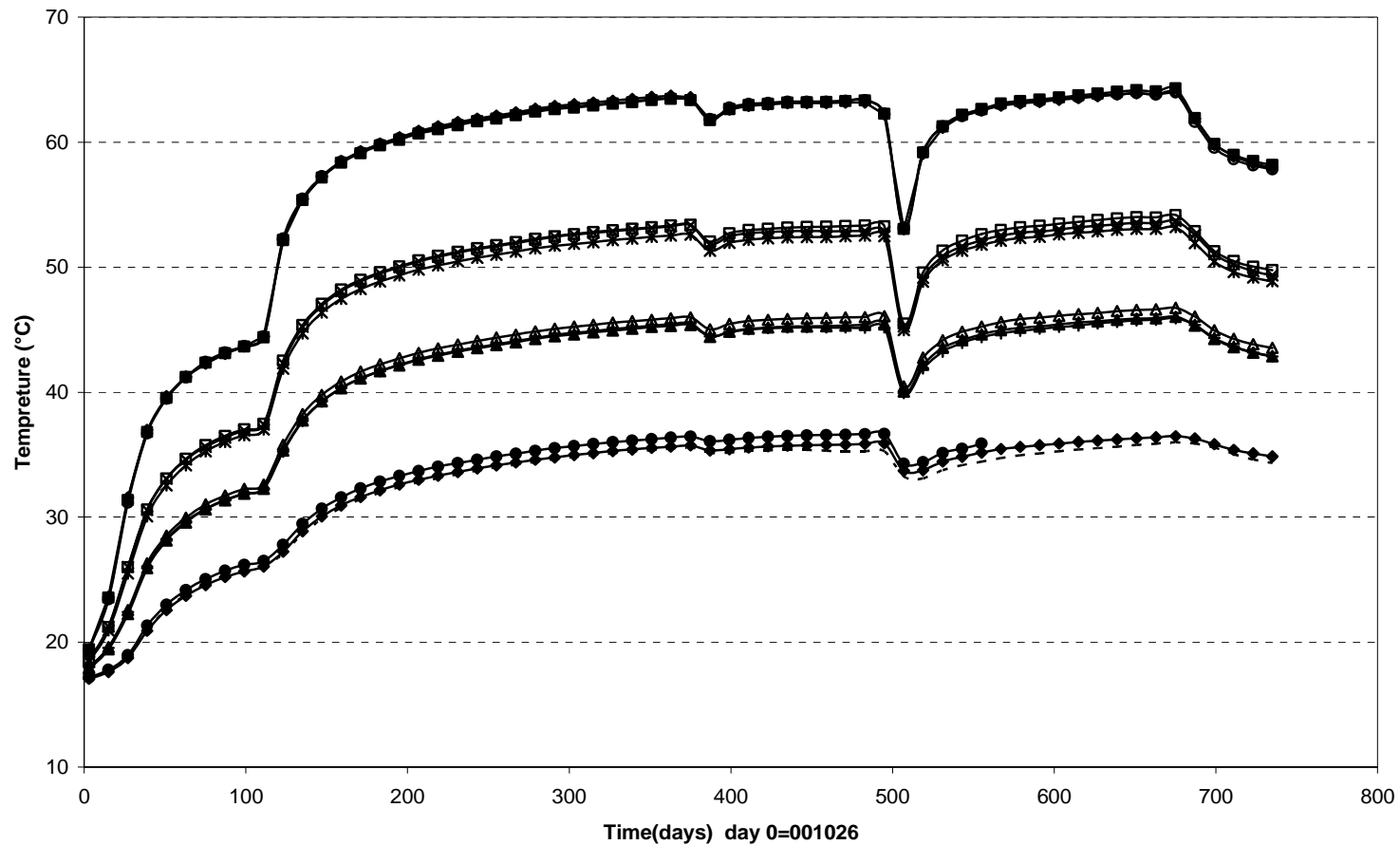


TR101(0\center\0,000)
 TR102(0\center\0,375)
 TR103(0\center\0,750)
 TR104(0\center\1,500)

Temperature in the rock - level 0,6 m (001026-021101) Thermocouple

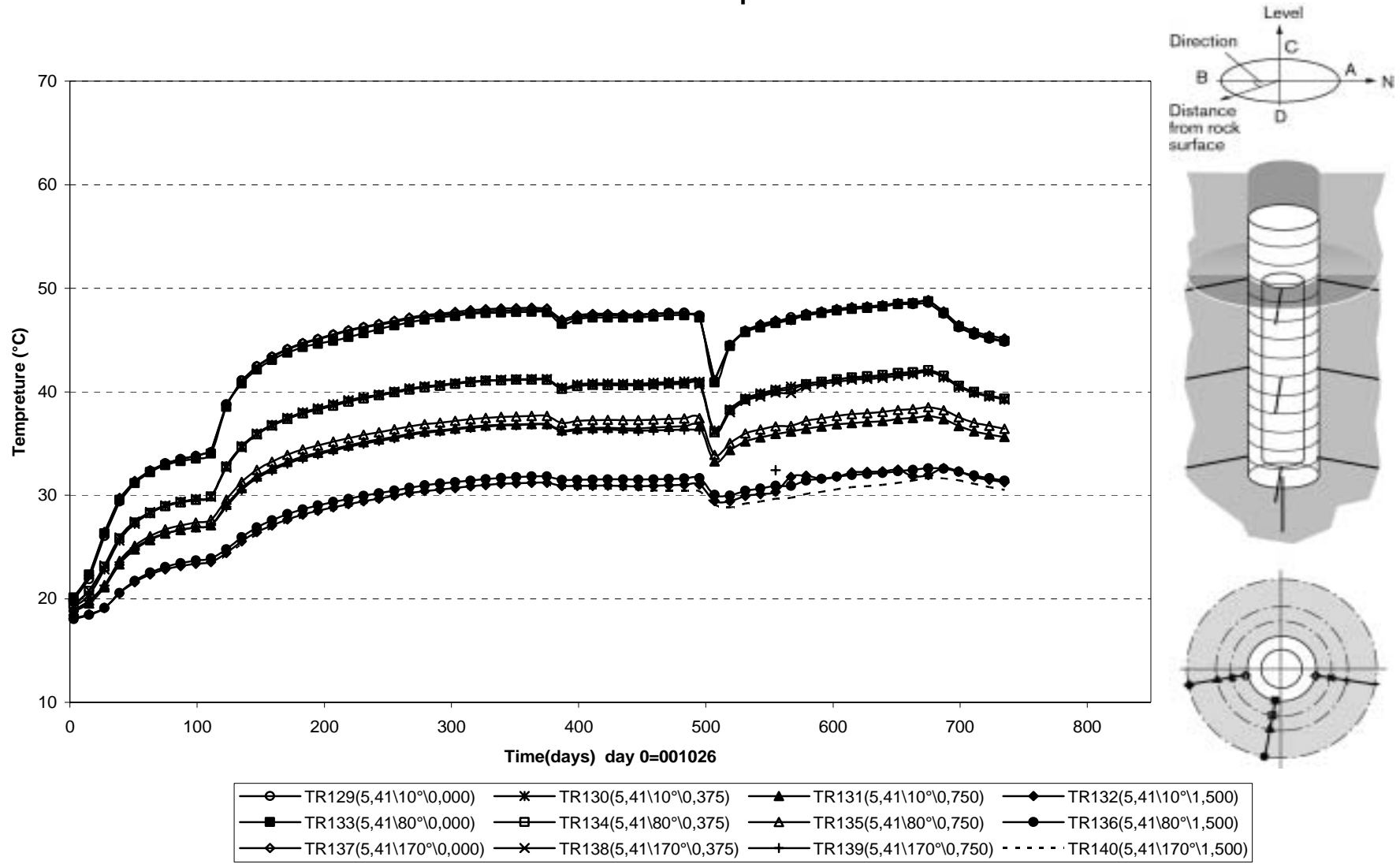


Temperature in the rock - level 3,01 m (001026-021101) Thermocouple

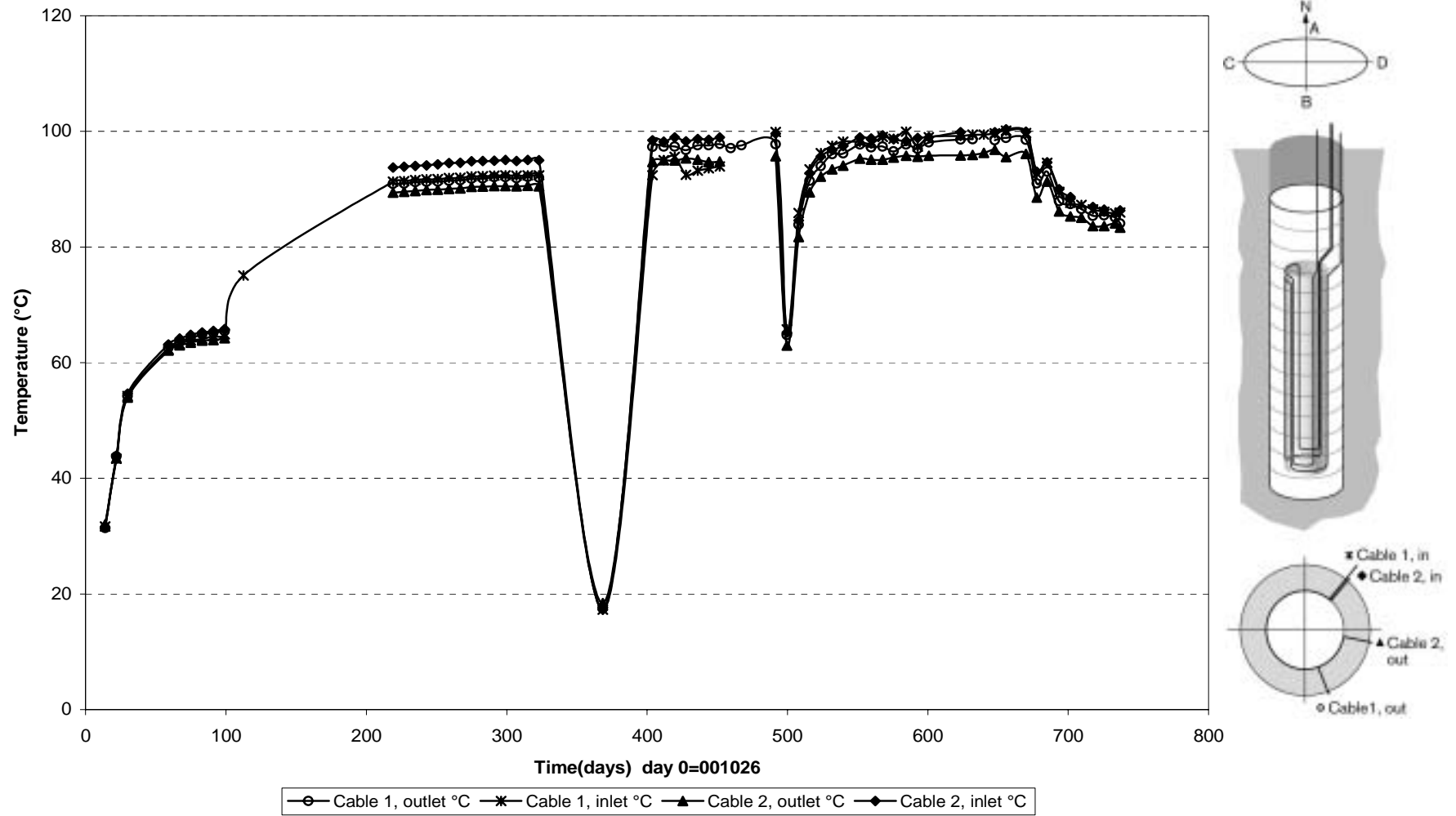


○ — TR117(3,01\10°\0,000)	* — TR118(3,01\10°\0,375)	▲ — TR119(3,01\10°\0,750)	◆ — TR120(3,01\10°\1,500)
■ — TR121(3,01\80°\0,000)	□ — TR122(3,01\80°\0,375)	△ — TR123(3,01\80°\0,750)	● — TR124(3,01\80°\1,500)
◇ — TR125(3,01\170°\0,000)	× — TR126(3,01\170°\0,375)	+ — TR127(3,01\170°\0,750)	- - - TR128(3,01\170°\1,500)

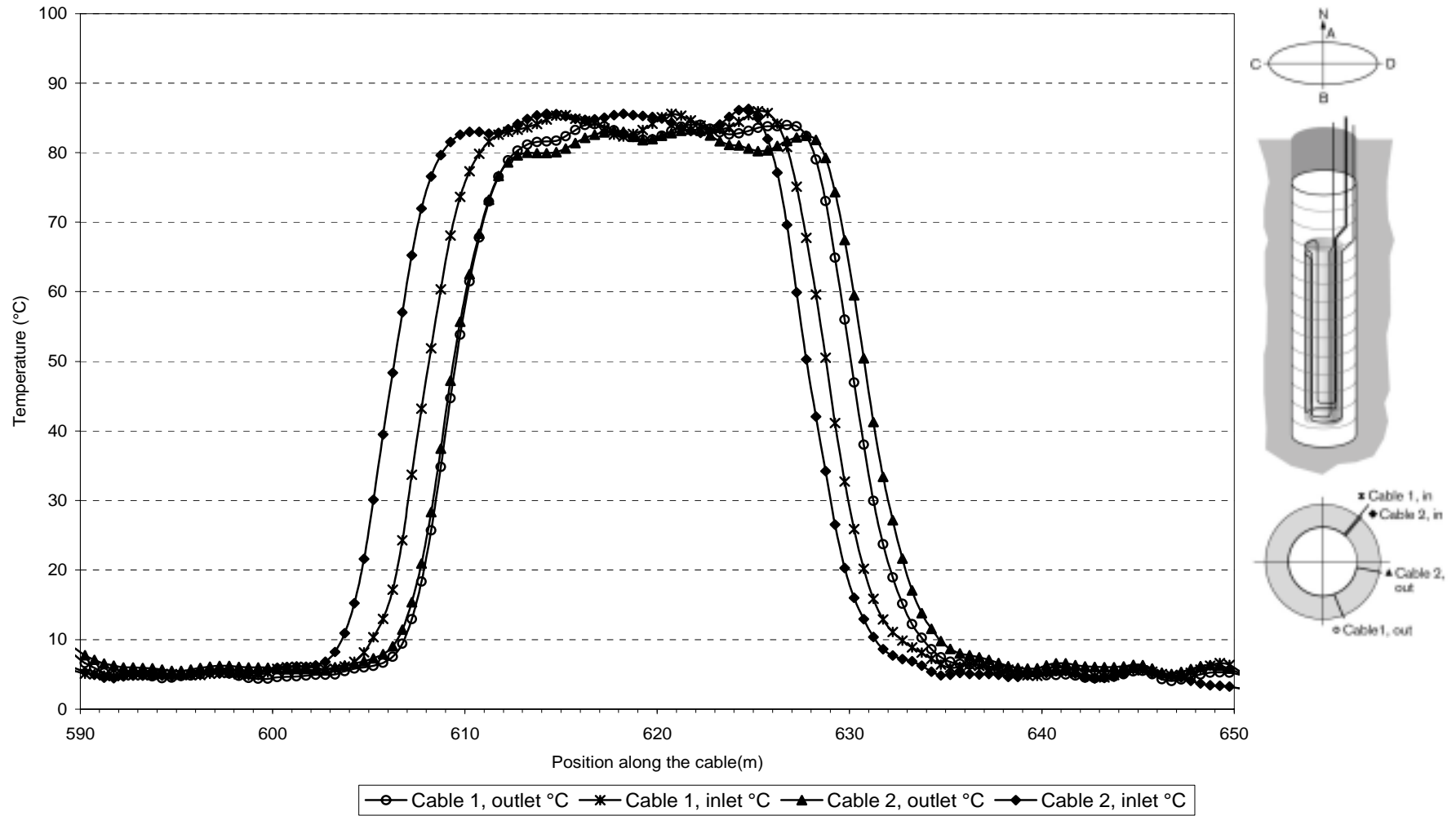
Temperature in the rock - level 5,40 m (001026-021101) Thermocouple



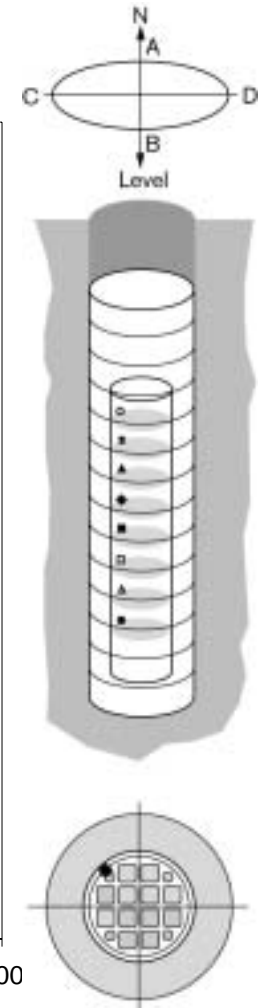
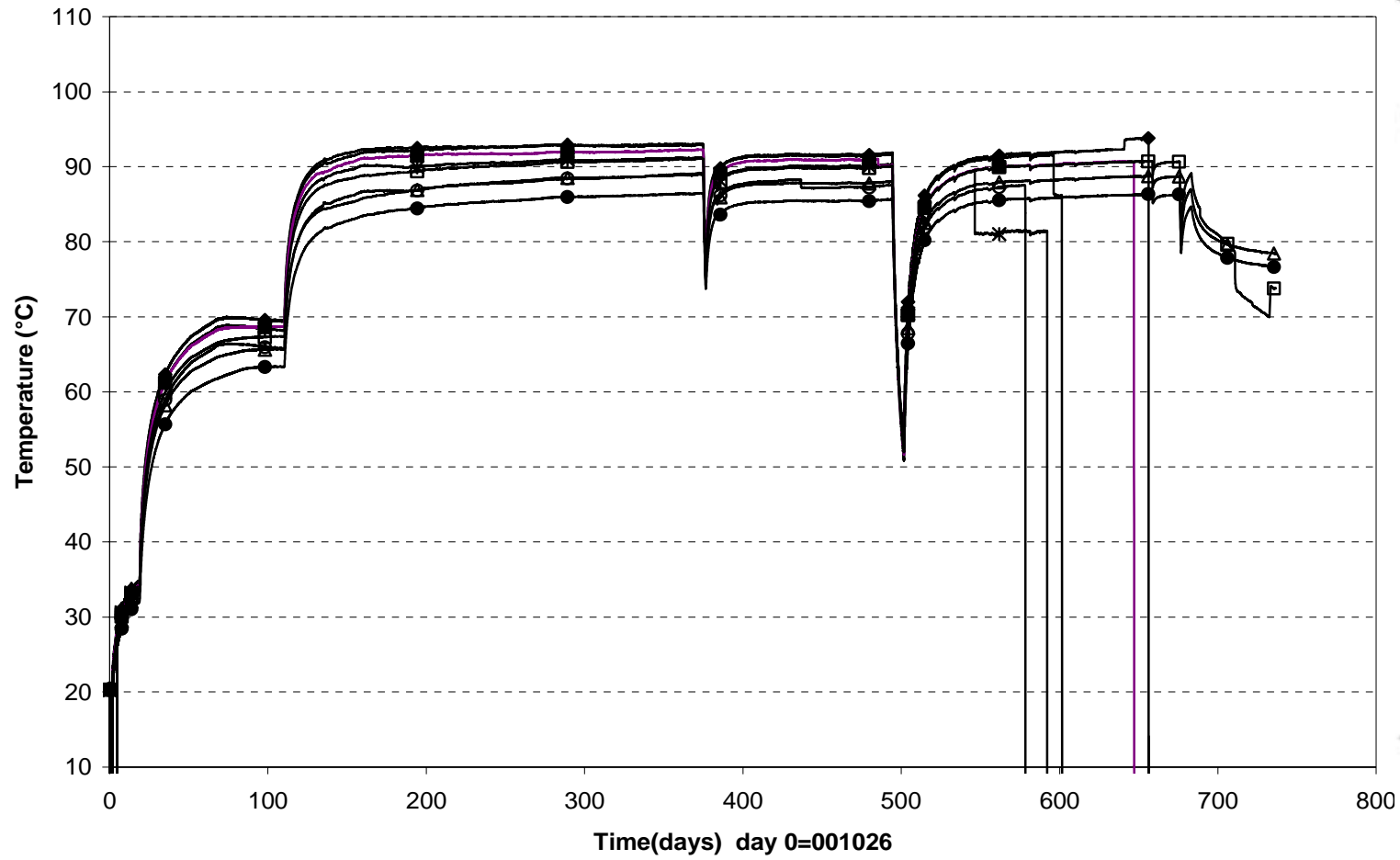
**Max.temperature on the canister surface (001026-021101)
Optical fiber cables**



Temperature profile on the canister surface (021101) Optical fiber cables

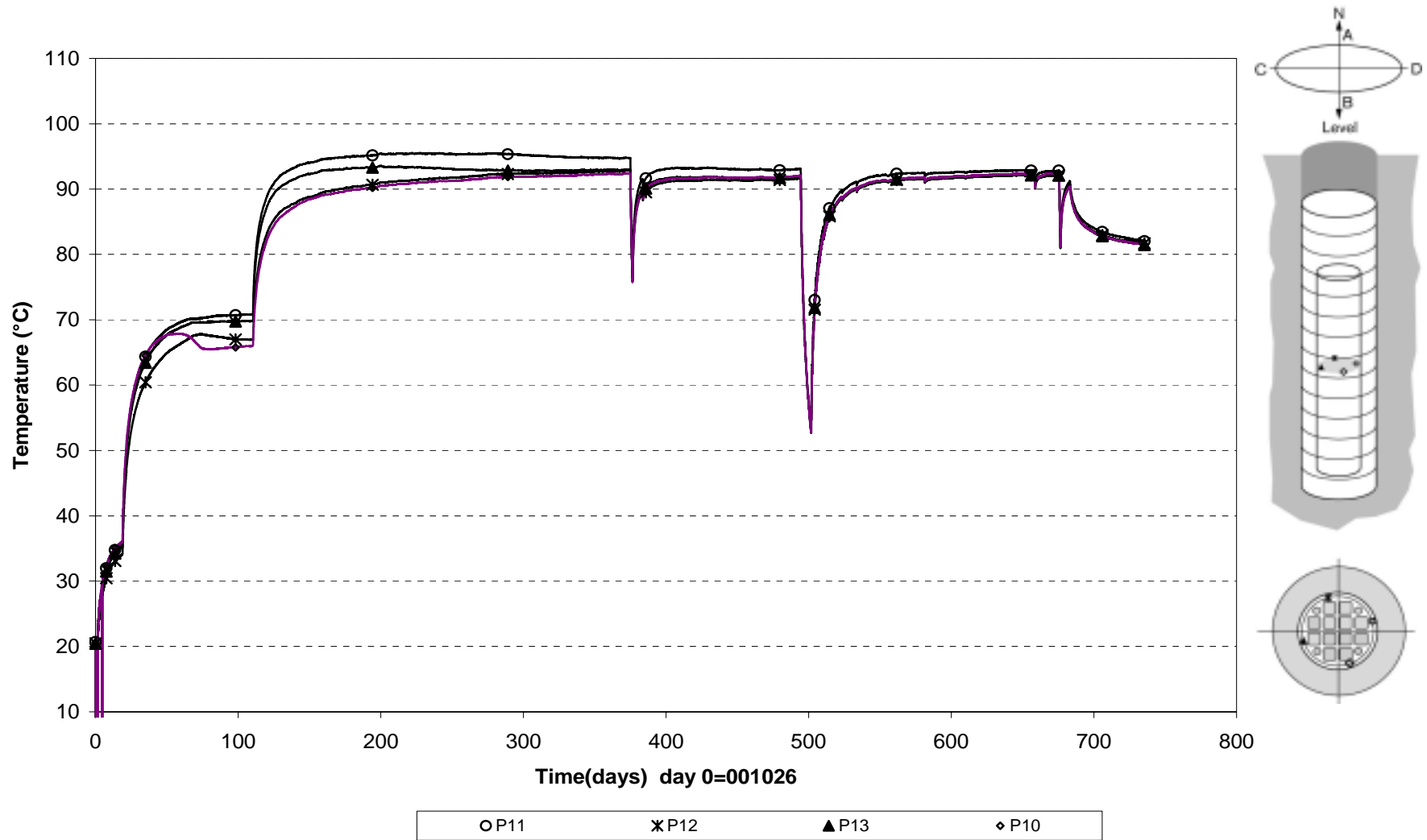


Temperature inside the canister (001026-021101)
PT-100

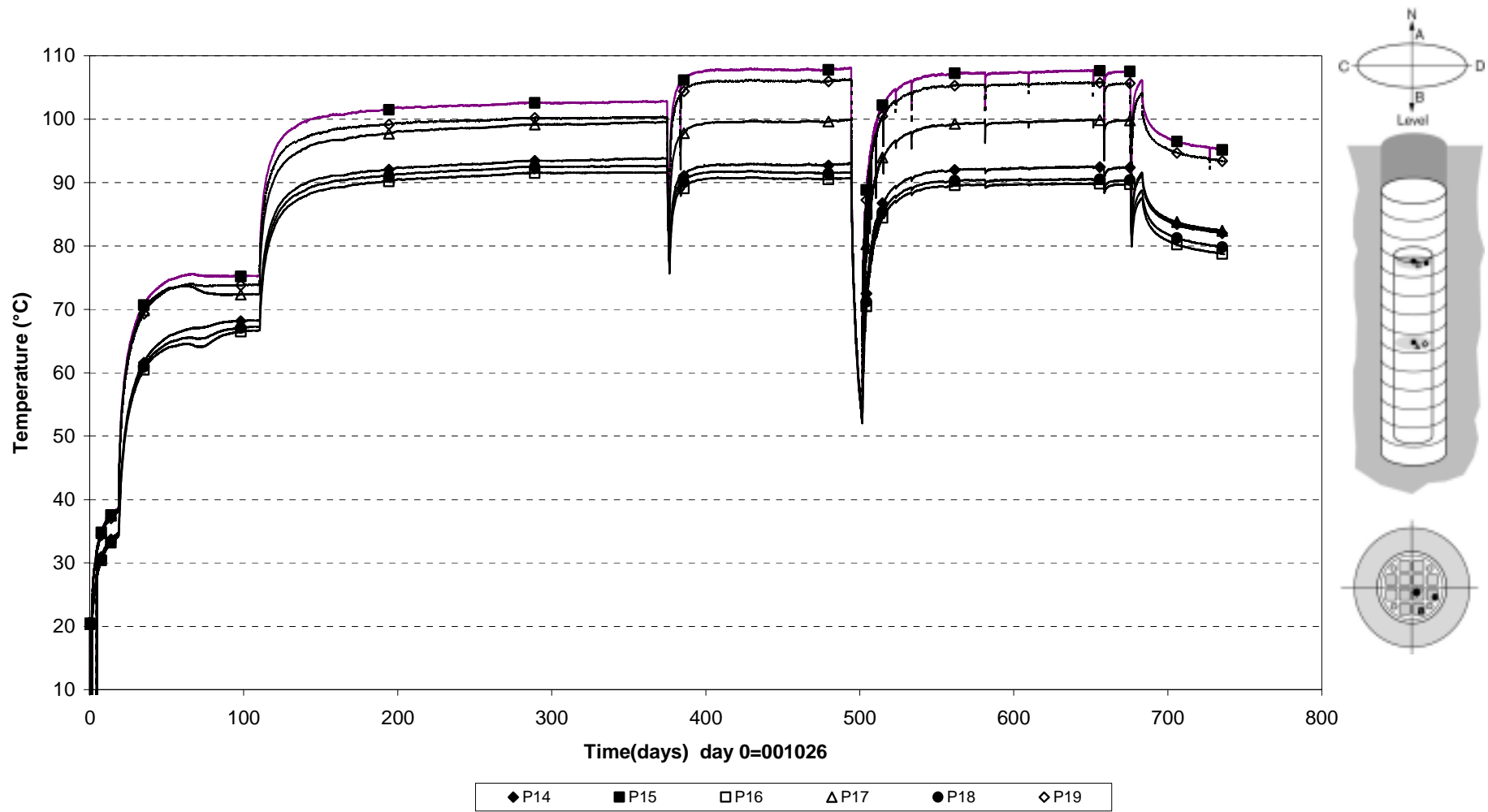


- P2
- ✕ P3
- ▲ P4
- ◆ P5
- P6
- P7
- △ P8
- P9

**Temperature inside the canister (001026-021101)
PT-100**



Temperature inside the canister (001026-021101)
PT-100



Appendix B



**STRESS AND STRAIN MEASUREMENT OF THE ROCK MASS
RETRIEVAL TEST AT ÄSPÖ**

Measuring period

2002-05-01 – 2002-10-31

Kennert Röshoff

Nancy Bono

2002-11-15

BergByggKonsult AB Ankdammsgatan 20 171 43, Solna, Sweden

Tel. 08-7595050 Fax 08-7595065

Contents		Page
1	EXTENT	83
2	TECHNICAL BACKGROUND	85
2.1	The vibrating wire embedment biaxial stressmeter	85
2.2	Embedded strain meters	85
2.3	Cement	85
3	FIELD MEASUREMENT	87
3.1	Installation work	87
3.2	Location of instruments	87
3.3	Registration	87
4	COMPUTER PROCESSING OF FIELD DATA	91
4.1	Evaluation of stresses	91
4.1.1	Radial deformations	91
4.1.2	Calculation of deformation to stresses	91
4.2	Evaluation of strain	92
4.2.1	Calculation of strain	92
4.3	Material parameters	92
4.4	Processing	93
5	RESULTS	95
5.1	Results of canister hole 1	99
5.1.1	Stress change for each biaxial stressmeter	99
	Stressmeter A1	99
	Stressmeter B1	100
	Stressmeter C1	101
	Stressmeter D1	102
5.1.2	Strainmeter A1:1, B1:1, C1:1, D1:1, D1:2	103
5.1.3	Strainmeter C1:2	103
	Results of canister hole 2	104
5.1.4	Stress change for each biaxial stressmeter	104
	Stressmeter A2	104
	Stressmeter B2	105
	Stressmeter C2	106
	Stressmeter D2	107
5.1.5	Strainmeter B2:1, C2:1, C2:2	108

1 EXTENT

BBK AB and NCC Teknik have, on commission of SKB, ÄSPÖ hard rock laboratory, performed rock mechanical measurements in the Repository tunnel at Äspö. The measurement program comprises of registration of the stress and the strain response around the two canister holes during drilling and heating of the rock mass.

In the first phase, the response of the rock mass was monitored during the drilling of the two canister holes (QPTD F69-00-21). This second phase includes the response registered during a heating phase. Hole 2, shown in Figure 3.1 and Figure 3.2, has a heating source while Hole 1 is open and not heated. The heating experiment started on 2000-10-27 and will continue for about five years.

The aim of the instrumentation is to monitor the stress changes due to heating of the rock mass in a canister hole. The strain meter is used to monitor the relative changes of strain of the intact rock and across fractures.

The commission extends over field measurement and evaluation.

BBK AB is responsible for measuring equipment, the mobilization, field measurement, the computer processing. BBK AB and NCC Teknik are responsible for the interpretation and report of the measurements.

This report presents the measurement results during the period of the heating phase from 2002-05-01 to 2002-10-31.

2 TECHNICAL BACKGROUND

2.1 Vibrating wire embedment biaxial stressmeters

The biaxial stressmeter, Geokon model 4350, is designed to measure compressive stress changes in rock, salt, concrete or ice. Principal stress changes are measured in the plane perpendicular to the borehole axes. The stressmeter consists of a high-strength steel cylinder that is grouted into a 60 mm borehole. Stress changes in the host material cause the cylinder to deform.

The radial deformation of the cylinder is measured by means of three pairs of vibrating wire sensors spaced at 60° intervals. Changes of stress produce corresponding changes in the resonant frequency of the sensors. These changes of frequency can be related to stress changes using factory-supplied calibrations. Longitudinal strain sensors and temperature sensors are also included in the stressmeter.

2.2 Embedded strain meters

The vibrating wire strain gages are designed for direct embedment in concrete. The strainmeter is 15 cm long and commonly used for strain measurement in foundations, piles, bridges, dams, tunnel liners etc.

The strain is measured using the vibrating wire principle. A length of a steel wire is tensioned between two end blocks that are embedded directly in concrete. Deformation (i.e. strain changes) of the concrete mass will cause the two end blocks to move relative to one another, thus altering the tension in the steel wire. The tension is measured by excitation of the wire and measuring its resonant frequency of vibration using an electro magnetic coil.

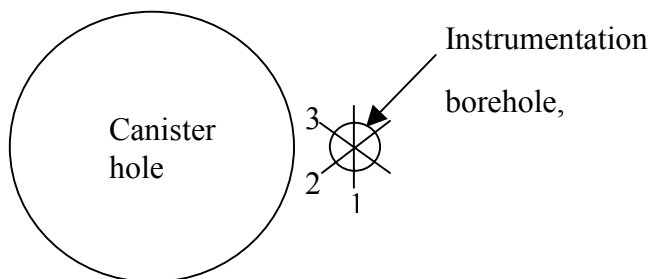
2.3 Cement

Special expansive grout was used to insure that the gage is in complete contact with the surrounding rock. The instruments are grouted in special cement from Denmark named Densitop T2. This cement is chosen to have as similar properties as the rock as possible. The compression strength is 150 MPa. The coefficient of expansion is approximate 8.5 microstrain/C° that is similar to hard rock as granite and as 85 % of common concrete.

3 FIELD MEASUREMENT

3.1 Installation work

Installation of the stressmeter gage is accomplished by inserting the gage into a grout-filled borehole using a setting tool and self-aligning setting rod.



The stress cell is orientated so that the first vibrating wire is orientated tangentially to the canister hole. The second string is orientated 60° from tangential direction and the third string is orientated 120° from tangential direction.

The strainmeters were fixed to a 6 mm glasfiber rod and pushed into the grout after the stress cell was installed.

3.2 Location of instruments

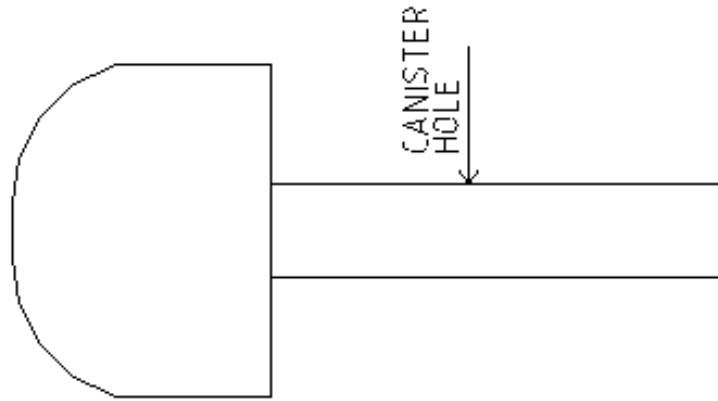
See figure 3.1 and figure 3.2.

3.3 Registration

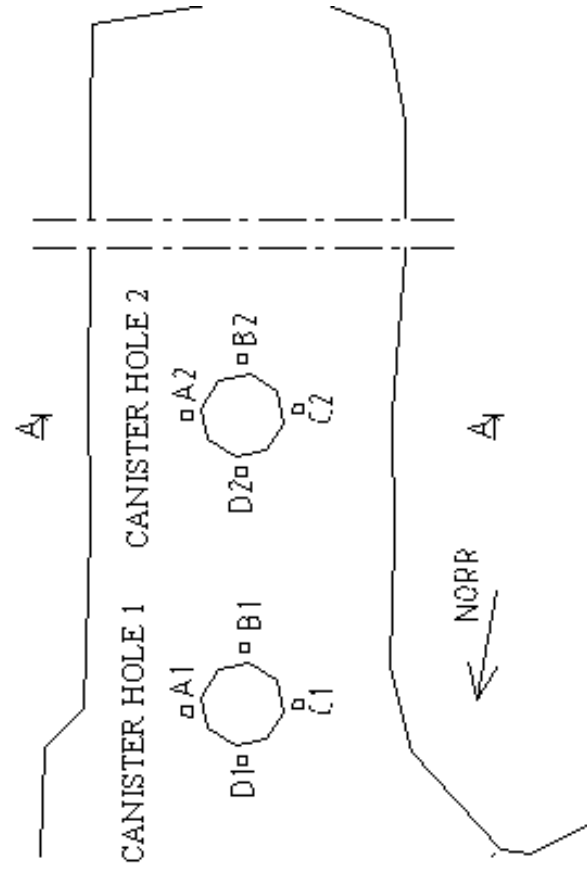
A datalogger type Campbell CR10X has captured the measurements, which have been recorded once every hour during the period 2000-10-01 to 2001-01-01, and once every six hours during the period 2001-01-03 to 2002-10-31.

MEASUREMENT LAYOUT

SECTION A-A



PLAN



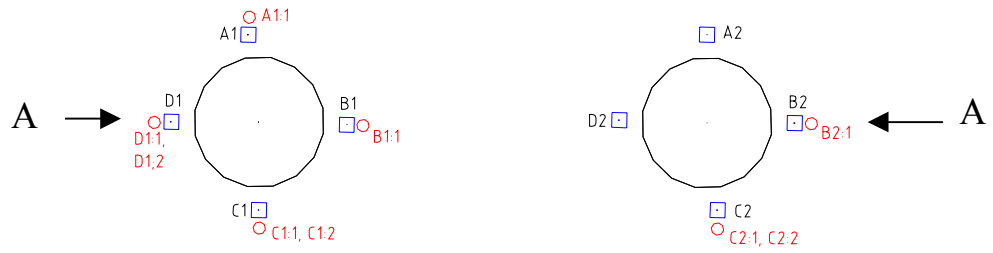
□ BOREHOLE LAYOUT

Figure 3.1 Measurement Layout

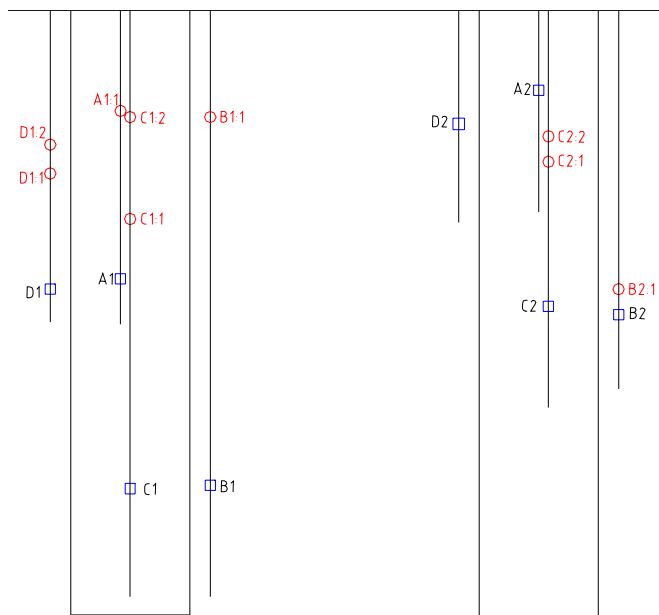
Canister Hole 1

Canister Hole 2

PLAN



SECTION A-A



□ Biaxial stressmeter

○ Deformationmeter

Figure 3.2 Location of instruments

4 COMPUTER PROCESSING OF FIELD DATA

4.1 Evaluation of stresses

The stress changes are evaluated from the measured deformations registered by the vibrating wires.

4.1.1 Radial deformations

Radial deformation for each of the strings are calculated with the equation:

$$V_r = (R_1 - R_0) * \text{Gagefactor} \quad (\text{in. or mm})$$

V_r = Radial deformation for each of the strings

R_1 = Deformation reading in digits (= frequency² / 1000)

R_0 = Deformation zero reading in digits (= frequency² / 1000)

4.1.2 Calculation of deformation to stresses

The magnitude and the direction of the stress changes are determined from the measured radial deformation of the sensor in three directions.

The equations below give the magnitude and the direction of the maximum stress increase and reduction in a plane perpendicular to the borehole axes:

Maximal stress increase

$$p = \frac{1}{2} \left[\frac{1}{3B} \left((2V_{r_1} - V_{r_2} - V_{r_3})^2 + 3(V_{r_2} - V_{r_3})^2 \right)^{1/2} + \frac{1}{3A} (V_{r_1} + V_{r_2} + V_{r_3}) \right]$$

V_{r_1} = Radial deformation for string 1

V_{r_2} = Radial deformation for string 2

V_{r_3} = Radial deformation for string 3

A, B = Coefficients depending on the sensor geometry and the material properties

Maximal stress reduction

$$q = \left[\frac{1}{3A} (V_{r_1} + V_{r_2} + V_{r_3}) - p \right]$$

The angle of the maximal stress increase

The angle in the plane perpendicular to the borehole axes is measured clockwise from the tangential direction of the canister hole.

$$\theta = \frac{1}{2} \cos^{-1} \left[\frac{V_{r_1} - A(p + q)}{B(p - q)} \right]$$

4.2 Evaluation of strain

Nine strain gages were installed in the same boreholes as the biaxial stressmeters.

4.2.1 Calculation of strain

Strain measurement were calculated as temperature compensated load related strain with the following equation:

$$\mu_{true} = (R_1 - R_0) * B + (T_1 - T_0)(C_1 - C_2)$$

μ_{true} = temperature compensated microstrain

R_1 and R_0 =Digits reading

B = batch calibration factor

C_1 and C_2 are the coefficients of expansion of steel and concrete, 12.2 microstrain/ C° and 8.5 microstrain/ C° .

4.3 Material parameters

Material parameters used in the calculations are as the following:

- Young's modulus of intact rock 69 Gpa
- Poisson's ratio of intact rock 0.25
- Coefficients of expansion of steel 12.2 microstrain/ C°
- Coefficients of expansion of concrete 8.5 microstrain/ C°

4.4 Processing

The raw data registered have been processed in Microsoft Excel software. The calculation and evaluation gathered from the deformations in the plane perpendicular to the borehole axes are presented as:

Temperature

Radial deformation of the three pairs of wires in plane perpendicular to borehole axes

Maximal stress increases and stress reduction in plane perpendicular to borehole axes

Orientation of maximal stress increase in plane perpendicular to borehole axes

Strain measurement

5 RESULTS

A summary of the results of the stress changes is presented in Table 1. These values represent total changes in stress magnitude and stress orientation during each reporting period during phase 2 (heating) together with maximum changes in stress magnitude and orientation recorded during phase 1 (drilling). Figure 5.1 presents graphically the maximum typical changes in stress magnitude and orientation during this reporting period from 2002-05-01 to 2002-10-31. These results are not compensated for temperature changes, nor are they compensated for longitudinal stress changes.

Although the measurements of stressmeters are affected by temperature, the temperature compensated results of stressmeters are not presented in this report because a further detailed study of the relationship between temperature and stressmeter measurements will be required in order to quantify these effects. In addition, the longitudinal stress changes are affected by temperature changes and for this reason these longitudinal measurements are not currently used on determination of radial stresses. Results of the biaxial stressmeter without temperature or longitudinal stress compensation, and the strainmeter with temperature compensation from each boreholes for the period 2002-05-01 to 2002-10-31 are summarized on the diagrams in section 5.1 and 5.2.

The diagrams in section 5.1 and 5.2 for each borehole display:

- Maximum stress increases and stress reductions in plane perpendicular to borehole axes.
- Orientation of maximum stress increase in plane perpendicular to borehole axes.
- Strain measurements presented in the diagrams are temperature-compensated with the unit of microstrain. Positive values represent elongation.

The data during this reporting period indicate that:

- The temperature is inhomogeneous around these two canister holes.

Hole 1

Around canister hole 1 (unheated) temperatures increased by about 2 to 3°C from May to the end of September and then dropped suddenly by about the same amount at the end of September. Following this drop, temperatures rose sharply again through the end of October. At the end of the reporting period temperatures were typically 23 to 24 °C, with the exception of B1. At stressmeter B1, which is nearest to canister hole 2, the temperature measurements at the end of the period were about 26.7°C

Hole 2

Around canister hole 2 (heated) the instruments located at greater depths (B2, C2 and B2:1) have maximum temperatures of about 57°C to 59°C. Instruments located at higher levels in Hole 2 have maximum temperatures of about 29°C to

30°C. The sudden drop and subsequent increase in temperature observed at Hole 1 was not seen in Hole 2.

- In canister hole 1 the stress changes during this reporting period have been small (approximately 1 to 2 MPa), and generally follow the gradual temperature change during the time period. The change in orientation of the stress field has also been very small and has reflected the temperature changes.
- In canister hole 2 the two stressmeters located at higher levels (A2 and D2) show small variations (1 to 2 MPa) which follow the measured temperatures, and the orientation of the stress field has also shown a change that follows the temperature curve, with changes of about 2 to 3 degree.

The two stress meters located at lower levels in canister hole 2 have shown larger stress changes during this reporting period. At B2 the stresses have increased by up to 8 Mpa during the reporting period. The stress magnitudes measured at gages 1-3 were greater than those recorded on gages 4-6. Due to the differences in individual gage readings, the calculated orientation of the stresses differed by about 9 degrees between the sets of gages.

At stressmeter C2 the stresses have increased by as much as 40Mpa during the period as measured in gages 1-3. The difference in magnitude measured in the two sets of gages has increased with gages 1-3 showing higher stress increases. The orientation of the stress field measured at the two sets of gages have converged and then diverged during this six month period, with the difference between the two sets of gages being about 13 degrees at the maximum.

The recorded data from two of the six radial gages, and one of the two longitudinal gages, within stressmeter C2 was -99999 on many occasions, which indicates that an error occurred while taking the reading. This had been observed during previous reporting periods, however the frequency of these 'zero readings' is increasing.

- Recorded changes in the strainmeters have been on the order of about 10 to 30 microstrain, and the measured changes in gage lengths have reflected the changes in temperature with an increase in temperature resulting in shortening of the gage length.

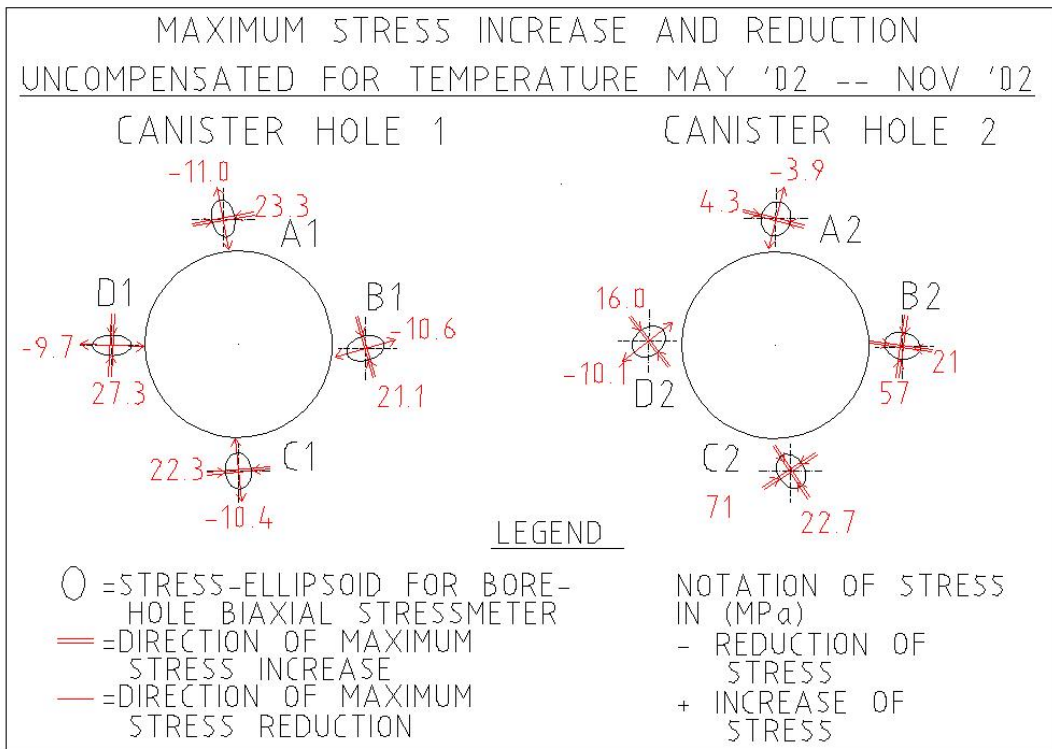


Figure 5.1 Maximum stress changes uncompensated for temperature

Stress-meter	Measuring period									
	Phase 1: Drilling phase					Phase 2: Heating phase				
	Typical max. stress increase (Mpa)		Typical max. stress reduction (Mpa)		Orientation of max. Stress increase (degree)	Typical max. stress increase (Mpa)		Typical max. stress reduction (Mpa)		Orientation of max. Stress increase (degree)
A1	17.0	-10.0	11.5	-10.0	22.7	-10.9	10.3	22.6	-10.8	10.3
B1	15.0	-11.0	17.0	-10.3	21.1	-10.3	16.8	26.9	-10.5	16.8
C1	12.0	-7.4	0	-9.9	21.9	-9.9	5.4	21.9	-9.8	5.4
D1	22.0	-11.0	0	-9.1	25.8	-9.1	0	26.3	-9.4	0
A2	5.0	-4.0	-11.0	-3.3	4.4	-3.3	-18.3	3.7	-3.3	-17.7
B2	11.0	-7.3	-7.5	-4.6	31.1	-4.6	-14.1	57.9 (*)	-4.6	-21.3
C2	11.0	-7.7	29.5	-6.6	29.1	-6.6	31.2	33.7 (*)	-7.6	30.2
D2	9.3	-7.2	38.5	-9.9	16.5	-9.9	38.7	16.2	-9.9	38.3

Stress-meter	Measuring period		
	Phase 2: Heating phase con't (see Note 5)		
	Period: 2002-05-01 to 2002-10-31		Orientation of max. Stress increase (degree)
A1	23.3	-11.0	10.4
B1	21.1	-10.6	15.9
C1	22.3	-10.4	5.3
D1	27.3	-9.7	-2.9
A2	4.3	-3.9	-13.9
B2	34 to 57	4 to 21	-0.6 to -8
C2	50 to 71	5.3 to 22.7	22 to 33
D2	16.0	-10.1	38.7

Notes:

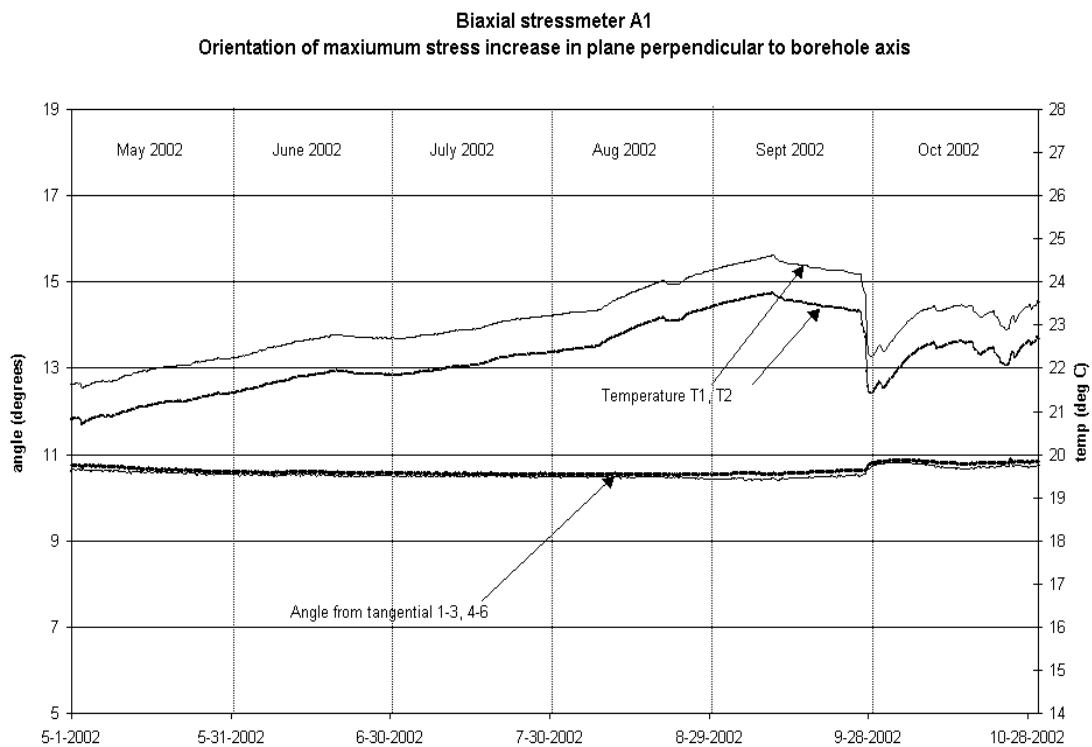
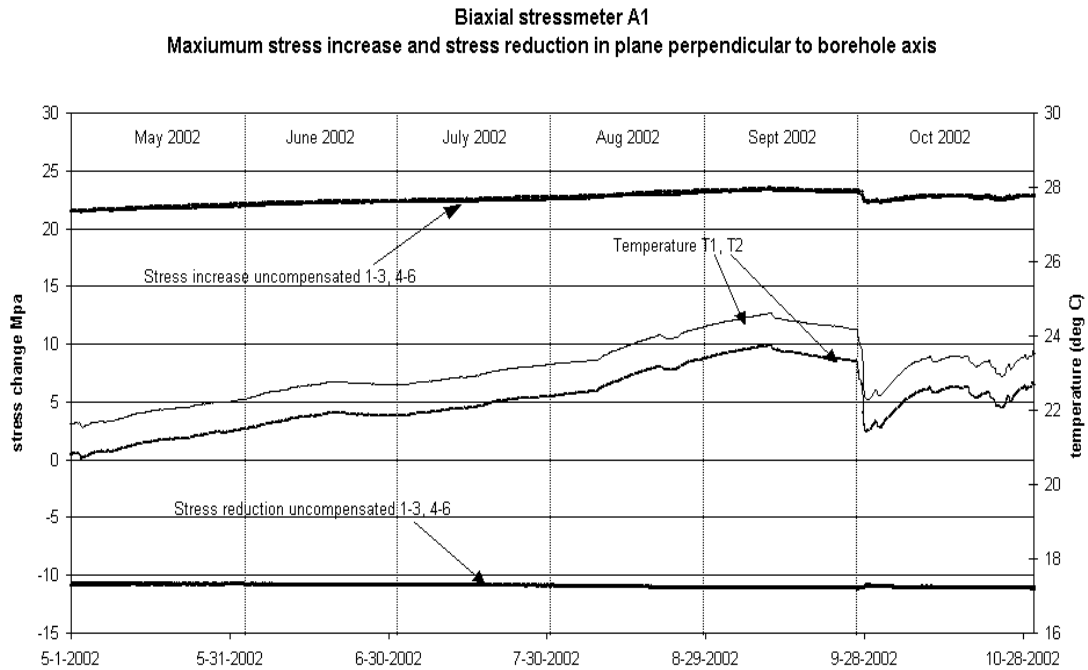
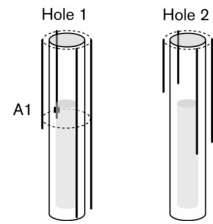
1. Positive values of stress indicate compression, negative values of stress indicate extension.
2. Positive values of orientation indicate anti-clockwise rotation, negative values of orientation indicate clockwise rotation.
3. Typical maximum stress increases and reductions represent maximum stabilised readings during the measuring period. (*) indicates that the reading had not stabilised during the measuring period.
4. Orientation of maximum stress increase is the orientation that corresponds to the typical maximum stress increase.
5. Calculation and processing methods revised during this reporting period to eliminate compensation for both temperature and longitudinal strains until further studies on these effects are carried out.

Table 1. Summary of results for stress measurements

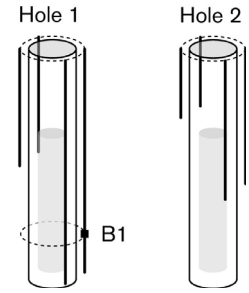
5.1 Results of canister hole 1

5.1.1 Stress change for each biaxial stressmeter

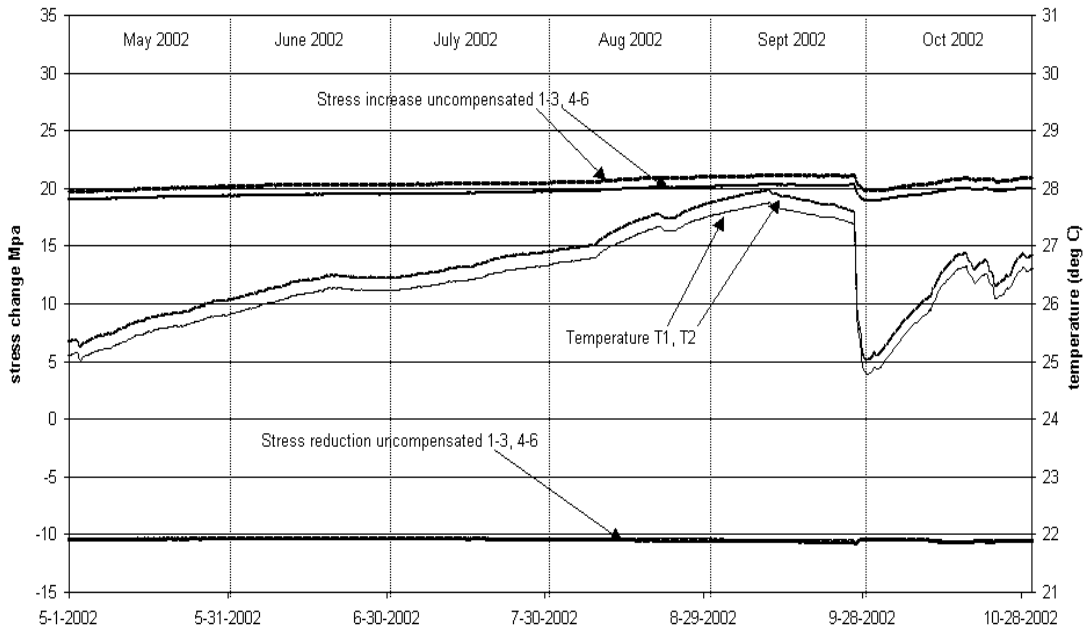
Biaxial stressmeter A1 uncompensated for temperature:



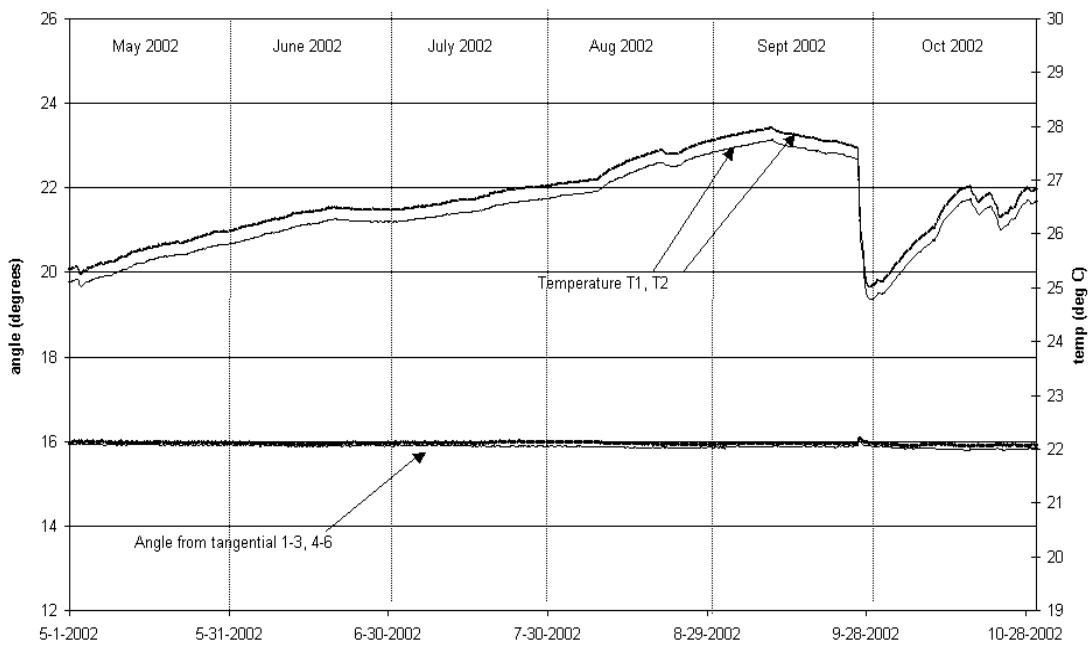
Biaxial stressmeter B1 uncompensated for temperature:



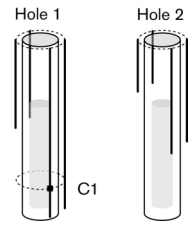
Biaxial stressmeter B1
Maximum stress increase and stress reduction in plane perpendicular to borehole axis



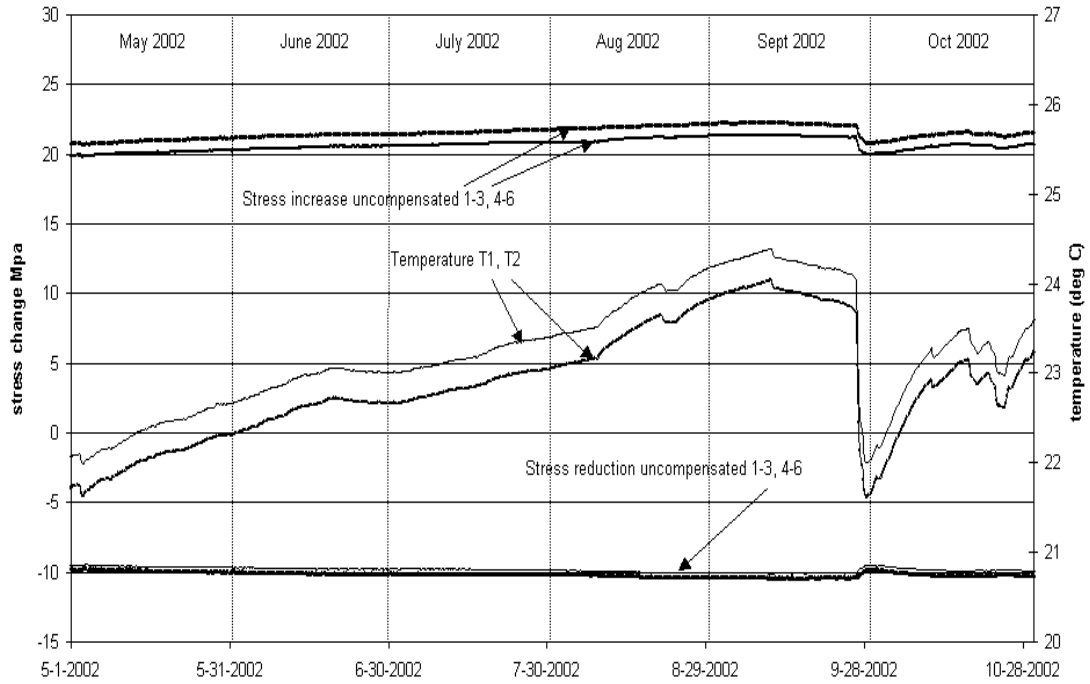
Biaxial stressmeter B1
Orientation of maximum stress increase in plane perpendicular to borehole axis



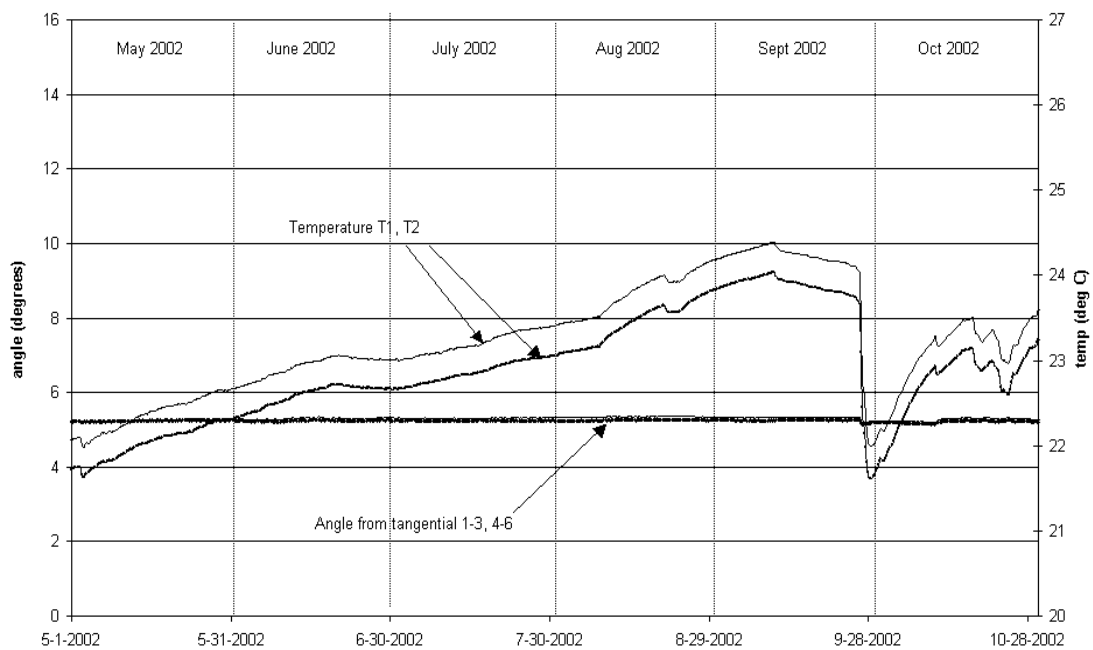
Biaxial stressmeter C1 uncompensated for temperature:



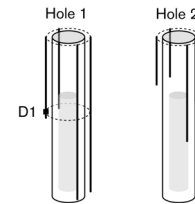
Biaxial stressmeter C1
Maximum stress increase and stress reduction in plane perpendicular to borehole axis



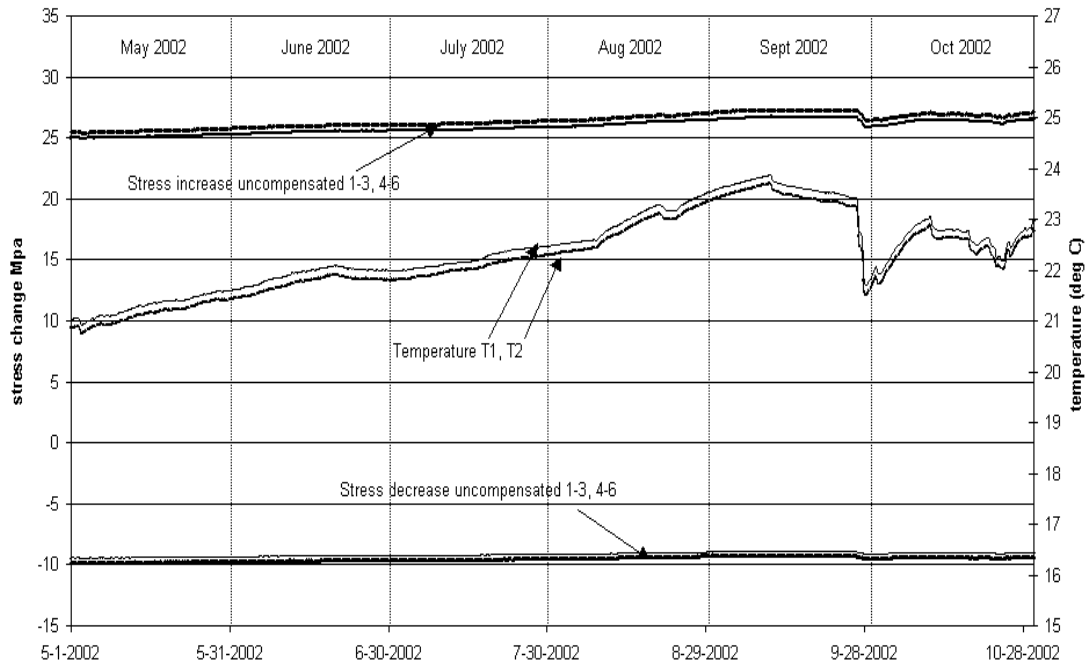
Biaxial stressmeter C1
Orientation of maximum stress increase in plane perpendicular to borehole axis



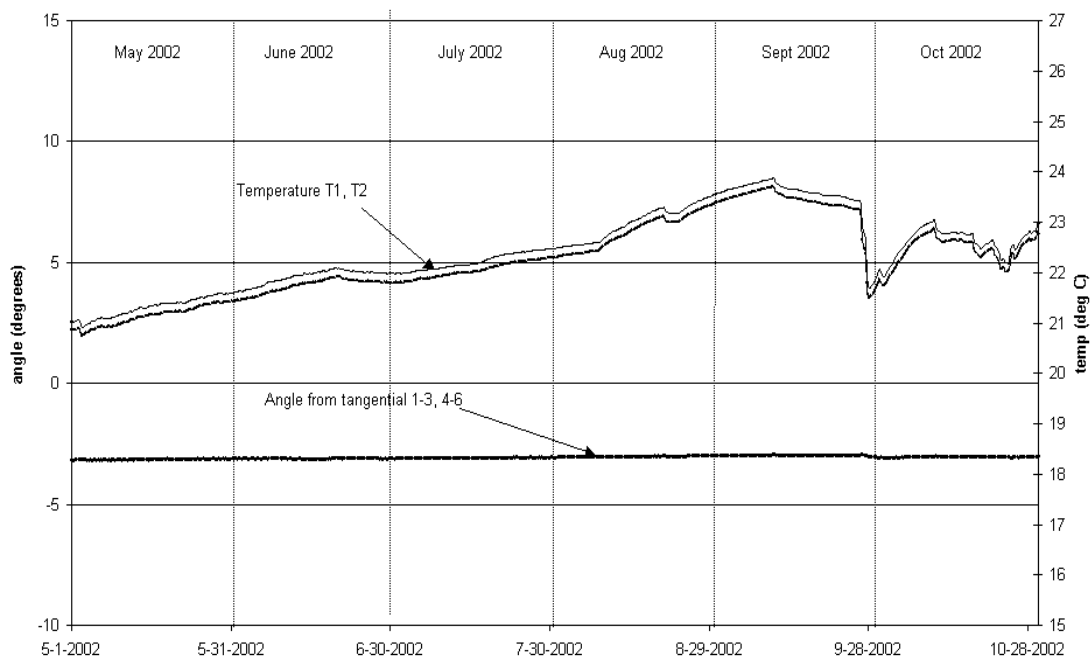
Biaxial stressmeter D1 uncompensated for temperature:



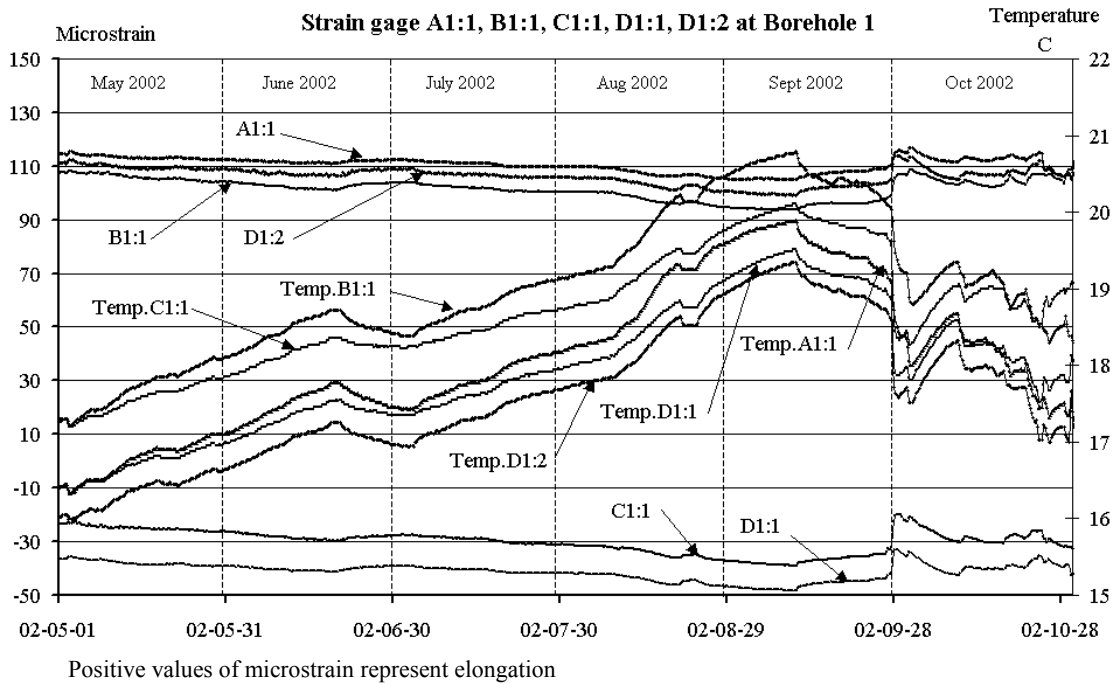
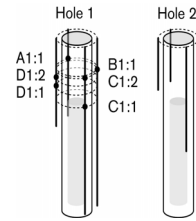
Biaxial stressmeter D1
Maximum stress increase and stress reduction in plane perpendicular to borehole axis



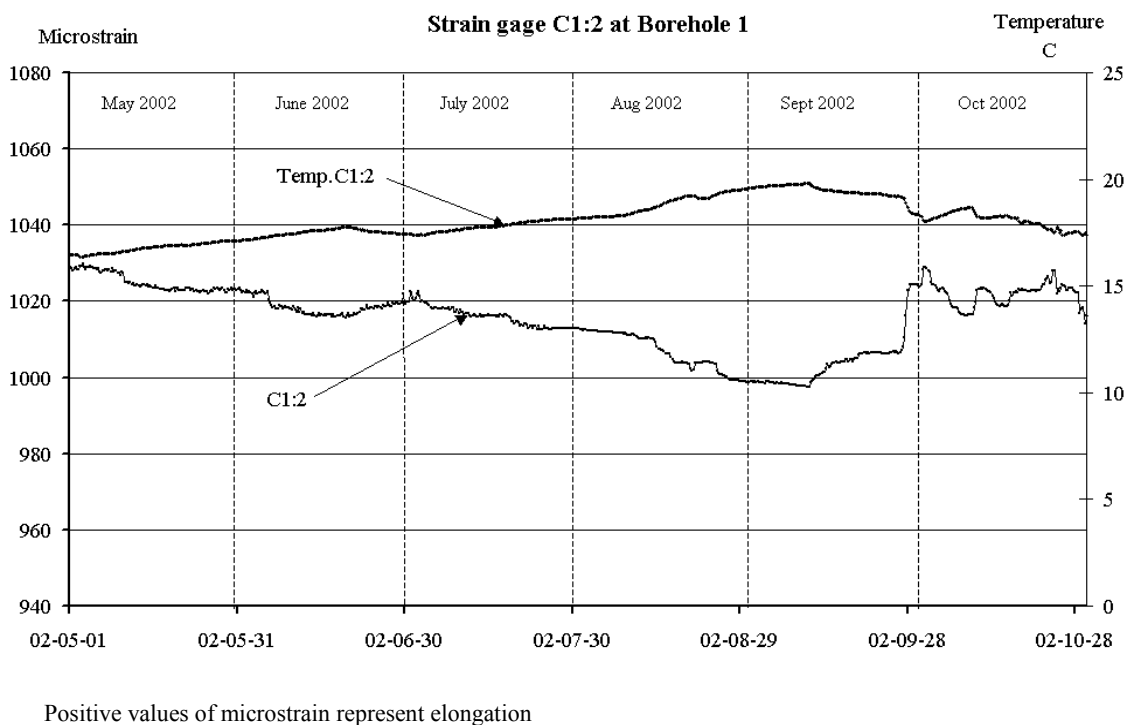
Biaxial stressmeter D1
Orientation of maximum stress increase in plane perpendicular to borehole axis



5.1.2 Strainmeter A1:1, B1:1, C1:1, D1:1, D1:2 (temperature compensated)



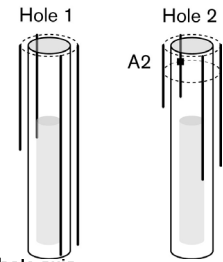
5.1.3 Strainmeter C1:2 (temperature compensated)



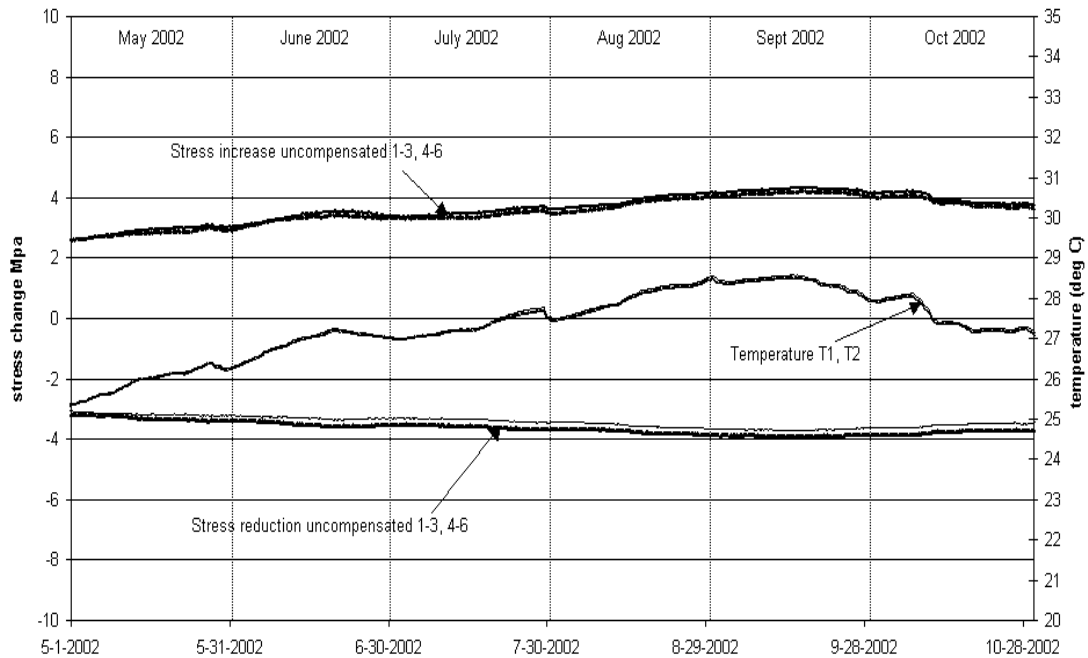
Results of canister hole 2

5.1.4 Stress change for each biaxial stressmeter

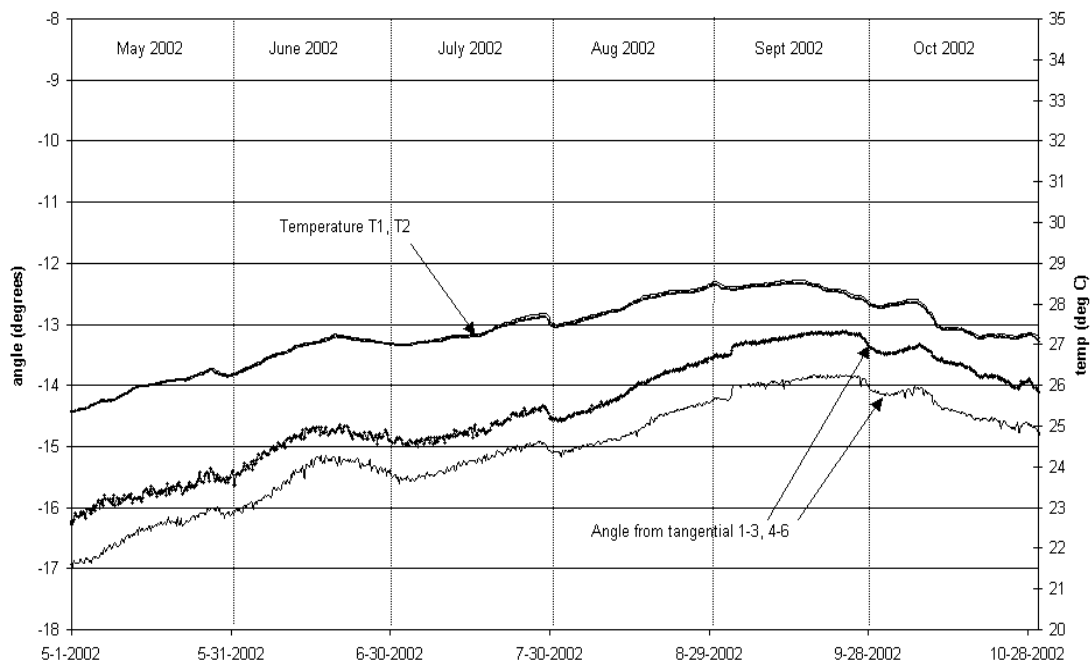
Biaxial stressmeter A2 uncompensated for temperature:



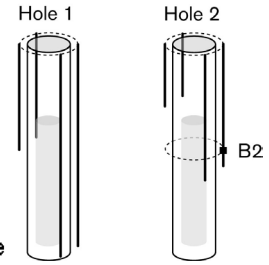
Biaxial stressmeter A2
Maximum stress increase and stress decrease in plane perpendicular to borehole axis



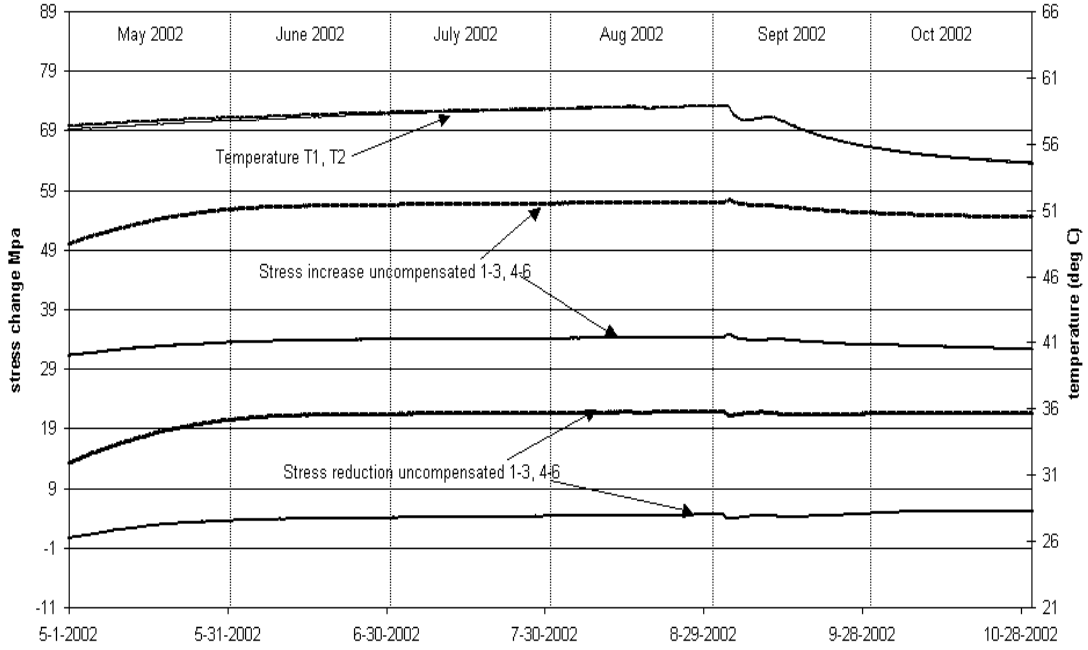
Biaxial stressmeter A2
Orientation of maximum stress increase in plane perpendicular to borehole axis



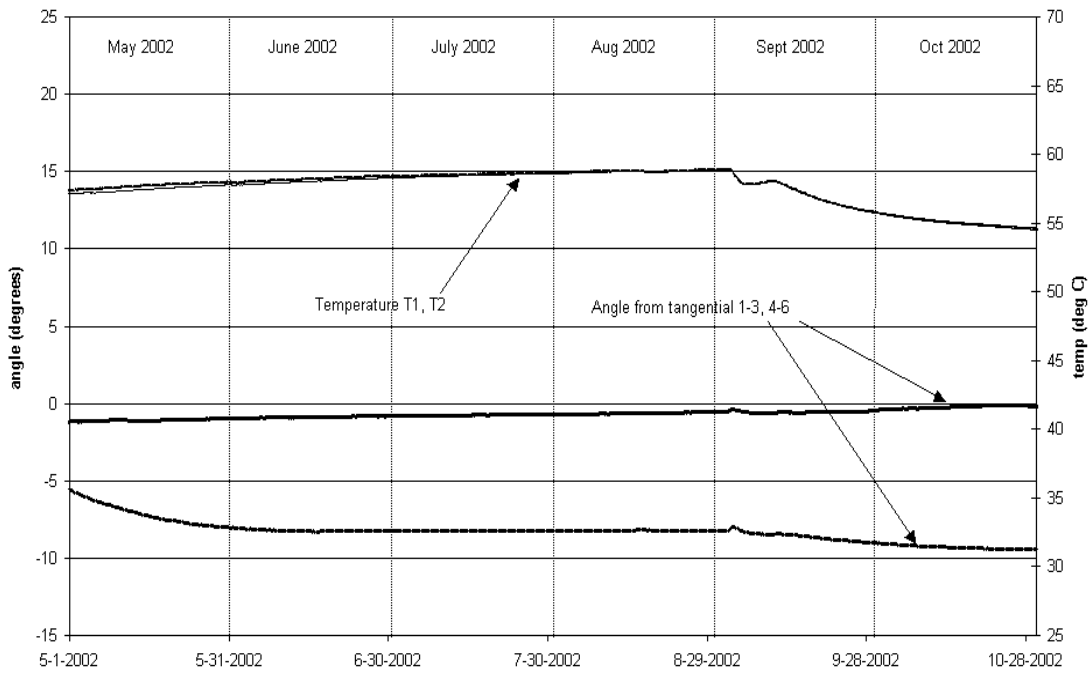
Biaxial stressmeter B2 uncompensated for temperature:



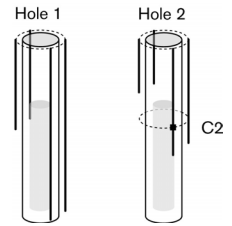
Biaxial stressmeter B2
Maximum stress increase (σ_1) in plane perpendicular to borehole



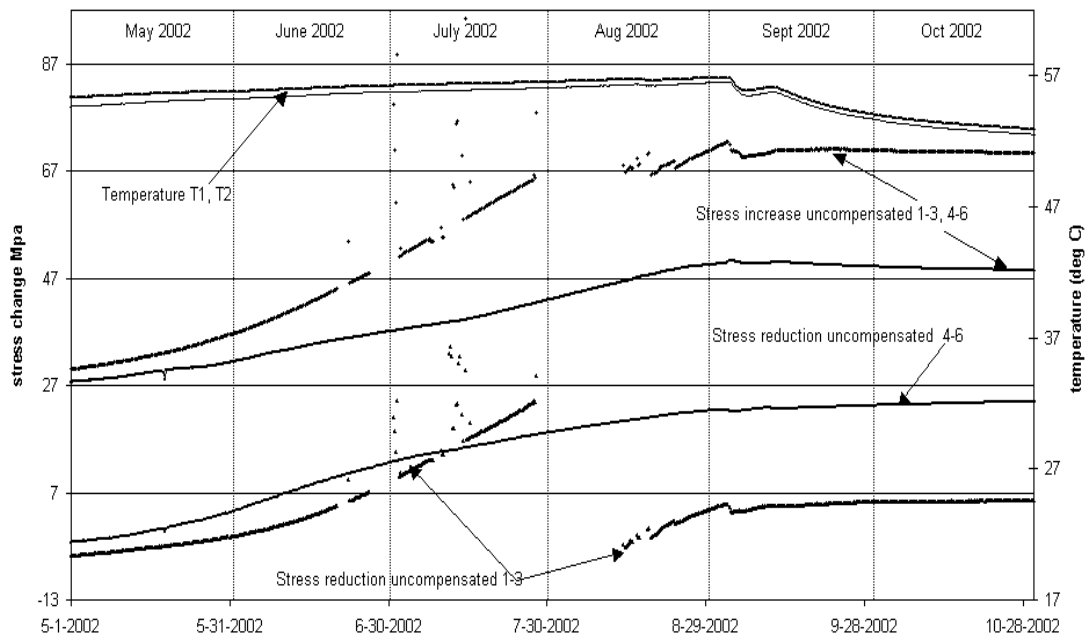
Biaxial stressmeter B2
Orientation of maximum stress increase (σ_1) in plane perpendicular to borehole



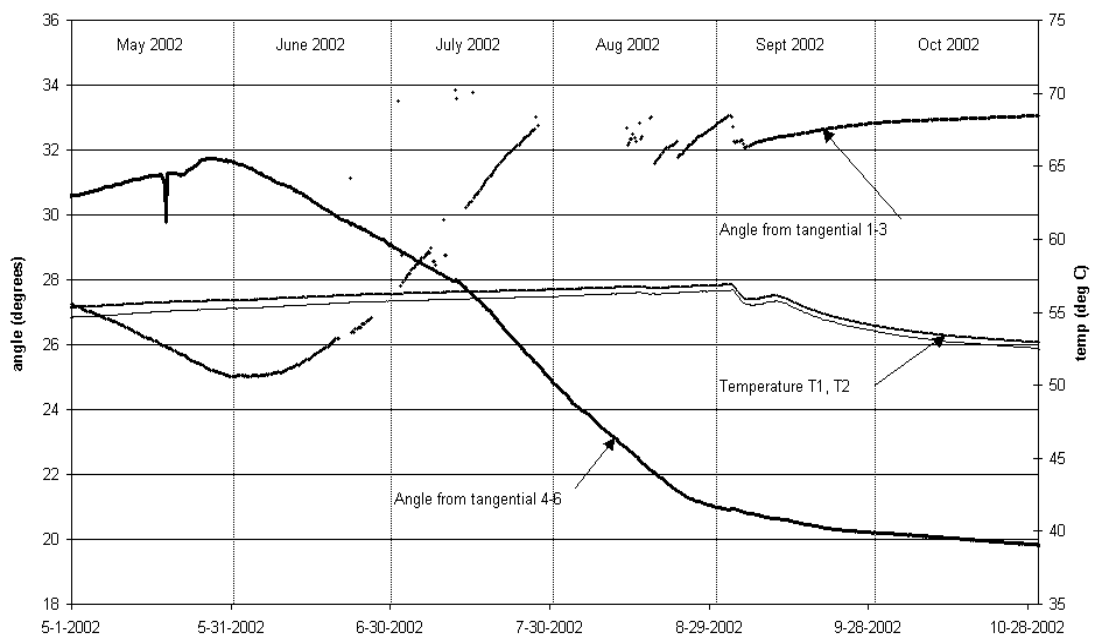
Biaxial stressmeter C2 uncompensated for temperature:



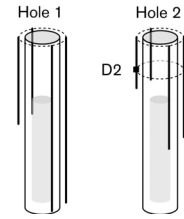
Biaxial stressmeter C2
Maximum stress increase and stress reduction in plane perpendicular to borehole axis



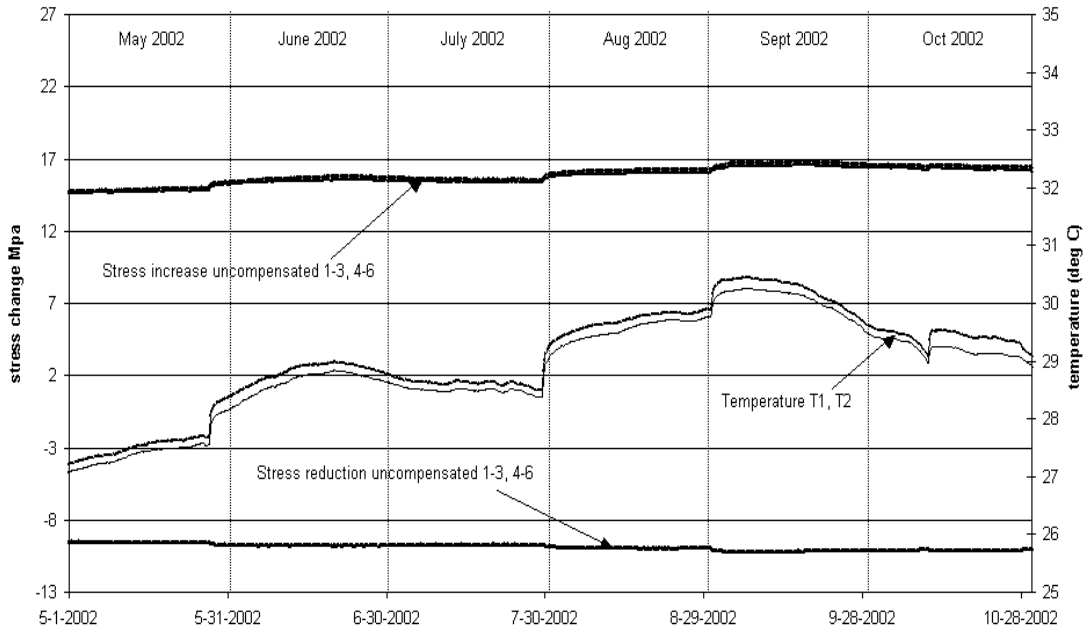
Biaxial stressmeter C2
Orientation of maximum stress increase in plane perpendicular to borehole axis



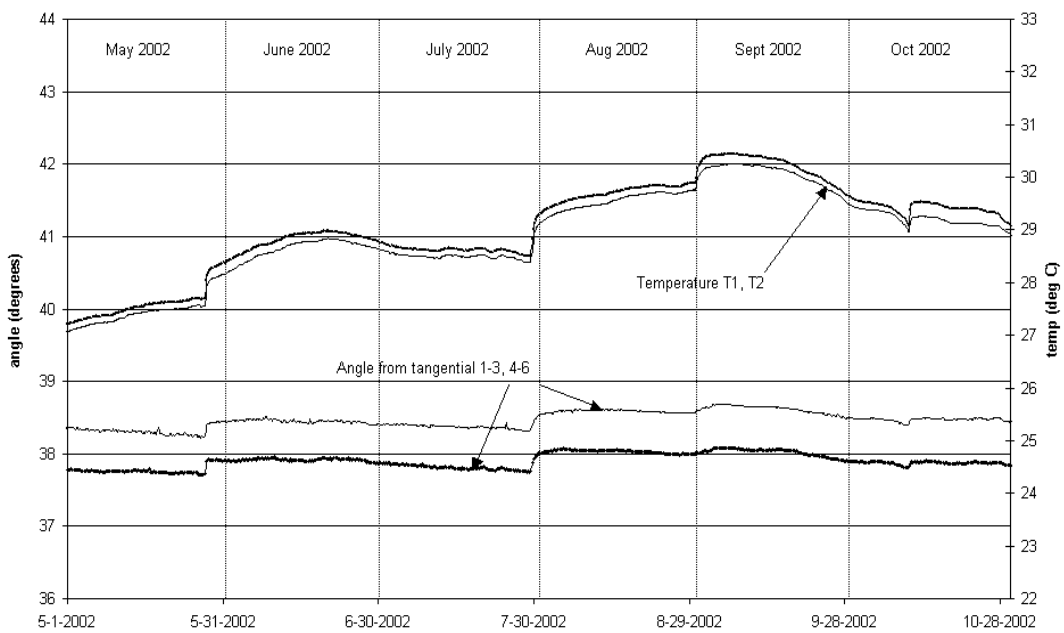
Biaxial stressmeter D2 uncompensated for temperature:



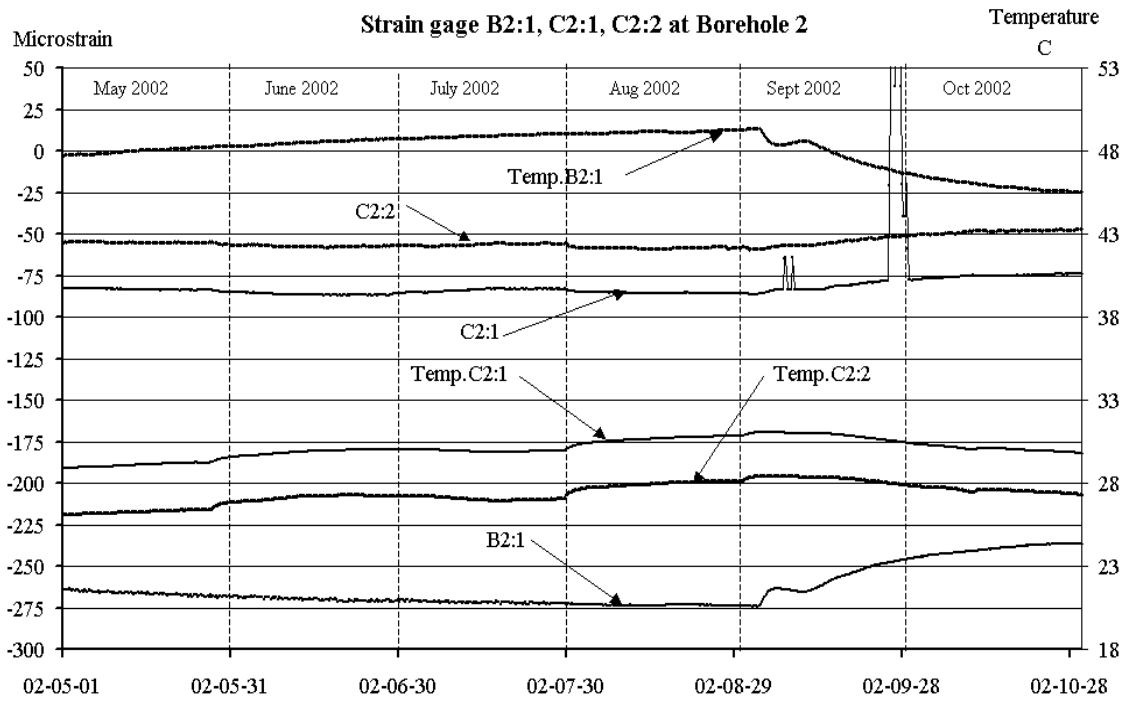
Biaxial stressmeter D2
Maximum stress increase and stress reduction in plane perpendicular to borehole axis



Biaxial stressmeter D2
Orientation of maximum stress increase in plane perpendicular to borehole axis



5.1.5 Strainmeter B2:1, C2:1, C2:2 (temperature compensated)



Positive values of microstrain represent elongation

